

2016

The molecular and mechanical mechanisms of the age-associated increase in the severity of experimental ventilator induced lung injury

Joseph Ames Herbert
jaherbster@gmail.com

Follow this and additional works at: <http://scholarscompass.vcu.edu/etd>

 Part of the [Other Biomedical Engineering and Bioengineering Commons](#)

© The Author

Downloaded from

<http://scholarscompass.vcu.edu/etd/4478>

This Dissertation is brought to you for free and open access by the Graduate School at VCU Scholars Compass. It has been accepted for inclusion in Theses and Dissertations by an authorized administrator of VCU Scholars Compass. For more information, please contact libcompass@vcu.edu.

Joseph Ames Herbert

Copyright 2016

ALL RIGHTS RESERVED

The molecular and mechanical mechanisms of the age-associated increase in the severity of experimental ventilator induced lung injury

A Dissertation submitted in partial fulfillment of requirements for the degree of Doctor of
Philosophy at Virginia Commonwealth University

by
Joseph Ames Herbert

**Virginia Commonwealth University
Richmond, Virginia
August, 2016**

Acknowledgement

I would like to thank all of the amazing people who helped me to achieve this goal. I would like to thank all of the members of both the Heise Lab and the interdepartmental VILI team for their consistently excellent scientific and professional support. I would also like to thank all members of my graduate committee for the time, effort, and support that they so generously contributed. I would like to give a special thanks to my mentor and friend Dr. Heise for showing me such unwavering faith and support over these past five years. I would also like to thank all of my family and friends for their support during this stressful time period. I would also like to give a special thanks to my girlfriend, Lauren, whose steadfast love and support have made this achievement possible.

TABLE OF CONTENTS

| | |
|--|------|
| List of Tables..... | VII |
| List of Figures..... | VIII |
| Abstract..... | XII |
| 1.0 Introduction..... | 1 |
| 1.1.0 Lung Anatomy and Physiology..... | 1 |
| 1.1.1 Generations of the Lung..... | 1 |
| 1.1.2 Alveolar Structure and Function..... | 5 |
| 1.1.3 Alveolar Epithelial Cells..... | 6 |
| 1.1.4 Alveolar Basal Membrane, ECM, and MACs..... | 10 |
| 1.2 Pulmonary Mechanics..... | 15 |
| 1.3.0 Ventilator Induced Lung Injury and Pulmonary Edema..... | 25 |
| 1.3.1 Impact of VILI..... | 25 |
| 1.3.2 Biotrauma..... | 28 |
| 1.3.3 Pulmonary Edema..... | 29 |
| 1.3.4 Alveolar Fluid Clearance..... | 30 |
| 1.3.5 VILI-Associated Edema..... | 31 |
| 1.3.6 Age, Edema, and VILI..... | 33 |
| 1.3.7 Fluid Support and Hemodynamics During MV..... | 33 |
| 1.4 ER Stress Background..... | 34 |
| 1.5 Specific Aims..... | 43 |
| 2.0 Conservative Fluid Management Prevents Age-Associated Ventilator Induced Mortality..... | 46 |

| | | |
|---------------|--|-----------|
| 2.1.0 | Introduction..... | 46 |
| 2.2.0 | Materials and Methods..... | 48 |
| 2.2.1 | Animal Use..... | 48 |
| 2.2.2 | Age Groups..... | 48 |
| 2.2.3 | Mechanical Ventilation..... | 48 |
| 2.2.4 | Fluid Support Protocol..... | 49 |
| 2.2.5 | Lung Mechanics..... | 50 |
| 2.2.6 | Euthanasia..... | 50 |
| 2.2.7 | Bronchoalveolar Lavage Fluid Collection..... | 50 |
| 2.2.8 | Bronchoalveolar Lavage Fluid Cytology..... | 51 |
| 2.2.9 | Bronchoalveolar Lavage Fluid Protein Concentration..... | 51 |
| 2.2.10 | Lung Histology..... | 51 |
| 2.2.11 | Lung Wet to Dry Ratios..... | 51 |
| 2.2.12 | Non-Ventilated Controls..... | 52 |
| 2.2.13 | Statistical Analysis..... | 52 |
| 2.3.0 | Results..... | 52 |
| 2.3.1 | Four Hour High Fluid Survival Rate..... | 52 |
| 2.3.2 | One Hour Lung Wet to Dry Ratios..... | 53 |
| 2.3.3 | Four Hour Bronchoalveolar Lavage Concentration..... | 55 |
| 2.3.4 | Bronchoalveolar Lavage Cytology..... | 55 |
| 2.3.5 | PV Loop Hysteresis..... | 56 |
| 2.3.6 | Lung Compliance..... | 59 |
| 2.3.7 | Total Lung Capacity..... | 59 |
| 2.3.8 | Airspace Enlargement..... | 60 |
| 2.4.0 | Discussion..... | 61 |
| 2.5.0 | Limitations..... | 69 |

3.0 The Role of ER Stress and Aging in an *In Vitro* Model of Ventilator

| | |
|--|----|
| Induced Lung Injury..... | 70 |
| 3.1.0 Introduction..... | 70 |
| 3.2.0 Methods..... | 73 |
| 3.2.1 ATII Cell Isolation and Culture..... | 73 |
| 3.2.2 ATII Cell Phenotyping..... | 73 |
| 3.2.3 CHOP Immunofluorescence..... | 74 |
| 3.2.4 Cell Stretch..... | 74 |
| 3.2.5 ER Stress Inhibition..... | 74 |
| 3.2.6 MTT Assay..... | 74 |
| 3.2.7 <i>mRNA Analysis</i> | 75 |
| 3.2.8 Media Protein Concentration..... | 75 |
| 3.2.9 Inflammatory Mediator Analysis..... | 75 |
| 3.3.0 Results..... | 75 |
| 3.3.1 Phenotyping..... | 75 |
| 3.3.2 CHOP Staining..... | 77 |
| 3.3.3 MTT Assay..... | 77 |
| 3.3.4 Inflammatory Gene Expression..... | 77 |
| 3.3.5 Media protein concentration..... | 74 |
| 3.4.0 Discussion..... | 76 |

4.0 VitC treatment attenuates VILI induced pulmonary edema and partially normalized pulmonary mechanics.....

| | |
|-------------------------|-----|
| 4.1.0 Introduction..... | 93 |
| 4.2.0 Methods..... | 91 |
| 4.2.1 Animal Use..... | 101 |

| | | |
|-------|--|-----|
| 4.2.2 | Age Groups..... | 101 |
| 4.2.3 | Mechanical Ventilation..... | 101 |
| 4.2.4 | VitC Treatment..... | 101 |
| 4.2.5 | Pulmonary Mechanics..... | 101 |
| 4.2.6 | Lung Wet to Dry Ratios..... | 101 |
| 4.2.7 | Data Analysis..... | 101 |
| 4.3.0 | Results..... | 102 |
| 4.3.1 | One Hour Lung Wet to Dry Ratios..... | 102 |
| 4.3.2 | PV Loop Hysteresis..... | 102 |
| 4.3.3 | Lung Compliance..... | 104 |
| 4.4.0 | Discussion..... | 104 |
| 5.0 | Summary, Implications and Future Directions..... | 105 |
| | References..... | 110 |
| | Vita..... | 126 |

List of Tables

Table 1: Cellularity in BALF. Data presented as absolute cell numbers in broncoalveolar lavage and as cell differentials (percentage of counted cells). Monocyte differential < Young Non-Ventilated and Old Non-Ventilated. Data are presented as mean +/- st.dev N=4 for Young Non-Vent, 3 for Young LVT – HF, 6 for Young HVT – HF, 3 for Young HVT – LF, 6 for Old Non-Vent, 4 for Old LVT – HF, 4 for Old HVT – HF, 5 for Old HVT – LF *p<0.05..... 55

List of Figures

Figure 1: Diagram of the divisions of the respiratory tract. Reprinted from McNulty et al³.....1

Figure 2: Respiratory Bronchioles transition from a terminal bronchiole, to respiratory bronchioles, to alveolar ducts, which terminate in alveolar sacs and individual alveoli. Reprinted from Kerr et al⁸ 3

Figure 3: Alveolus Diagram. Reprinted from public domain⁹4

Figure 4: Diagram of the alveolar epithelium 6

Figure 5: Diagram of the alveolar mechanics A. without surfactant and B. with surfactant. Reprinted from Sherwood et al¹⁷9

Figure 6: Alveolar epithelial barrier histology. Reprinted from Kerr et al⁸ 11

Figure 7: (left) Alveolar capillary lined by endothelial cell. (right) wo cell air blood alveolar barrier. Reprinted from Wiebel et al¹⁸ 13

Figure 8: Collagen and Elastin fiber networks surrounding alveolar epithelium. Reprinted from Toshima et al²⁰ 14

Figure 9: Alveolar Macrophage Attacking E Coli Bacteria. Image copyright Dennis Kunkel Microscopy, Inc²² 15

Figure 10: (left) Crumpled lung collagen ECM. (right) Inflated lung collagen ECM. Reprinted from Toshima et al²⁰ 18

Figure 11: Pressure volume loops obtained from cat lung submerged in saline. Reprinted from Harris et al²⁵ 20

Figure 12: PV graph of combined chest and lung wall mechanics. Reprinted from Harris et al²⁵ 23

Figure 13: Graph of lung inflation below FRC. Reprinted from Harris et al²⁵ 24

Figure 14: Flow chart of the mechanisms of VILI. Reprinted from Carrasco et al³¹ 26

Figure 15: Diagram of the alveolar mechanisms of VILI. Reprinted from Reynaud et al³⁰ 27

Figure 16: A schematic energy landscape for protein folding. Reprinted from Reynaud et al⁶⁷. 36

Figure 17: Regulation of protein folding in the ER. Reprinted from Reynaud et al⁶⁷ 38

Figure 18: Diagram of ER Stress Pathway. Reprinted from Reynaud et al⁷² 40

Figure 19: Time dependent ER stress pathway. Reprinted from Hetz et al⁷⁹ 41

Figure 20: 4Hr Survival Rate. Survival rate in the Old HVT-HF group was significantly less than all other groups. Data is presented as survival percentage N = 10 for Young LVT-HF, 10 for Young HVT-HF, 3 for Young HVT-LF, 7 for Old LVT-HF, 12 for Old HVT-HF, 8 for Old HVT-LF
*** p<0.001 53

Figure 21: A. 1Hr Lung Wet to Dry Ratios. There was a group wise statistically significant difference across age with old groups having significantly greater lung wet to dry ratio than young. The Young HVT-HF group was significantly greater than in the Young Non-Ventilated group. The Old HVT-LF group was significantly less than in all other old groups respectively. Data are presented as mean +/- st.dev N = 4 for Young Non-Vent, 4 for Young HVT-HF, 4 for Young HVT-LF, 4 for Old Non-Vent, 4 for Old HVT-HF, 5 for Old HVT-LF. **B. 4Hr Lavage Protein Concentration.** The Old HVT-HF group concentration was significantly greater than that of all other old groups respectively. N = 4 for Young Non-Vent, 4 for Young LVT-HF, 7 for Young HVT-HF, 3 for Young HVT-LF, 4 for Old Non-Vent, 4 for Old LVT-HF, 4 for Old HVT-HF, 5 for Old HVT-LF *p<0.05..... 54

Figure 22: A. Representative 4Hr PV Loop for a Young LVT-HF subject. B. Representative 4Hr PV Loop for an Old LVT-HF subject. C. Representative 4Hr PV Loop for a Young HVT-HF subject. D. Representative 4Hr PV Loop for an Old HVT-HF subject..... 56

Figure 23: A. 1Hr PV Loop Hysteresis. Hysteresis in the Old HVT-HF group was significantly greater than Young HVT-HF and Old HVT-LF groups. Data are presented as mean +/- st.dev N=7 for Young HVT-HF, 7 for Young HVT-LF, 9 for Old HVT-HF, 12 for Old HVT-LF. **B. 4Hr PV Loop Hysteresis.** Hysteresis of the Old HVT-HF group was greater than that of the Old LVT-HF and Old HVT-LF groups. N=5 for Young LVT-HF, 6 for Young HVT-HF, 3 for Young HVT-LF, 5 for Old LVT-HF, 4 for Old HVT-HF, 5 for Old HVT-LF *p<0.05 **p<0.01 57

Figure 24: A. 1Hr Lung Compliance. There was a significant group wise across age with the old groups having a greater compliance than the young. 1Hr lung compliance in the Old HVT-HF group was significantly greater that of the Old HVT-LF group. Data are presented as mean +/- st.dev N=11 for Young HVT – HF, 4 for Young HVT – LF, 14 for Old HVT – HF, 7 for Old HVT – LF. **B. 1Hr Total Lung Capacity.** There was a significant group wise difference across age with the old groups having a greater TLC than young. 1Hr TLC in the Old HVT-HF group was significantly greater that of the Old HVT-LF group. N=4 for Young HVT – HF, 4 for Young HVT – LF, 14 for Old HVT – HF, 14 for Old HVT – LF. **C. 4Hr Lung Compliance.** There was a significant group wise difference across age with the old groups having greater lung compliance than the young. 4Hr lung compliance in the Old HVT-HF group was significantly greater that of the Old 0Hr and Old HVT-LF groups. N=11 for 0Hr Young, 7 for Young LVT – HF, 8 for Young HVT – HF, 3 for Young HVT – LF, 16 for 0Hr Old, 6 for Old LVT – HF, 4 for Old HVT – HF, 6 for Old HVT – LF. **D. 4Hr Total Lung Capacity.** There was a significant group wise difference across age with the old groups having a greater TLC than young. 4Hr TLC in the Old HVT-HF group was significantly greater that of the Old HVT-LF group. N=11 for 0Hr Young, 7 for Young LVT – HF, 9 for Young HVT – HF, 3 for Young HVT – LF, 16 for 0Hr Old, 6 for Old LVT – HF, 4 for Old HVT – HF, 6 for Old HVT – LF, *p<0.05 **p<0.01 ***p<0.001 ****p<0.0001 58

Figure 25: A, B, C, D, E, F. Representative 4Hr histological H&E images of A. Young LVT-HF, B. Young HVT-HF, C. Young HVT-LF, D. Old LVT-HF, E. Old HVT-HF, and F. Old HVT-LF lung sections respectively 60

Figure 26: Airspace Enlargement. There was a statistically significant groupwise difference across age with old groups having significantly greater enlargement than young. Enlargement was greater in the Old HVT-HF group than in all others. Data are presented as mean +/- st.dev N = 3 for Young Non-Vent, 6 for Young LVT-HF, 6 for Young HVT-HF, 3 for Young HVT-LF, 3 for Old Non-Vent, 3 for Old LVT-HF, 4 for Old HVT-HF, 3 for Old HVT-LF **p<0.01 61

Figure 27: Representative 20X surfactant C images of A. Old 24Hr and B. Young 24Hr cells. Green are pro-SPC positive cells, blue are nuclei stained with DAPI 76

Figure 28: Representative 20X 4Hr histological CHOP images of A. Young LVT-HF, B. Old LVT-HF, C. Young HVT-HF, D. Old HVT-HF lung sections. Yellow are CHOP positive cells, blue are nuclei stained with DAPI 76

Figure 29: Normalized MTT absorbance values. A. MTT values for Young 5% 24hr and 96hr groups were significantly higher than static controls. MTT Value for Young 15% 4hr group was significantly higher than static control, B. MTT value for Old 5% 96hr group was significantly greater than static control. MTT value for old 15% 96hr was significantly lower than static control. Data presented as mean +/- st.dev n=3 *p<0.05..... 77

Figure 30: Age, stretch, and ER inhibitor induced inflammatory gene expression. A,B. Old 24Hr Static ER Control, Old 24Hr Stretch ER Control, Old 24Hr Static ER Inhibited, Old 24Hr Stretch ER Inhibited, normalized to Old 24Hr Static ER Control. Columns are fold change differences in gene expression. Data are presented as mean +/- st. deviation, n=3, *p<0.05..... 78

Figure 31: Age and stretch induced inflammatory gene expression. A. Young 24Hr Static, Old 24Hr Static, Young 24Hr Stretch, Old 24Hr Stretch normalized to Young 24Hr Static. B. Young 24Hr Static and Old 24Hr Static normalized to Young 24Hr Static. Columns are fold change differences in gene expression. Data are presented as mean +/- st. deviation, n=3 79

Figure 32: Age and stretch induced inflammatory gene expression. A. Young 24Hr Static and Old 24Hr Static normalized to Young 24Hr Static. B. Young 24Hr Static and Young 24Hr Stretch normalized to Young 24Hr Static. Columns are fold change differences in gene expression. Data are presented as mean +/- st. deviation, n=3, *p<0.05 80

Figure 33: Age and stretch induced inflammatory gene expression. A,B. Old 24Hr Static and Old 24Hr Stretch normalized to Old 24Hr Static. Columns are fold change differences in gene expression. Data are presented as mean +/- st. deviation, n=3, *p<0.05 81

Figure 34: Age and stretch induced inflammatory gene expression. A,B. Young 24Hr Stretch and Old 24Hr Stretch normalized to Young 24Hr Stretch. Columns are fold change differences in gene expression. Data are presented as mean +/- st. deviation, n=3, *p<0.05..... 82

Figure 35: Age and stretch induced inflammatory gene expression. A,B. Old 24Hr Stretch ER Control and Old 24Hr Stretch ER Inhibited normalized to Old 24Hr Stretch ER Control. Columns are fold change differences in gene expression. Data are presented as mean +/- st. deviation, n=3, *p<0.05 83

- Figure 36: Age and stretch induced inflammatory gene expression. A,B. Old 24Hr Stretch ER Control and Old 24Hr Stretch ER Inhibited normalized to Old 24Hr Stretch ER Control. Columns are fold change differences in gene expression. Data are presented as mean +/- st. deviation, n=3, *p<0.05 84**
- Figure 37: Cell media protein concentration. A,B,C,D,E,F,G,H. Old 24Hr Static ER Control, Old 24Hr Stretch ER Control, Old 24Hr Static ER Inhibited, Old 24Hr Stretch ER Inhibited. Data are presented as mean +/- st. deviation, n=3, *p<0.05 85**
- Figure 38: 1Hr Lung Wet to Dry Ratios. The Old HVT-HF-LF and Old HVT-HF-VitC groups were significantly lower than that of Old non-ventilated and Old HVT-HF groups. Data are presented as mean +/- st.dev N = 3, *p<0.05..... 102**
- Figure 39: 1Hr PV Loop Hysteresis. Hysteresis in the Old HVT-LF and Old HVT-HF-VitC group were significantly greater than Old HVT HF. Data are presented as mean +/- st.dev N=3, *p<0.05.103**
- Figure 40: 1Hr Lung COmpliance. Lung Compliance in the Old HVT-LF group was significantly lower than Old HVT-HF. Data are presented as mean +/- st.dev N=3, *p<0.05 103**

Abstract

Background

The majority of patients requiring mechanical ventilation are over the age of 65 and advanced age is known to increase the severity of ventilator-induced lung injury (VILI) and mortality. However, the mechanisms which predispose aging ventilator patients to increased mortality rates are not fully understood.

Pulmonary edema is a hallmark of VILI and the severity of edema increases with age. Ventilation with conservative fluid management decreases mortality rates in acute respiratory distress (ARDS) patients, but has not been investigated in VILI. We hypothesized that age-associated increases in pulmonary edema promote age-related increases in ventilator-associated mortality. Endoplasmic reticulum (ER) stress can disrupt cellular functions and plays a key role in many disease states. The severity of ER stress also increases with age. We hypothesized that age-associated increases in ER stress also increase in the severity of VILI.

Finally, serum Vitamin C (VitC) levels also decrease with age. VitC treatments have been shown to decrease mortality rates in murine models of ARDS by and attenuate pulmonary edema. We hypothesize that VitC treatments will attenuate ventilator induced pulmonary edema in our aged murine subjects.

Methods

Mechanical Ventilation: Young and old mice were mechanically ventilated with either high tidal volume (HVT) or low tidal volume (LVT) for with either liberal or conservative fluid support. One group received VitC treatment prior to ventilation.

Cell Stretch: Alveolar epithelial cells (ATECs) from young and old mice were harvested, cultured, and mechanically stretched. Treatment groups received ER stress inhibitor 4-PBA.

Results

Both advanced age and HVT ventilation significantly increased inflammation, injury, and decreased survival rates. Conservative fluid support significantly diminished pulmonary edema decreased mortality rates. VitC treatments significantly decreased pulmonary edema and improved pulmonary mechanics. Mechanical stretch promoted ER Stress and upregulated proinflammatory gene expression and secretion in aged ATECs. ER stress inhibition attenuated all of these effects.

Conclusion

Conservative fluid management alone attenuated age-associated increases in ventilator-associated mortality. VitC treatments decreased pulmonary edema and partially restore pulmonary mechanics in old mice ventilated with HVT. ER stress inhibition decreased stretch induced proinflammatory gene expression and protein secretion in aged mechanically stretched ATEC cells.

CHAPTER 1

INTRODUCTION

1.1.0 Lung Anatomy and Physiology

In humans the chief function of the lungs is to facilitate the exchange of carbon dioxide and oxygen between our blood stream and the atmosphere. In addition to respiration the lungs perform numerous other important biological functions which include providing the expiration of air needed for phonation, extra buoyancy when we are immersed in water, a supplemental method of thermoregulation, and the lungs mucosal layer and leukocytes act as an important second line of defense against inhaled infectious agents and other harmful environmental factors^{1,2}.

1.1.1 Generations of the Lung

The physical pathway through which air moves is known as the respiratory tract. The respiratory tract begins as a single airway but as it moves distally it divides. Every division is roughly a bifurcation and each is ascendingly enumerated as generation (figure 1).

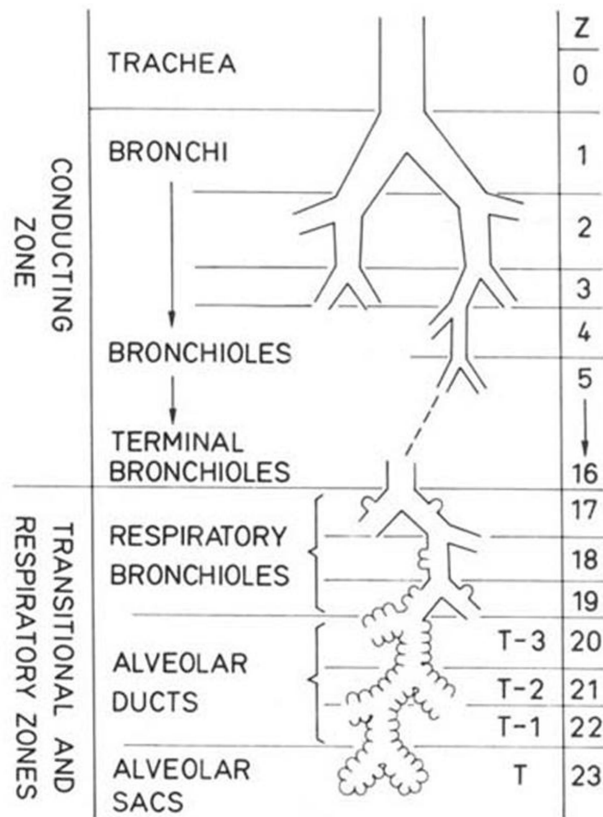


Figure 1: Diagram of the divisions of the respiratory tract. Reprinted from McNulty et al³.

The first 16 generations (divisions 0 through 15) of the respiratory tract are called the conduction zone and include the nose, pharynx, larynx, trachea, bronchi, bronchioles, and terminal bronchioles. Because each generation of divisions roughly doubles the number of pathways in the respiratory tract the final generation of the conduction zone has approximately 32,270 pathways or roughly 2^{15} . The primary function of the conducting zone is to act as a passageway through which air is able to

reach the rest of the respiratory tract. In addition the conduction zone filters, heats, and humidifies the inhaled air all of which aid in respiration. The conduction zone is also the site of phonation^{1,4}.

Additionally, the conduction zone acts as the body's first line of defense against inhaled pathogens and harmful environmental factors. The epithelium of the conducting airways contains goblet cells which secrete high molecular weight mucus glycoproteins which entrap inhaled irritants, particles and micro-organisms. These same epithelium are also lined with motile cilia which function to move the entrapped material up and out of the respiratory tract^{1,5-7}

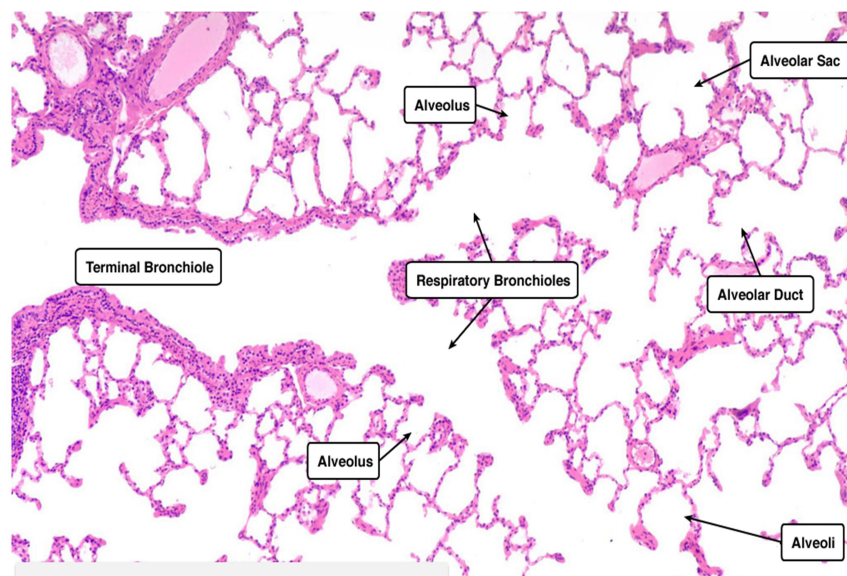


Figure 2: Respiratory Bronchioles transition from a terminal bronchiole, to respiratory bronchioles, to alveolar ducts, which terminate in alveolar sacs and individual alveoli. Reprinted from Kerr et al⁸.

The remaining nine generations (divisions 16 through 24) of the respiratory tract are known as the respiratory zone and contain the respiratory bronchioles, alveolar ducts, alveolar sacs, and the individual alveoli (figure 2). As its name suggest the respiratory zone is the region in which all of the respiration takes place. The functional

biological units of respiration are small space filled fluid lined sacs called alveoli (figure 3) through which carbon dioxide and oxygen are exchanged with the bloodstream¹.

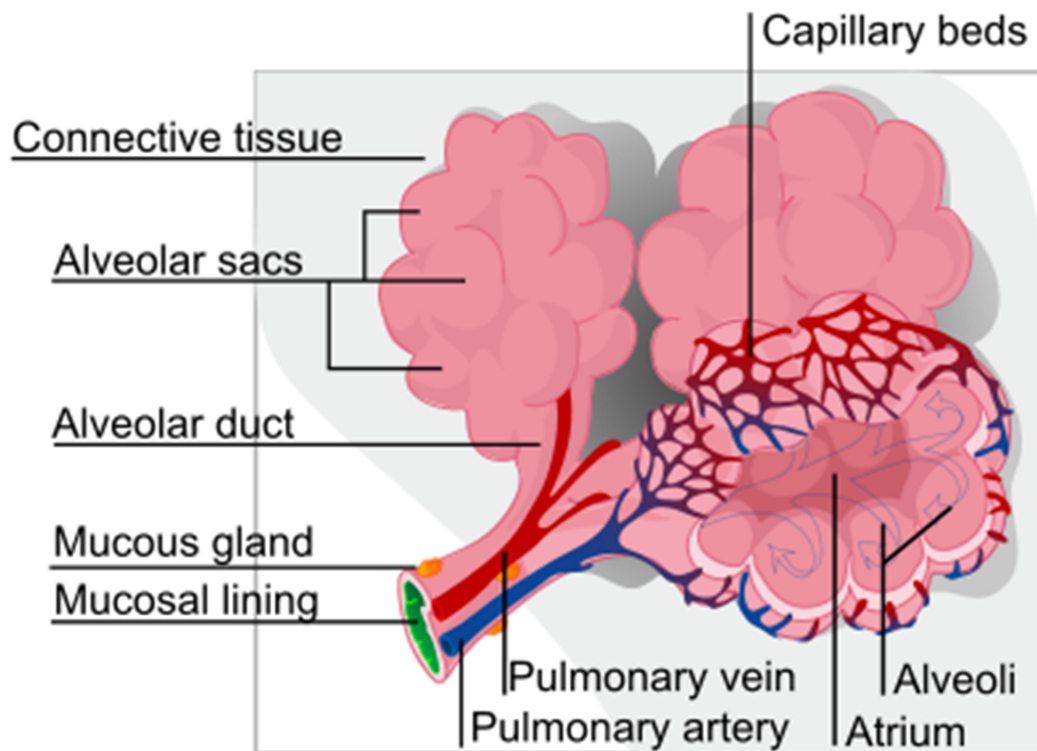


Figure 3: Alveolus Diagram. Reprinted from public domain⁹

As the bronchioles go through successive generations of division eventually around their 6th generation (the 17th generation of the respiratory tract overall) they begin to express individual alveoli as outgrowths. With each successive generation, the number of individual alveolar outgrowths increases.

This continues as the respiratory bronchioles eventually divide into the alveolar ducts which are heavily lined with alveoli. Each alveolar duct terminates with 2-3 large clusters of alveoli called an alveolar sac. The terminal ends of the alveolar ducts occur

at the 23rd division which means that there are roughly 16.8 - 25.2 million alveolar sacs in the adult lungs.

Each sac contains roughly 20 alveoli which mean that there are roughly 350-500 million alveoli in each pair of adult human lungs. The alveolar sacs contain the largest concentration of alveoli in the body. The individual alveoli on the respiratory bronchioles and the alveolar ducts are responsible for roughly 10% of the gas exchanged during respiration and the alveoli contained in alveolar sacs are responsible for the remaining 90%^{1,5,10}.

1.1.2 Alveolar Structure and Function

In total the alveolar walls, or interalveolar septa, account for 99% of the interior surface area of the lungs which in adult humans is about 100 to 150 square meters. The alveoli share these septa among neighboring alveoli which makes it impossible to make an exact distinction between the individual alveoli. When a 2D section of lung parenchyma is viewed it closely resembles dense foam with the major difference being that the alveolar sacs eventually open to alveolar ducts which interconnect and lead back up the respiratory tract^{1,2,5}. The alveoli have two kinds of openings in addition to the main opening to the alveolar duct.

The first type of openings are called pores of Kohn and serve to interconnect neighboring alveoli. The second type of openings are called canals of Lambert and connect the alveoli to the terminal respiratory bronchioles. Both of these openings have the same basic function which is that they allow air to pass collaterally between the

alveoli and bronchioles. This creates an interdependence in the alveolar air pressure which helps to stabilize them and helps air to reach underinflated alveolus¹

1.1.3 Alveolar Epithelial Cells

The alveolar septa are covered with two morphologically distinct types of pneumocyte cells.

Detailed anatomy of the respiratory membrane

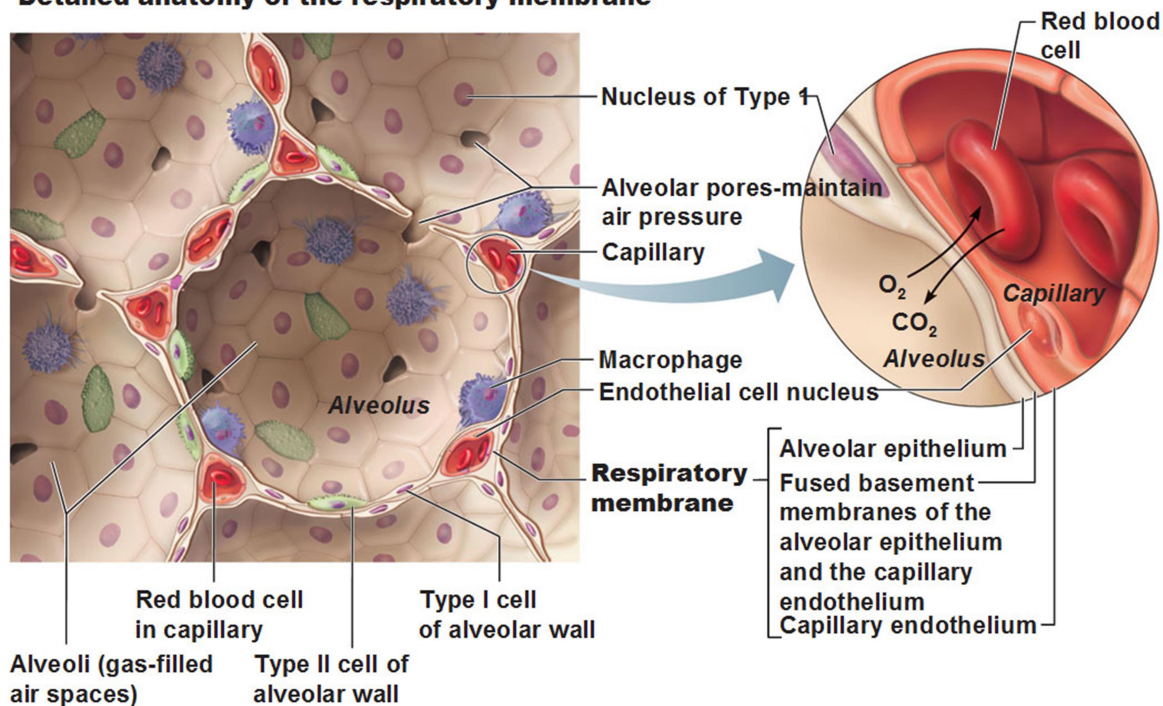


Figure 4: Diagram of the alveolar epithelium. Reprinted from Antranik et al¹⁴.

ATI pneumocytes (ATIs) are squamous epithelial cells which means that they are flat, stretched out, and create a tile like cell layer. They cover both the inner and outer surface of the alveolar septa (figure 4). ATI cells are also relatively large (diameter of ~ 50 to 100 μm and volume of ~ 2,000 to 3,000 μm^3). ATII pneumocytes are cuboidal epithelial cells. They exist only on the interior surface of the alveolar septa and protrude into the interior space of the alveolar sacs. They are relatively small compared to the

ATI cells (diameter $\sim 10 \mu\text{m}$ and volume of ~ 450 to $900 \mu\text{m}^3$). Even though ATI cells comprise only 8% of the cells found in the alveolar region, because of their larger size and their extremely stretched flattened arrangement they cover 95% of the alveolar surface, the rest being covered by the AII cells^{7,15}.

It has long been assumed that since ATI cells form the surface across which essentially all of the gas is exchanged during respiration that they have significant functionality with regards to facilitating this process. However, the physiological role of ATI cells in respiration is still yet to be fully elucidated. Despite this shortcoming our understanding of their role in innate host defense and in alveolar fluid clearance has developed considerably in the recent past. The Na^+ gradient that drives fluid absorption across the alveolar epithelial barrier is created by active transport through the Na-K-ATPase pump, the 1a and 1b subunits of which are the most common Na pump subunits in alveolar epithelial cells. In one study a cell specific deletion of the 1b subunits in ATI's created a significant decrease in alveolar fluid clearance¹⁶. However, this knockout did not lead to increased pulmonary edema in either hyperoxia induced or ventilator induced lung injury models relative to similarly injured wild type controls.

Thus while ATIs involvement in alveolar fluid clearance is clear their exact role is yet to be fully elucidated. Additionally, it has recently been discovered that the inflammatory response of ATI cells to inflammation and injury is more acute than that of AII's¹⁷. In one study, relative to similarly cultured AII's, isolated ATI's were shown to exhibit both a higher level of inflammatory gene expression in control groups, when treated with LPS, when cocultured with alveolar macrophages, and when cultured with treated media from LPS treated macrophages¹⁸.

It is also known that ATI cells are generally unable to proliferate¹⁵ which leads to one of the two primary functions of ATII cells. ATII cells are responsible for mediating all primary replenishment of injured or dead alveolar epithelial cells. When either ATI or ATII cells die and are sloughed off they leave a nude section of the basement membrane. When this occurs resident ATII cells divide and repopulate the area. They then either remain as ATII cells or transdifferentiate into an ATI cells depending on which cell type they are replacing¹⁵.

The second primary function of ATII cells is to synthesize surfactant, store it in vesicles called lamellar bodies, and secrete it as needed into the alveolus. Surfactant serves the important job of decreasing the surface tension on the inside of the alveoli.¹⁹ The insides of the alveoli are coated with water, the molecules of which form hydrogen bonds with one another. Below the surface water molecules are surrounded on all sides by other molecules so the forces are in equilibrium. However, at the air liquid interface the forces are unbalanced which causes surface molecules to attach more strongly to each other than to the air. This gives rise to a surface tension the result of which is that the water molecules on the interior of the alveoli are highly attracted to each other. This has the effect of creating a contractile force which both attempts to collapse the alveoli and makes it more difficult to open them (figure 5). The surfactant produced by the ATII cells counteracts this surface tension by laying on the surface of the water and interrupting the hydrogen bonds^{7,15,20}.

Law of LaPlace:
 Magnitude of inward-directed pressure (P) in a bubble (alveolus) = $\frac{2 \times \text{Surface tension } (T)}{\text{Radius } (r) \text{ of bubble (alveolus)}}$

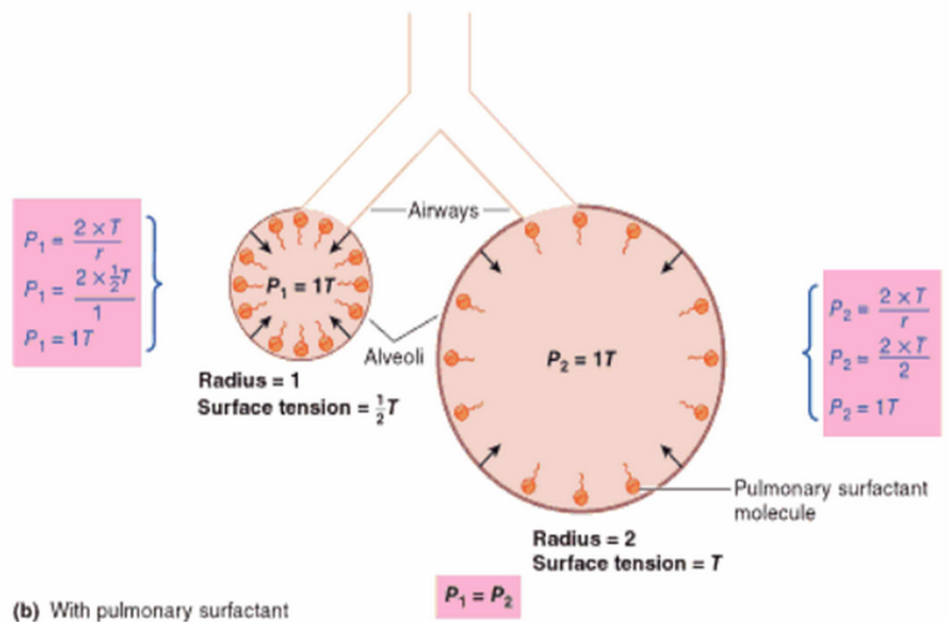
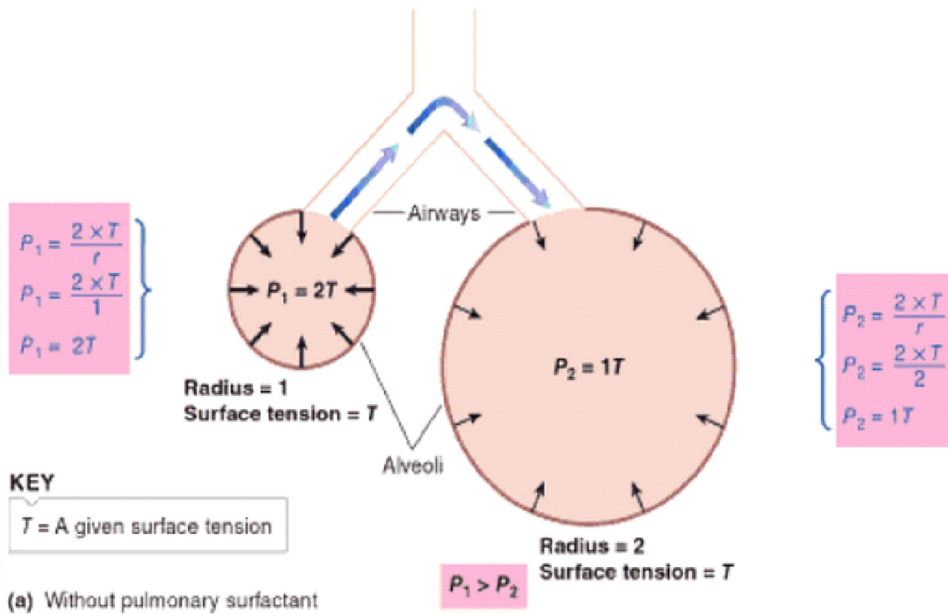


Figure 5: Diagram of the alveolar mechanics **A.** without surfactant and **B.** with surfactant. Reprinted from Sherwood et al¹⁷.

This decrease in surface tension aids in normal lung function in two important ways. Firstly the strength of the surface tension of the water inside the alveoli without

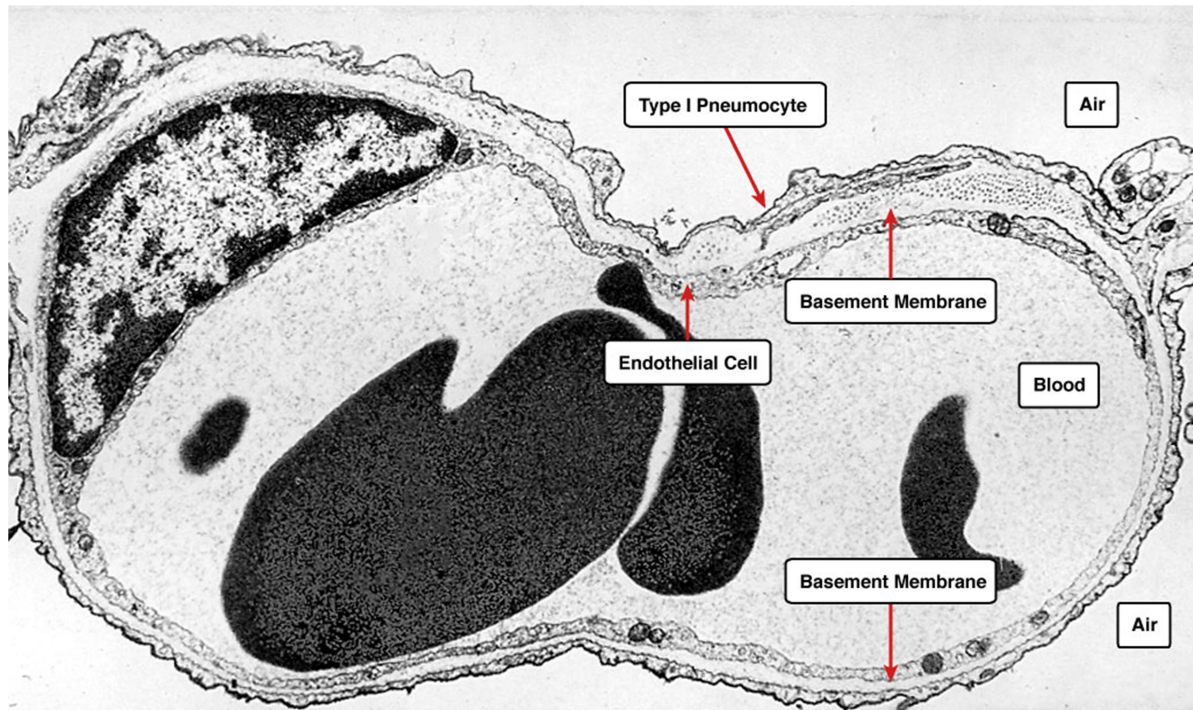
any surfactant present would be such that unassisted inflation of the lungs would not be possible. The Second important function of the surfactant is to stabilize the air flow between neighboring alveoli. According to the law of Laplace the collapse pressure on a sphere is inversely proportional to its radius (figure 5A). This means that the pressure needed to collapse a smaller alveolus is much less than the pressure required to collapse a larger one. And since the alveoli collaterally linked through several openings, this means that normally if one alveolus were less inflated than a neighbor to which it was attached, all of the air would naturally flow out of the smaller alveolus into the larger one and the smaller alveolus would totally collapse^{1,17}

The reason why this does not in general happen is because the surfactant decreases the surface tension more on the less inflated alveoli than on the more inflated ones. This is simply a result of the fact that the smaller alveolus has the same amount of surfactant as the larger alveolus but a smaller interior surface over which the surfactant is spread (figure 5B). And with a more surfactant units per area on the surface, the surface tension of the alveolus is more completely disrupted. The net result is that that the collapsing pressure for the alveoli is essentially independent of their inflation which means that they are stabilized with regards to one another^{2,17}.

1.1.4 Alveolar Basal Membrane, ECM, and MACs

Directly beneath the ATI and ATII cells both on the interior and exterior of the alveoli is the alveolar basement membrane. Inside of the basement membrane is an interstitial space. Contained in this interstitial space are several very important cell types and structures. Of primary importance are the abundant capillaries that fill this space.

These capillaries have an outer covering that consists of a thin basement membrane. Directly inside of this basement membrane is a single cell thick endothelial layer of squamous cells which create the capillary wall. Inside of these capillaries are a



constant flow of erythrocytes and plasma¹⁸

Figure 6: Alveolar epithelial barrier histology. Reprinted from Kerr et al⁸.

As the alveoli are ventilated oxygen passes from the open space of the alveolar sac into the alveolar septa then through the ATI cells then through the alveolar basement membrane. Once inside the septal wall the oxygen passes through the interstitia, then through the capillary basement membrane, then through the outer membrane of the endothelial cells, then through the cytoplasm, then through the inner membrane into the plasma of the capillary and finally into the erythrocytes themselves. And carbon dioxide traverses the same path in the opposite direction^{5,21}. Because the

gas exchange that takes place during respiration is passive it is extremely important that the distance that the gasses traverse be as short as possible (figure 6).

There are several physiological adaptations of the capillary endothelia that help to facilitate this. The endothelial cells have fewer organelles than other similar endothelial cells which allow the capillary wall to be stretched particularly thin across certain areas. Those organelles that they do have are gathered closely to the nucleus which is itself usually organized axially with the septal wall and or towards the junctions between ATI cells. This means that while the cells are thick in the regions around the nucleus they are able to remain very thin for most of their surface that is oriented towards the ATI cells of the alveolar septa. This thin region of the endothelium that lies parallel with the alveolar septa is additionally thinned by the fusing of the outer endothelial membrane with the capillary basement membrane. The result is that on the face of the endothelium oriented towards the alveolar septa the entire capillary endothelium is composed of two thin membranes with a tiny amount of intercalated cytoplasm that's width totals only 20nm. At some places the entire barrier between the alveolar air and the blood stream is only 200nm (figure 7).

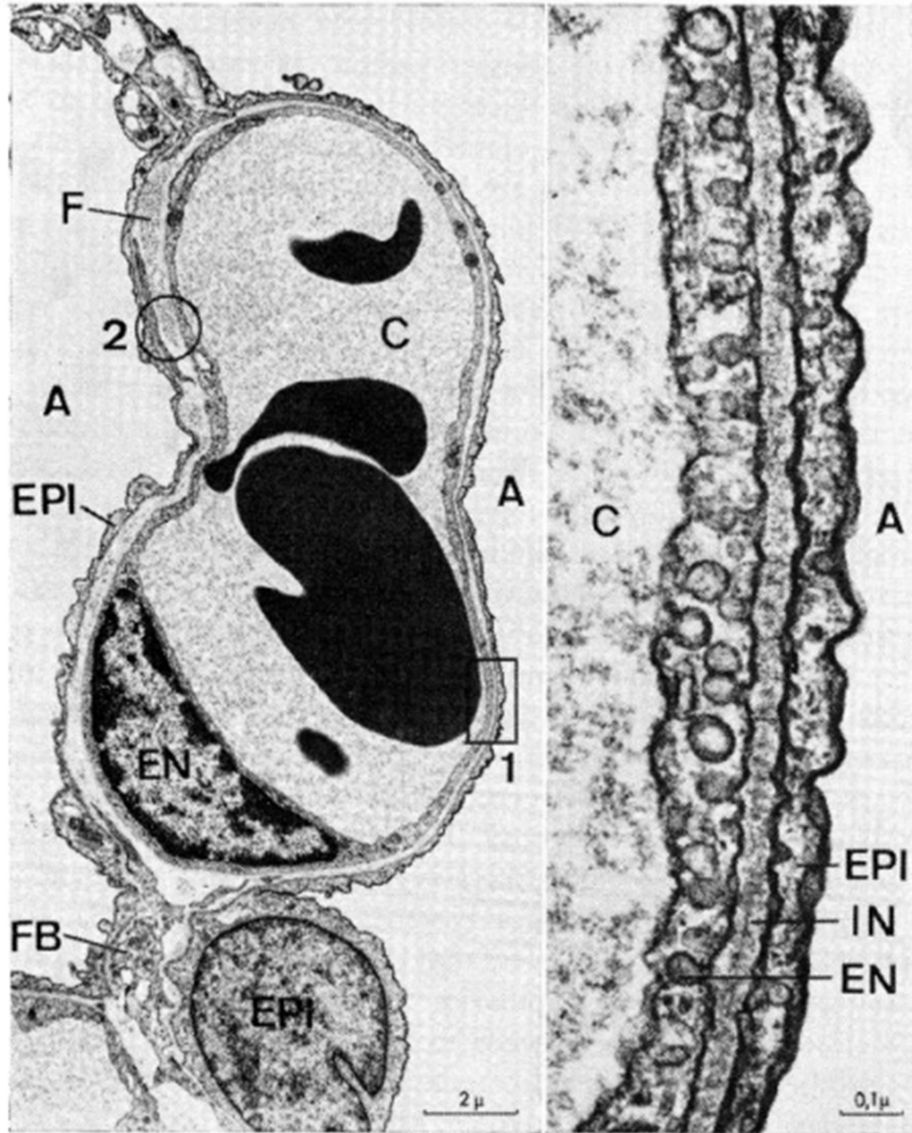


Figure 7: (left) Alveolar capillary lined by endothelial cell. (right) Two cell air blood alveolar barrier. Reprinted from Wiebel et al¹⁸.

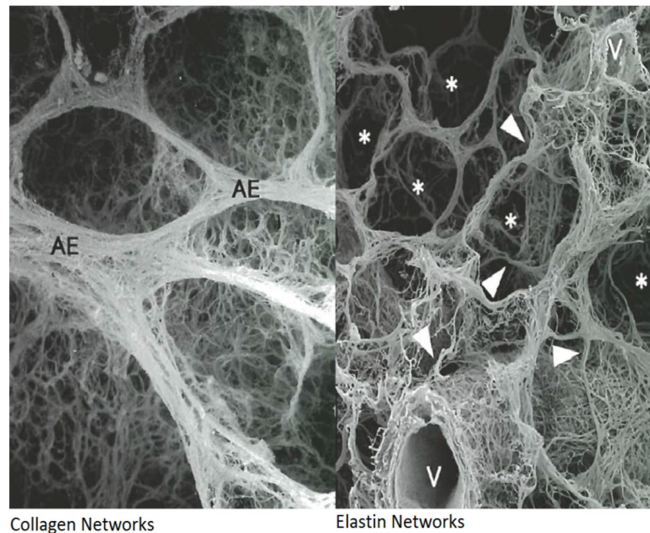


Figure 8: Collagen and Elastin fiber networks surrounding alveolar epithelium. Reprinted from Toshima et al²⁰.

Additionally in this interstitial space there are fibroblasts that manufacture collagen and elastin fibers. These fibers form bundles that create a collagen and elastin network that extend from the large airways down to the alveoli and make up the basis for the physical structure of the septal walls and the lung parenchyma itself (figure 8). These fibers form dense rings around the alveolar entrances and in the case of elastin they are interconnected with the elastin networks of the blood vessels. These fiber networks are responsible for a major component of the lungs mechanical behavior which we will discuss shortly^{5-7,21}.

Finally, patrolling the interior space of the alveolar septa are alveolar macrophages that migrate around and phagocytose cellular debris, foreign cells, and other harmful pathogens (figure 9). Collectively the lung parenchyma are comprised of the bronchioles, bronchi, blood vessels, alveolar ducts, alveolar sacs, individual alveoli, and interstitial cells and structures^{7,22}

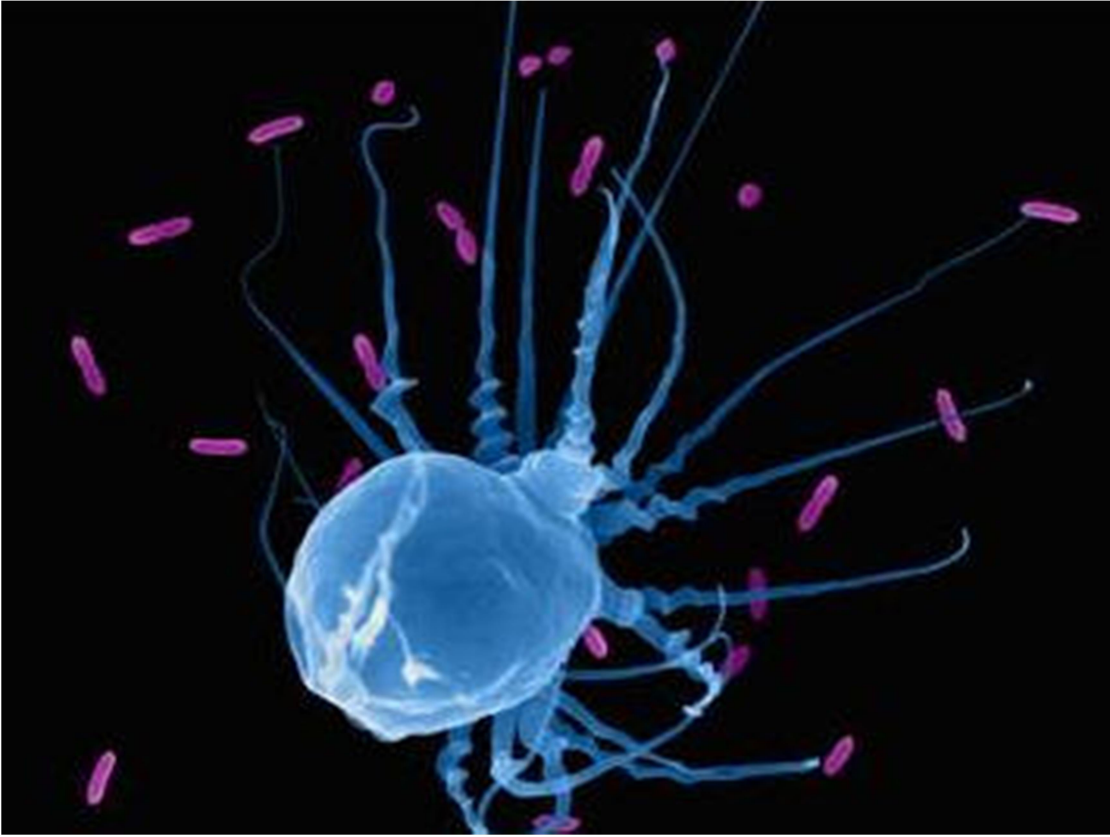


Figure 9: Alveolar Macrophage Attacking E Coli Bacteria. Image copyright Dennis Kunkel Microscopy, Inc²³.

1.2 Pulmonary Mechanics

Normal respiration requires that the respiratory zone be continually ventilated, a process consisting of cycles of the inspiration and subsequent expiration of air. The body achieves ventilation of the respiratory zone by physically changing the dimensions thoracic cavity in which the lungs reside. The cavity itself is bounded by on the top and sides by the thoracic wall by the and by the diaphragm on the bottom. The thoracic wall is comprised of a layer of interior and exterior intercostal muscles imbedded into which are the ribs. The diaphragm is a thin musculotendinous dome shaped structure that separates the thoracic and abdominal cavities^{7,24}

Immediately surrounding the lungs is a serous membrane called the visceral pleura. Opposed to it and lining the interior of thoracic wall and diaphragm is another serous membrane called the parietal pleura. There is a thin fluid filled region in between them called the interpleural space. Systemic circulation provides the parietal pleura with high-pressure blood which causes it to constantly secrete fluid into this space while the visceral pleura is constantly reabsorbing fluid from the space. The interpleural space is of extreme importance to the normal function of the lungs because in addition to providing lubrication for the movement of the lungs in the thoracic cavity, the fluid provides an airtight seal that causes the two membranes to adhere to one another. This means that any increasing volume of the thoracic cavity itself also increases the volume of the lungs and therefore increases the volume of the respiratory tract. This decreases the internal air pressure of the respiratory tract which in turn creates an inspiration of air. A subsequent decrease in the volume of the thoracic cavity increases the pressure in respiratory tract and expires the air¹.

Additionally the interpleural space is important because of the recoil pressure it applies to the lungs. As we will discuss in more detail later, the elastic nature of the lungs causes them to have a constant recoil pressure. Normally this would cause them to collapse, however since the interpleural space is air tight the recoil pressure of the lungs sets up a negative pressure in the interpleural space which balances the recoil pressure of the lungs and keeps them from collapsing. Because of this, any puncture to the interpleural space that allows air to enter results in the collapse of one or both lungs.

The expansion of the thoracic cavity is achieved by the contraction of the respiratory muscles. During normal or 'quiet' breathing the principle muscle responsible for the expansion of the thoracic wall is the diaphragm with some help from the exterior intercostal muscles. During quiet breathing the diaphragm contracts and distends 1-2 cm downwards and the thoracic cavity is expanded while the contents of the abdominal cavity are compressed. In more forceful breathing the expansion of the thoracic wall benefits from an increased contribution from a large group of accessory muscles distributed across in the thoracic, back, neck and abdomen. Additionally during maximal breathing the diaphragm can distend up to 10 cm^{7,24}.

During cycles of normal ventilation the expiration ends while the airways still have a positive volume in order to prevent the collapse of the alveolar sacs. We will discuss the importance of not collapsing the alveoli momentarily. During a normal maximal inspiration the lungs volume increases approximately fourfold compared to its end expiratory minimum. This means that the dimensions of the lung are expanding by roughly a factor of $4^{1/3} = 1.6$. Most of this expansion occurs in the alveoli and alveolar ducts and is isotropic due to surface properties of the liquid on the alveoli and their collateral airflow²⁴.

During inspiration the parenchymal fibers go from being crimped to being straightened out (figure 10). Additionally the septal walls begin the inspiration containing undulations or "crumples" which get smoothed out as the alveoli begin to inflate. Because these fibers contain elastin, when they are stretched much of the energy used to stretch them is converted to mechanical potential energy instead of

being converted to heat. This stored energy means that when lung tissue is expanded it develops contractile force. This contractile force and the one created by the alveolar surface tension combine to create the lung's elastic recoil^{21,24}.

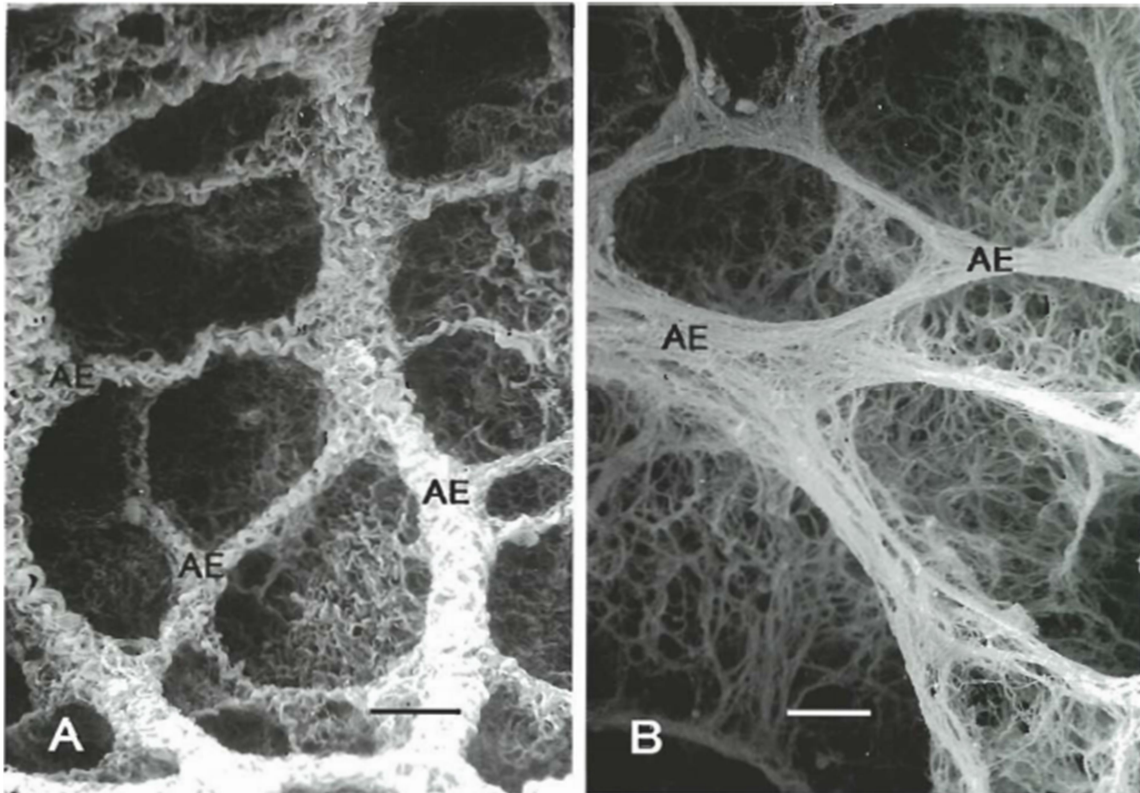


Figure 10: (left) Crumpled lung collagen ECM. (right) Inflated lung collagen ECM. Reprinted from Toshima et al²⁰.

The elastic properties of lung tissue are generally referred to as compliance and are written as $C = \Delta V / \Delta P$ where ΔV and ΔP are change in lung volume and lung pressure respectively. This equation means that compliance is defined as the reciprocal of elasticity. Therefore to better understand the mechanical properties of the lungs it is important to determine the compliance of both healthy and diseased lungs at all of the pressures and volumes experienced during ventilation. This is generally done

by ventilating a lung and measuring the pressure at the airway opening. However, in order to use our equation, we must modify it to account for two additional important mechanical factors. Firstly, our equation must reflect the work that the lung does on the air as it circulates. Secondly, the thoracic wall to which the lung is attached has elastic properties of its own which means that the recoil pressure it generates must be included in our equation as well. When considering these effects if we assume that the lungs have one degree of freedom (isotropic expansion) then the equations of motion become²⁵:

$$P_{AO} = V/C + V'R + V''I - P_{tho}$$

Where P_{AO} is the pressure at the airway opening, P_{tor} is the pressure generated thoracic walls elastic recoil, V is lung volume, V' is gas flow, R is airway resistance, V'' is convective gas acceleration, I is impedance, and C is the previously mentioned compliance.

From this equation we can clearly see the advantages of examining the compliance of the lung using a model in which the lung is not in motion while measurements are being taken (static pressure-volume analysis). Additionally because of the effect of the pressure exerted by the chest wall there is also merit to examination of a lung that has been excised from the thoracic cavity. Furthermore as previously discussed both the collagen and elastin fibers and the surface tension of the alveoli contribute to the lungs elastic recoil. Since the surface tension of the alveoli are dependent on their having an air liquid interface the effect of the alveolar surface

tension could be effectively removed by using an experimental model in which the lungs as ventilated with liquid instead of air. This allows the recoil forces of the lung parenchyma to be studied independently. Figure 11 contains the pressure volume loops of an excised cat lung ventilated with both air and saline.

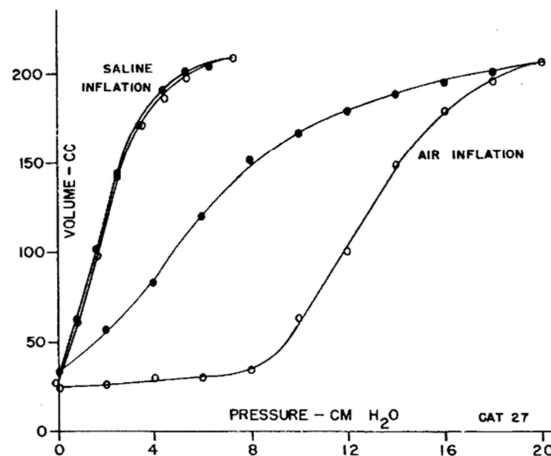


Figure 11: Pressure volume loops obtained from cat lung submerged in saline. Reprinted from Harris et al²⁵

Figure 11 contains two very important features. The first is that the recoil pressures are greater at every volume in the air filled lung than in the saline filled lung. This means that the surface tension of the alveoli have a substantial effect on the amount of force needed to inflate the lungs. One obvious implication of this effect is that liquid ventilation can achieve inspiration and expiration of the lung with the application of lower pulmonary pressure than conventional gas ventilation^{24,25}.

The second important feature of the graph is that there is a much greater separation between the inflation and deflation limbs of the air filled lung than the saline filled lung. At any given volume the air filled lung has a much greater recoil pressure

during its inflation that its deflation. Because the graph is of pressure versus displacement the difference in the two graphs represents the hysteresis of the lungs during ventilation. Therefore this graph demonstrates that the majority of the hysteresis of the lungs during ventilation is due to the surface tension of the alveoli^{7,24,25}.

While giving us information about the role of alveolar surface tension, this model fails to investigate the relationship of the elastic recoil of the thoracic wall and that of the lungs. In order to do investigate this we must first create an equation that relates the compliance of the lungs and that of the thoracic wall independently and in combination. If we treat the thoracic wall and the lungs like two elements in series the equation for the compliance of the combined system is equal to the sum of the reciprocal of the two elements individually or:

$$1/C_{RS} = 1/C_L + 1/C_{TW}$$

Where C_{TW} is the compliance of the thoracic wall, C_L is the compliance of the lungs, and C_{RS} is the compliance of the combined respiratory system. C_L and C_{TW} can then be calculated independently. At pressures controlled through mechanical ventilation the changes in the volume of the wall can be directly observed as the distention of the diaphragm is inferred from of the movement of the abdomen.

When the C_L , the C_{TW} , and the resultant C_{RS} values are measured, calculated, and graphed respectively for an adult human we get the graph in figure 12 as a result. TLC is total lung capacity, FRC is function reserve volume (the volume of air remaining

in the lungs after normal exhalation) and RV is residual volume(the volume of air in the lungs after maximal exhalation)^{7,24,25}.

The graph in figure 12 has several important features. Firstly when we look at the graph of the lung compliance we see that at its minimum volume its pressure and volume never go to zero. Additionally as its volume increases its compliance has a relatively linear region then drops off sharply. This is the type of behavior we would expect to see in biological tissue whose elastic properties come from elastin and collagen fibers since we know that they have a tendency to behave in a linearly elastic fashion until they are fully stretched out then have a sharp drop off in compliance. Secondly when we observe the thoracic wall graph we see that it has no elastic recoil pressure when its volume is equal to around 4L (figure 12). When its volume is less than 4L it has a negative recoil pressure which means it attempts to expand. Additionally because the thoracic wall's compliance decreases with decreasing volume, the amount of pressure needed to continue to decrease its volume continues to increase. When we analyze the combined graph we soon see why this is important.

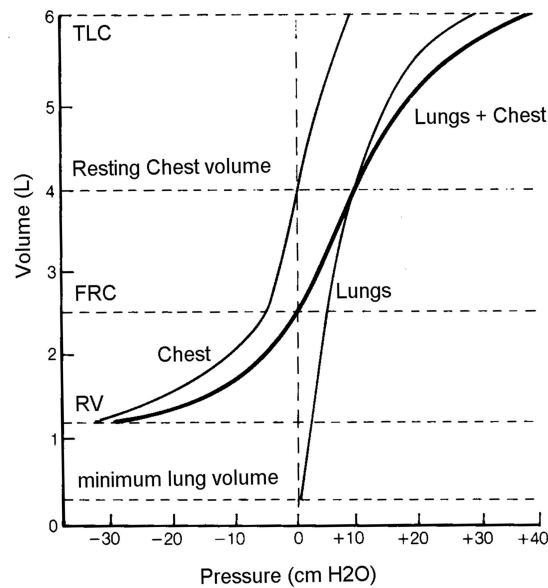


Figure 12: PV graph of combined chest and lung wall mechanics. Reprinted from Harris et al²⁵

The net effect of the combination of the two graphs is that at low volumes the negative elastic recoil pressure of the thoracic cavity dominates the compliance of the system. This is beneficial because for all volumes lower than the FRC the recoil pressure on the lungs attempts to inflate them. This means that inflating the lungs from any volume below the FRC to the FRC takes no energy which helps to maintain the residual lung volume needed to prevent the alveoli from collapsing. And at larger volumes the elastic recoil of the lungs dominates the system which is beneficial because it both allows the mechanical energy of inspiration to be stored physically in the arrangement of the fibers so that expiration requires less energy, and it prevents the over inflation of the lungs and alveoli^{7,24,25}.

In order to determine if there are any other mechanical benefits to the function of the lungs during respiration contributed by the elastic properties of the lungs we can observe the pressure-volume graphs for experiments in which the lungs are made to

inflate at pressures below the FRC. In this experiment cats were ventilated using a negative pressure ventilators beginning at pressures both above and below their FRC (figure 13). The most important features of this graph are that while the pressure-volume curve for the expirations seems to be independent of the starting volume, the curve of the inspiration is shifted downwards when the lungs are inflated from below the FRC. This means that it requires more energy and more energy is lost when the lungs inspiration begins below the FRC.

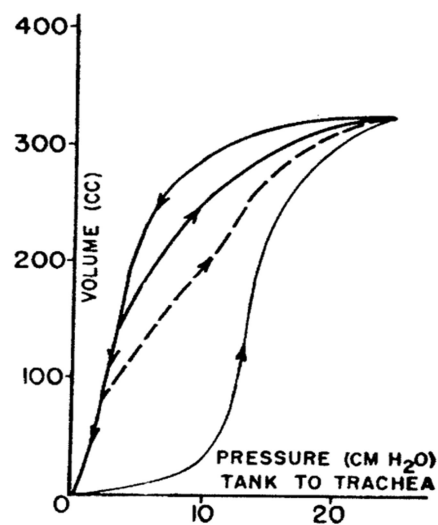


Figure 13: Graph of lung inflation below FRC. Reprinted from Harris et al²⁵.

We can also note that this graph (figure 13) has a much lower hysteresis than the one we observed previously in the air ventilated cat lung. This seeming disagreement can be resolved by replicating this experiment with an excised lung^{7,24,25}.

Here we see a similar set of pressure-volume curves when the initial volume for this extracted of lung is close FRC for the intact lung. However, we see that if we allow the lungs initial volume to go to zero and the lungs and alveoli to completely collapse we get a graph that matches our first experimental graph of the excised cat lung. From this

was can clearly see that the amount of energy lost to hysteresis when the lungs are allowed to fully collapse is significantly larger than the amount of energy lost to during normal ventilation²⁵.

1.3.0 Ventilator Induced Lung Injury and Pulmonary Edema

Many pathophysiological states can result in a person's inability to adequately ventilate their lungs with spontaneous breathing which makes mechanical ventilation a necessary and potentially lifesaving clinical intervention. These pathological states include Acute Lung Injury (ALI), Acute Respiratory Distress Syndrome (ARDS), Pneumonia, Asthma, and Chronic Obstructive Pulmonary Disease (COPD)²⁶⁻²⁸. It is estimated that annually there are 800 thousand hospitalizations in the United States requiring mechanical ventilation with an estimated in-hospital mortality rate of 34.5%. This represents 2.7 episodes of mechanical ventilation and .9 deaths per 1000 individuals in the U.S. This means that pathological conditions requiring mechanical ventilation lead to more deaths annually than breast cancer and prostate cancer combined. The national costs of mechanical ventilation are estimated at \$27 billion dollars per year and account for 12% of all hospital costs in the United States²⁹.

1.3.1 Impact of VILI

Despite its necessity as a potentially life-saving clinical intervention, mechanical ventilation (MV) can result in ventilator induced lung injury (VILI). The three proposed mechanisms of VILI are over-distention of the alveoli (volutrauma), cyclic recruitment

and derecruitment of the alveoli (atelectatrauma), and secondary injury caused by the stretch or injury-induced release of inflammatory cytokines (biotrauma) ^{27,30}(figure 14).

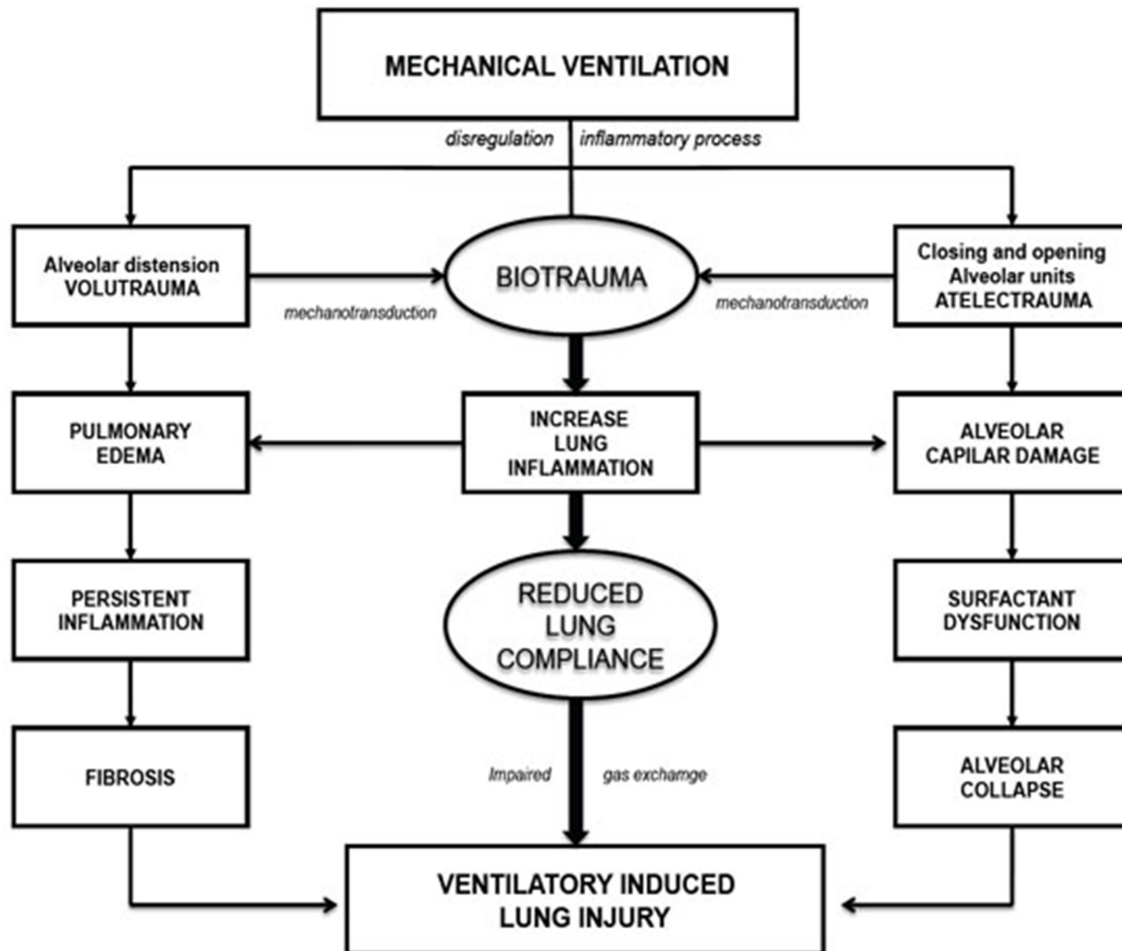


Figure 14: Flow chart of the mechanisms of VILI. Reprinted from Carrasco et al³¹

The largest population of patients requiring MV is the elderly²⁹, and age is a known predictor for the severity of VILI³². As people age the chest wall becomes less compliant, the lung parenchyma loses elasticity, the average alveolar diameter increases, and overall lung capacity diminishes ^{10,33}. Additionally over time the lungs capacity to recover from injury diminishes and its inflammatory responses increase³⁴.

These physiological changes in the aging lung correlate to each of the proposed mechanisms of VILI. Accordingly age is a predictive factor in the severity of VILI; however, the exact relationship between age and the severity of VILI is currently unknown. The increase in the severity of VILI with patient age combined with the increased need for ventilation and mortality rate among the elderly makes the investigation of this relationship even more important.

A consistent feature in all of the proposed mechanisms of injury is that they occur at the level of the alveoli²⁷ (figure 15). This would seem to suggest that there is a meaningful substantive difference between the physiological and mechanical behaviors of healthy lung alveoli under spontaneous breathing and in alveoli being injuriously mechanically ventilated. It would also seem to suggest that there are age related changes in these physiological and mechanical behaviors that play an important role in the severity of VILI.

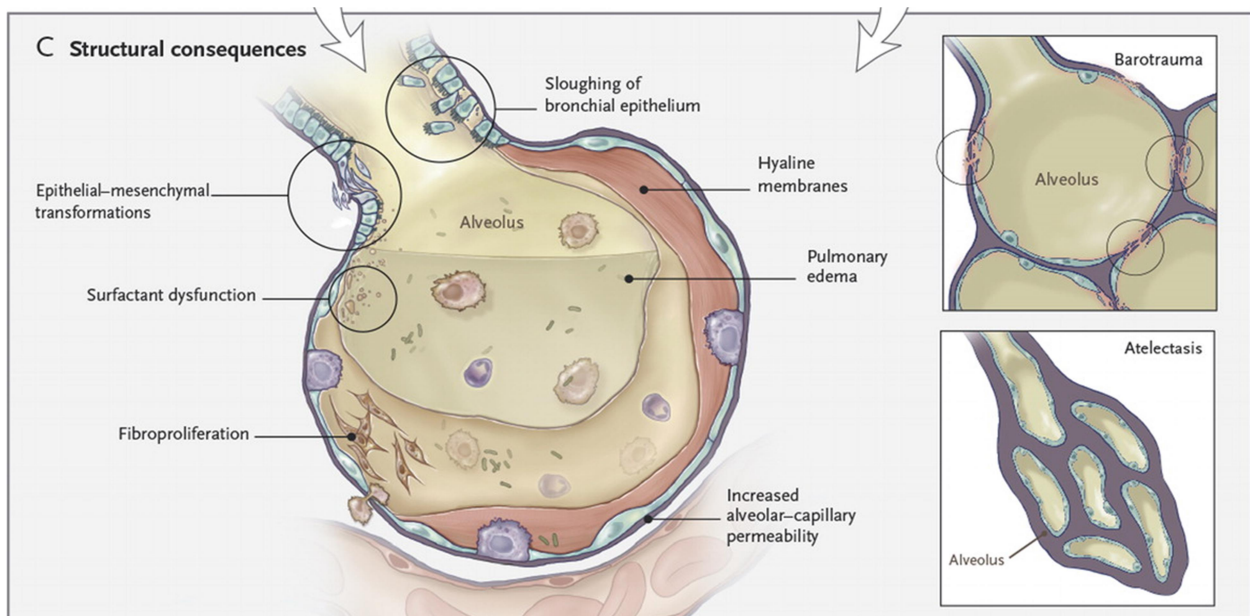


Figure 15: Diagram of the alveolar mechanisms of VILI. Reprinted from Reynaud et al³⁰

1.3.2 Biotrauma

Both through mechanotransduction and cell/tissue injury, MV has been shown to up-regulate the production and excretion of inflammatory cytokines in the lung, which in turn can further aggravate lung injury. Stress failure of the alveolar barrier (decompartmentalisation) and stress failure of the plasma membrane (necrosis) have been shown to release cytokines into the lung as well as into systemic circulation ³⁵. Mechanotransduction is also sufficient to cause the release of cytokines into the lung. In one study, Broncho alveolar lavage fluid (BALF) concentrations of TNF- α and interleukin (IL) 6 were elevated in infants without prior lung injury who were treated with MV for whom no clinically obvious harmful effects of MV were observed ³⁶.

In addition to the release of cytokines, biotrauma is an upstream regulator for the recruitment and extravasation of leucocytes in the lung^{37,38}. The biotrauma associated with adult acute lung injury and neonatal chronic lung disease has also been shown to delay leucocyte apoptosis^{39,40} and cause apoptosis of pulmonary epithelial cells.

Not surprisingly the immune and inflammatory response by to injurious mechanics stretch is not localized to the lungs⁴¹. The majority of patients who die from acute respiratory distress (ARDS) die from multiple organ dysfunction syndrome (MODS)⁴¹. Concentration differences across the lung (difference between arterial and mixed venous) of inflammatory mediators have been detected in patients with ALI with ARDS^{42,43}, indicating a significant release of these pro-inflammatory molecules by lung tissue. In one study, rabbits treated with injurious MV showed significantly increased renal apoptosis, renal dysfunction, and small intestine apoptosis compared to rabbits

receiving a protective ventilation strategy⁴⁴. An ARDS network study has also shown that after three days with either high or low tidal volume MVs, patients with low tidal volumes have lower serum level of IL-6, increased organ failure-free days, and lower mortality than those with high tidal volume ventilation^{45,46}. Understanding the mechanisms of VILI-associated biotrauma could prove critical for increasing survival in ventilated patients.

A direct investigation of the effect that age has on the lungs immune and inflammatory response to mechanical stretch and ventilation can be accomplished in a relatively straightforward manner using scientific methods currently in use. The alveolar epithelial cells of young and elderly mice can be harvested, grown in culture, and exposed to cyclic mechanical stretch^{40,47}. Those cells can then be assayed for cell damage/survival/proliferation, their media can be assayed for the presence of inflammatory cytokines and total protein, and their proinflammatory gene expression can be measured using QPCR. Likewise young and elderly mice can be mechanically ventilated; the mechanical properties of their airways as a whole can be measured, their airways can be lavaged with saline to collect and measure inflammatory mediators and their lungs can be fixed and analyzed with histology/microscopy. These are all methods of analysis that we employed our study to measure and quantify the effect of how aging affect the lung and how this in turn affects the severity of VILI.

1.3.3 Pulmonary Edema

In the human body, the existence of interstitial colloidal osmotic pressure and capillary filtration pressure causes the filtration of about 20 liters of water out of the blood stream

into the surrounding tissues per day. This creates a need for an opposing gradient in order to prevent the accumulation of filtered water in these tissues (edema). In the absence of pathological conditions, these gradients roughly balance one another with approximately 17 liters of water being filtrated directly back into the circulatory system and the remaining 3 liters being taken up by the lymphatic system and then returned to circulation⁴⁸.

This balance is of particular importance in the distal lung because pulmonary gas exchange occurs at the air liquid interface of the alveoli and thus maintenance of this interface critical for normal lung function. Not surprisingly the accumulation of water in the lung alveoli (pulmonary alveolar edema) can lead to dramatic dysfunction of pulmonary gas exchange and is potentially fatal^{9,48}.

Both increases in vascular pressure, increases in alveolar vascular permeability, and increases in alveolar epithelial barrier permeability have been demonstrated to drive pulmonary edema. Additionally each of these forms of dysfunction are known to exist in various pathological lung conditions including acute respiratory distress syndrome (ARDS) and ventilator induced lung injury (VILI)⁴⁹.

1.3.4 Alveolar Fluid Clearance

In the healthy lung, the mechanism for the clearance of alveolar edema is primarily linked to that the transportation of sodium and chloride ions out of the alveolus into the alveolar capillaries and surrounding interstitial space. This creates an osmotic pressure gradient which drives alveolar fluid clearance into the bloodstream, pleural space, and lymphatic system. Both alveolar epithelial ATI and ATII cells (ATIs, ATIIIs) contain

sodium/potassium ATPase pumps (Na/K-ATPase). In addition ATI cells contain the epithelial sodium channel (ENaC), the nonselective cation channels (NCC), the cyclic nucleotide-gated channels (CNG), and other selective cation channels (SCC). Chloride ions are able to pass through alveolar epithelium through either a trans or paracellular route^{48,50}.

The gradient that is caused by sodium transport causes water to be transported by both aquaporin (AQP) 1, and 5, and through paracellular pathways. However, the exact breakdown of how this happens is not immediately clear. There is experimental evidence that in young rats that have AQP-1 and 2 knockout out, both separately and together, that there is no significant inhibition of alveolar edema clearance. However, it has also been demonstrated that the experimentally induced up regulation of the expression of AQPs that were down regulated by age restores age related losses in pulmonary edema clearance function in aged mice⁵⁰⁻⁵².

1.3.5 VILI-Associated Edema

Edema is a hallmark complication of VILI and acts through several distinct pathways. VILI has been shown to increase lung microvascular pressure and transmural pressure and to drive water filtration into the alveolus. Mechanical ventilation (MV) has also been shown to inactivate surfactant within the alveolus. This increases alveolar surface tension which in turn has been shown to increase filtration from the microvasculature into the alveolus^{52,53}.

All of these effects however contribute insufficiently to pulmonary edema to account for the pathophysiological state caused by MV. Instead it is a VILI induced

increased in the alveolar epithelial barrier permeability that accounts for the majority of the observed edema. It is known that VILI-associated volutrauma can strongly promote pulmonary edema. In one study, during static inflation of sheep lungs the equivalent pore radius of the alveolar epithelial barrier (an indicator of barrier permeability) increase from 1 to 5 nm. This fivefold increase was sufficient to allow albumin to diffuse freely across the barrier, indicating a major compromise to barrier integrity. This increased permeability persisted or even increased after the cessation of inflation, confirming that epithelial barrier damage and not vascular pressure were driving this increase in permeability⁵².

Additionally, multiple animal models have also shown that when MV with high peak pressures causes pulmonary edema, histological analysis inevitably reveals stress failure of the alveolar barrier (decompartmentalisation), stress failure of the plasma membrane (necrosis), visible denuding of the epithelial basement membrane, and gaps in the capillary epithelium^{50,52,53}.

In addition to primary lung injury sustained through volutrauma, secondary injury to the lungs and systemic organs systems through the release of inflammatory cytokines (biotrauma) is another major mechanism in the pathogenic process of VILI. Inflammatory cytokines are known to have a profound effect on epithelial barrier integrity. TNF-alpha and IL-1, 6, and 8 are all known to increase the leakiness of tight junctions, and are all associated with VILI Induced biotrauma⁵⁴. In this way, VILI is able to contribute to edema through both direct insult to the alveolar barrier integrity, and through the release of inflammatory cytokines which further compromise membrane permeability^{41,53}.

1.3.6 Age, Edema, and VILI

Increased age is known to increase the severity of both VILI and edema separately. The changing mechanical properties of the aging lung lead to increases in lung compliance which increases the lung susceptibility to over-distention during MV^{27,29,41,55,56}. Additionally, the aging lung also exhibits an increasingly dysregulated immune/inflammatory response to injury which has a generally pro-inflammatory effect^{57,58}. It has been shown in rats that increased age leads to increased lung damage/inflammation and animal mortality in rats that are ventilated with high tidal volumes compared to young rats⁵⁹. This is in good agreement with the murine data we present in chapter two. It has also been shown that age is a predictive factor in the incidence and severity of pulmonary edema. Aging is known to decrease the expression of AQP 1 and 5 in the alveolar membrane of rats which leads to an increase in pulmonary edema⁶⁰. Additionally, our own data presented in chapter two demonstrate that elderly mice treated with injurious MV show both increases in pulmonary edema and decreases in 4 hour survival compared to similarly ventilated younger mice.

1.3.7 Fluid Support and Hemodynamics During MV

MV has a strong effect on a patient's hemodynamics. Overall, MV has a tendency to decrease blood pressure and cardiac output. In addition to strong insult to the cardiovascular system, prolonged dysfunction of the circulation is also extremely stressful on a patient's renal system. These MV related complications can prove to be

fatal to patients with already in compromised pathophysiological states^{49,61}. For this reason there is a general concern among clinicians regarding an attempt to normalize the hemodynamics of ventilator patients. Although the exact effects are still being debated, fluid support has been shown to increase the blood pressure and improve the overall hemodynamics in ventilated rats⁶¹. However, the same study showed that these rats, while having improved hemodynamics, displayed increases in edema and anemia. Additionally, in human ventilation patients it has been shown that conservative fluid management strategies decrease pulmonary edema.

These results may at first be somewhat surprising since it has been established ventilation induced pulmonary edema is caused primarily by decreases alveolar membrane permeability and not modified hemodynamics in the alveolus. Thus the impact of this and other studies that correlate high volume fluid-management with pulmonary edema is that once alveolar barrier permeability is compromised, only minor increases in intravascular pressure and drops in oncotic pressure are required to generate large edema. The molecular aspects that influence pulmonary edema, both upstream and downstream, are currently understudied. One key player in the mechanism may be stress in the endoplasmic reticulum.

1.4.0 ER Stress Background

Protein molecules are vital players in virtually every cellular process. However, their useful bioactivity is not an innate property imbued through their synthesis by the ribosomes alone. Instead each nascent polypeptide chain must go through a conformational change into its characteristic or 'native' 3 dimensional form in order to

have its full physiological functionality^{62,63}. Every part of the protein formation process that occurs after translation of the polypeptide chain by is known as protein folding. For proteins that are eventually to be secreted out of the cell or sorted to other organelles this folding takes place takes place in the cisternae of the Endoplasmic Reticulum (ER)³⁷.

The ER itself is a membrane enclosed organelle performing numerous cellular functions including lipid biosynthesis and calcium storage and sequestration. However, arguably the most important function of the ER is its role as the site of protein folding as the majority of its resident proteins are dedicated to this process⁶⁴. An N-terminal signal sequence on these proteins interacts with a signal recognition particle (SRP) which lead the RNA, Ribosome, polypeptide complex to the ER. Once docked, the sequence is translated directly into the luminal environment of the ER. The folding process itself may start as soon as the nascent polypeptide chain begins to enter the ER while the rest of the chain is still undergoing translation. Thus the N-terminus of the polypeptide chain may undergo folding while the while the C-terminal is still being synthesized^{64,65}.

The native states of almost all proteins correspond to the three dimensional conformation of their nascent polypeptide coil that are the most thermodynamically stable under physiological conditions⁶⁶. Therefore although one might imagine a linear set of consecutive folding steps that leads each protein from nascent to native, the protein instead meanders down an energy landscape (figure 16).

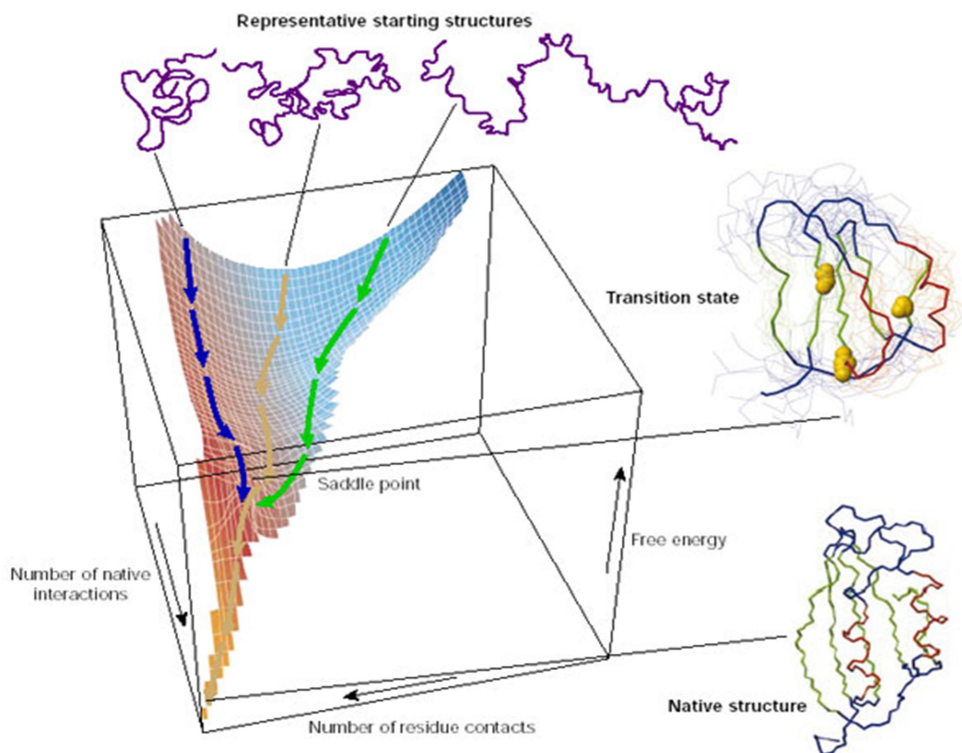


Figure 16: A schematic energy landscape for protein folding. Reprinted from Reynaud et al⁶⁷.

And although the potential paths are many, at each step the protein chooses a new conformation that further reduces its free energy until, if all goes well, it arrives at its native conformation. This means that ultimately it is the amino acid sequence itself that determines native conformation of each resultant protein⁶⁶.

However, because it is a stepwise process, it is a certainly the case that at intermediate stages of this process some regions that would normally be hidden inside the protein during its native conformation are exposed to the crowded milieu of the ER⁶⁸. This leaves intermediately folded proteins vulnerable and prone to inappropriate interactions with other molecules. In the case of exposed hydrophobic residues intermediate or misfolded proteins will have a strong tendency to aggregate together. In all as many as 30% of synthesized proteins never attain their fully native conformation⁶⁹.

All hope is not lost however. The cell has evolved a quality control system to bolster the success of this folding process. The folding process inside the ER is assisted at every stage by molecular chaperones and ER folding enzymes⁶⁵. Molecular chaperones are proteins that aid other proteins to attain their native conformation but are not part of the final protein structure. In the ER protein folding process the primary function of the molecular chaperones is to shield the hydrophobic binding sites of the intermediate or misfolded proteins. Different chaperones specialize in assisting at various different stages of the folding process. Some chaperones assist the nascent protein as they are being translocated into the ER while others aide the final conformation into native proteins. But in all cases along this continuum these chaperones effectively sequester the proteins and provide them with a privileged folding environment to prevent premature folding or aggregation. There are still other chaperones that have the ability to 'rescue' misfolded or aggregated proteins and allow them to attempt to refold properly^{66,70}(figure 17).

But for proteins who are hopelessly misfolded or aggregated there are multiple chaperones and folding sensors that have the ability to identify them. These proteins

are then transported outside of the cell and degraded. Because there are very few protein folding chaperones anywhere else in the body it is crucial that highly efficient quality control system be in place to prevent misfolded proteins from being packaged transported out of the ER⁷¹.

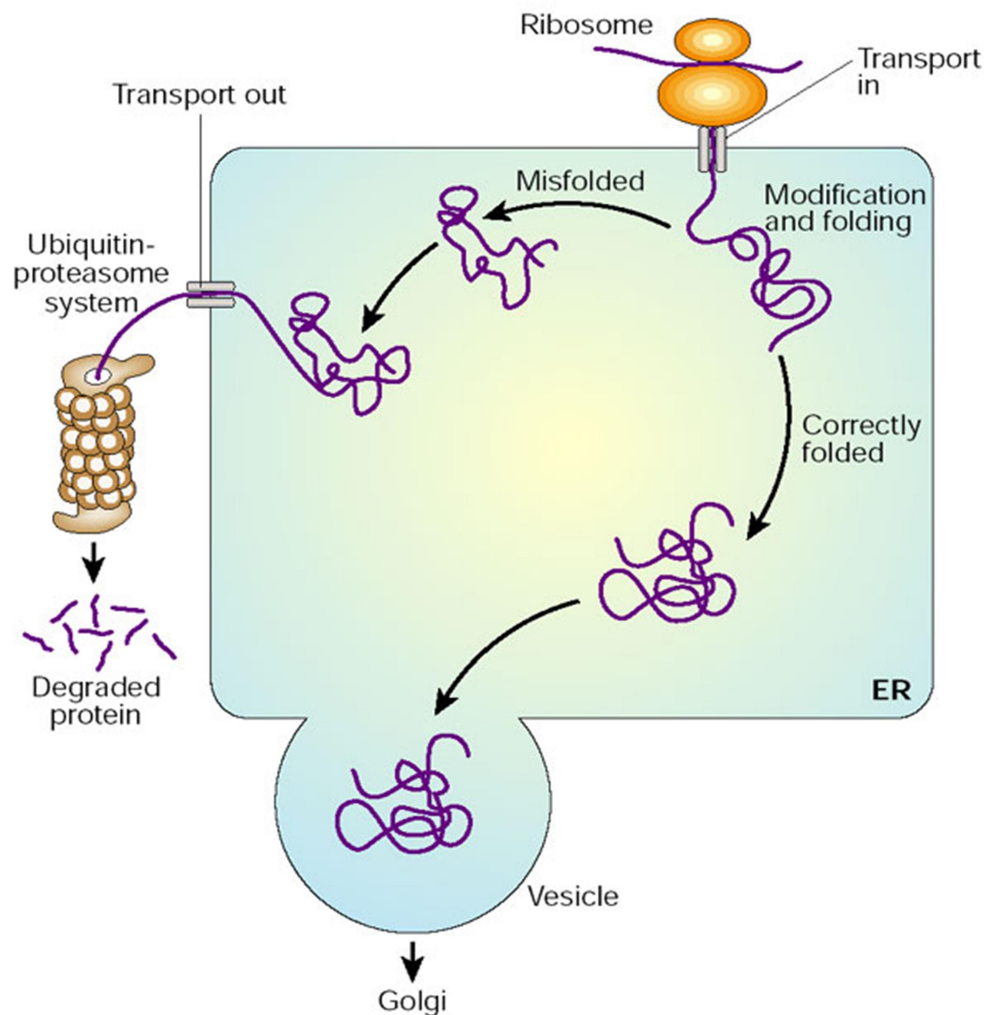


Figure 17: Regulation of protein folding in the ER. Reprinted from Reynaud et al⁶⁷

As the folding of the ER proteins is guided by the chemical forces acting on the polypeptide sequences, the maintenance of homeostasis of the ER environment is critical for this process. There are many pathophysiological conditions however that can

perturb this delicate balance including disruptions in calcium homeostasis, glucose/energy deprivation, redox changes, ischemia, hyperhomocystinemia, and viral infections and mutations. This impairment in folding can cause an increasing accumulation of unfolded and/or aggregated proteins known as ER Stress⁷².

The evolved response to ER Stress is known as the unfolded protein response (UPR) and consists primarily of three branches. The signaling of each branch is transduced across the ER membrane through a one of three transmembrane proteins: PKR like ER kinase (PERK), inositol requiring element-1 (IRE-1), and activating transcription factor 6 (ATF6). Each of these three proteins are held inactive by being bound to BiP, a peptide-dependent ATPase and member of the heat shock 70 protein family. However, when the unfolded/aggregated proteins begin to accumulate BiP dissociates from the three signaling molecules and they become active (figure 18)⁷³.

IRE1 dimerizes then auto-transphosphorylates. It then produces the mRNA which encodes unspliced x box-binding protein 1 (XBP1u) to produce active transcription factor spliced (XBP1s)⁷⁴. XBP1s which includes the transcription factors for several molecular chaperones including BiP and GRP94. XBP1s also encodes for the transcription of genes associated with ER-associated degradation (ERAD). The net effect is an increase in the available protein folding chaperones and an upregulation of the degradation of misfolded proteins.

PERK phosphorylates initiation factor eukaryotic translation initiator factor 2 α (eIF2 α) which inhibits general translation into the cell with the exception of BiP and ATF4 which are instead translated more efficiently⁷⁵. PERK also inhibits several transcription factors. This general decrease in the rate at which proteins are being

transcribed into the ER gives the protein folding apparatus extra time to try to clear the accumulation of misfolded proteins. PERK also upregulates Nrf2 which upregulates antioxidant response⁷⁶. This is of particular importance in understanding the therapeutic potential of VitC to attenuate ER stress. VitC is a powerful anti-inflammatory and antioxidant⁷⁷ both of which have the potential to strongly interact with the ER stress pathway.

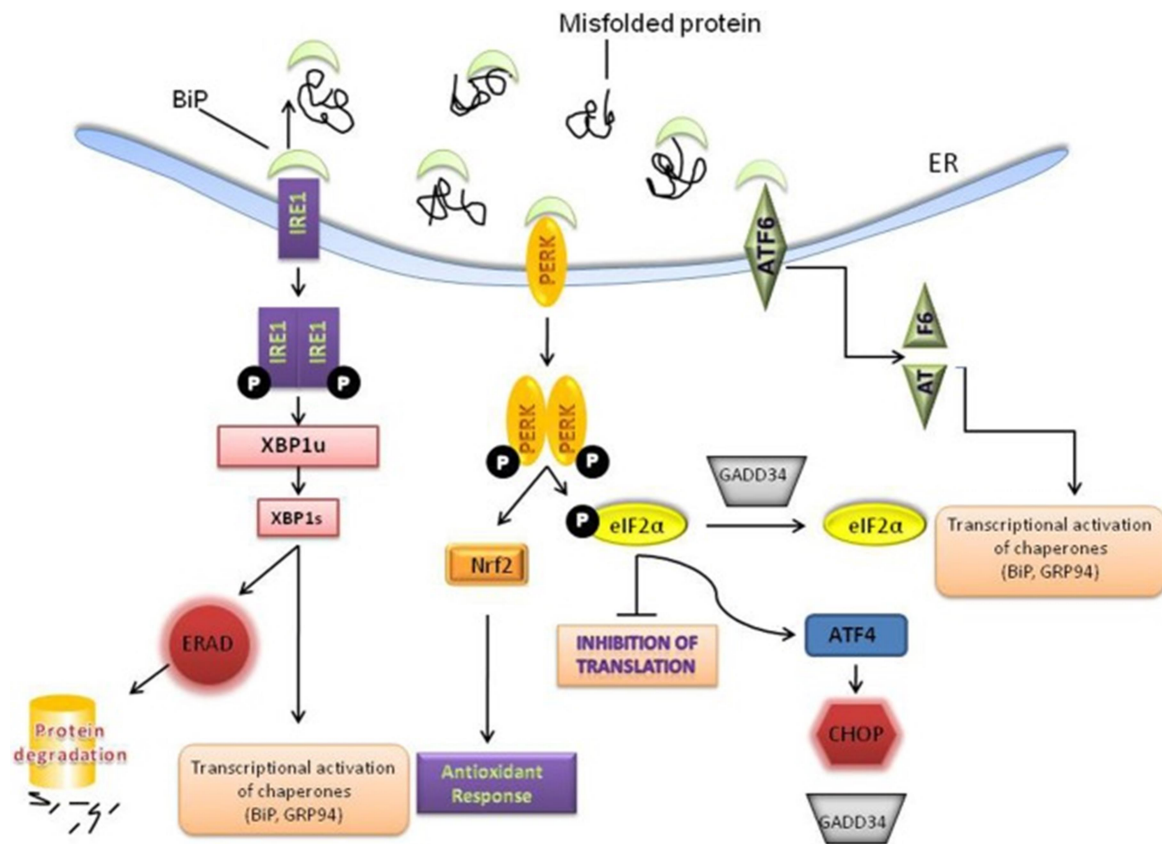


Figure 18: Diagram of ER Stress Pathway. Reprinted from Reynaud et al⁷²

ATF6 is localized in the ER membrane when the ER is unstressed. When cleaved from BiP ATF6 is transported to the golgi apparatus where it is cleaved. The cytosolic dominant fragment (ATF6f) upregulates expression of the gene encoding for

ERAD and XBP1⁷⁸. As discussed above the upregulation of these genes stimulates degradation of misfolded proteins.

If the ER stress continues unabated however it leads to pro-apoptotic signaling and cell death. The ER stress induced is mediated primarily through C/EBP homologous protein (CHOP) also known as growth arrest and DNA damage 153 (GADD 153) which downregulates the anti-apoptotic protein BCL-2, induces the expression of some BH3-only proteins and upregulates growth arrest and DNA damage-inducible 34 (GADD34)⁶⁵. CHOP is downstream of both the PERK and ATF6 pathways. The PERK induced eIF2 α in the presence of sustained ER stress will upregulate nuclear factor-kappaB (NF κ B) and ATF4. And under prolonged ER stress ATF4 in turn upregulates CHOP. IRE1 α may upregulate p53 which along with ATF4 and CHOP may upregulate BH3-only proteins⁷⁹.

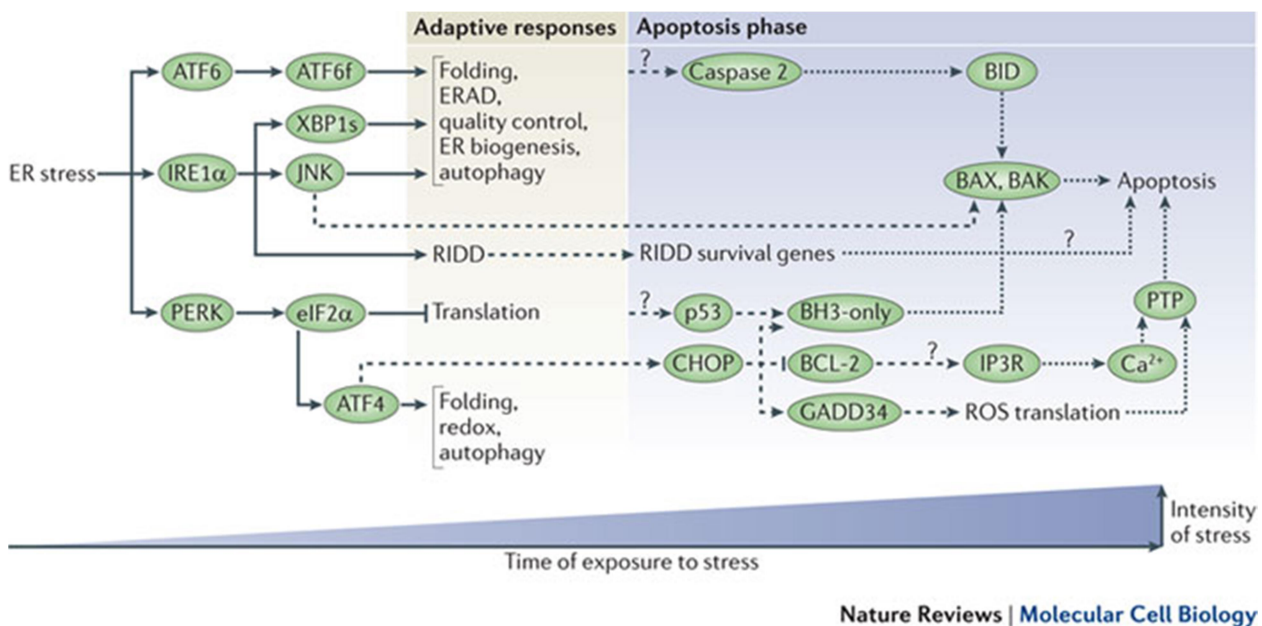


Figure 19: Time dependent ER stress pathway. Reprinted from Hetz et al⁷⁹.

As we can see from the above diagram there is a balance between adaptive responses to ER stress and the apoptosis phase whose nature is such that failure to sufficiently resolve the UPR will upregulate apoptosis (figure 19)⁷⁹. Predictably there are many disease states in which ER stress plays a key role.

We know that as people age there is a general shift away from the adaptive phase of the UPR towards the apoptotic signaling pathway⁷². In addition to promoting inflammation, this age-associated decrease in the efficiency of the UPR also leads to the accumulation of insoluble proteins or plaques in a variety of organs including the liver, spleen, or brain. This in turn contributes to a host of age-associated pathologies including age-related neurodegenerative disorders. For example protein aggregation is a hallmark of Alzheimer's disease, Parkinson's, and prion disease⁸⁰. It was experimentally determined that under basal conditions that the expression of chaperones calnexin, protein disulfide isomerase (PDI), and Grp78 are downregulated in the aged hypothalamus⁸¹. Each of these chaperones is a constituent in the normal protein folding process. Conversely, ubiquitination which plays a key role in the apoptotic arm of the UPR pathway is increased in the aged hippocampus. The downstream effects of this pattern were experimentally confirmed as well. When ER stress was induced in young VS old rats via intra-hippocampal lactacystin injection the old rats expressed less folding chaperones and Caspase-12 and young did not⁸¹.

Key protein folding chaperones BiP, PDI, calnexin and GRP94 also become increasingly impaired with age^{82,83}. Over time these chaperones become increasingly oxidized which may impair their functionality. For several of these chaperones reductions in oxidation correlate significantly with diminished enzymatic activity.

The universality of both aging and ER stress makes any interaction between them as ubiquitous as even the most common of pathologies. It is thus not surprising that as we continue to further investigate this interaction that we are compiling an ever growing list of diseases of aging in which ER stress is a key factor. Our ultimate goal is to discern the role of aging and ER stress in VILI.

1.5 Specific Aims

Despite its necessity as a potentially life-saving clinical intervention, MV can result in ventilator induced lung injury (VILI). The proposed mechanisms of VILI (volutrauma/, atelectrauma, biotrauma) were discussed in chapter one of this dissertation. Also as we discussed previously age is a predictive factor in the severity of VILI and the largest population of patients requiring MV is the elderly. However, the exact relationship thought which age-associated changes in pulmonary physiology interact with VILI is not well understood which has made it difficult for physicians to create age-dependent ventilator protocols or preventative treatments for VILI.

We hypothesized that there is an overall age-associated increase in the severity of the ventilator induced lung injuries that act to promote pulmonary edema. We hypothesized that this upregulation of edema promoting stimulus synergizes with a general and independent age-associated increase in the susceptibility to and severity of pulmonary edema. Furthermore we hypothesized that this age-associated increase in the severity of VILI induced pulmonary edema itself promotes further injury and inflammation which in turn positively feeds back to further promote edema and injury.

We believed this VILI induced positive feedback loop through the pulmonary edema pathway is ultimately an important cause of the age-associated increase in ventilator-associated mortality. And finally we hypothesize that since the primary mechanical driving force which filters fluid into the lungs is trans pulmonary pressure, if we administered a low fluid protocol to our murine subjects it would attenuate their age-associated increase in VILI-associated edema, inflammation, injury and mortality.

We tested this hypothesis *in vivo* by mechanically ventilating young (8 weeks) and old (20 months) mice with either a high tidal volume (HVT) or low tidal volume (LVT) ventilation protocols and with either a conservative or liberal fluid treatment protocol. During ventilation we measured subjects' pulmonary mechanics and mortality rates. Concluding ventilation we measured pulmonary edema, histological lung injury, and relative cytokine population in the alveolar lavage fluid.

Specific Aim 1: Measure the effect of novel low fluid treatment protocol on the age-associated increase in the severity of VILI and ventilator induced mortality.

We also hypothesized that the known age-associated increase in the susceptibility and severity of ER stress is a causal mechanism in the age-associated increase in the severity of ventilator-associated biotrauma. We hypothesized that old ATII cells themselves exhibit greater inflammation and injury downstream of an age-associated increase in mechanical stretch induced ER stress. Additionally, since we hypothesized ER stress as being upstream of this age-associated increase in stretch induced

inflammation and injury, we further hypothesized that treatment with an ER stress inhibitor would attenuate both the ER Stress and inflammation/injury as well. We tested this hypothesis *in vitro* by harvesting and culturing the alveolar epithelial ATII cells of young and old mice, exposing them to cyclic mechanical stretch, and measuring their inflammation and injury. Cells were treated with either an ER stress inhibitor or sham control.

Specific Aim 2: Determine if ER stress is an upstream regulator of age-associated mechanical stretch induced inflammation and injury in primary alveolar epithelial ATII cells.

In mice, VitC deficiency has been shown to increase the severity of acute lung injury (ALI) and pulmonary edema. Treatment with injections of VitC has been proven to attenuate these effects both in VitC deficient and sufficient mice[8]. Knowing the mechanistic role that pulmonary edema plays in the age-associated increase in the severity VILI, we hypothesized that VitC treatments would resolve edema and confer a protective effect on old murine ventilation subjects.

Specific Aim 3: Evaluate the efficacy of VitC as a treatment for Edema and VILI in old mice.

When taken together, these data greatly enhance our working understanding of the mechanistic relationships that drive the age-associated increase in the severity of VILI.

Even more importantly the resolution of each of these aims provides a much needed therapeutic target for preventative VILI treatments.

2.0

Conservative Fluid Management Prevents Age-Associated Ventilator Induced

Mortality

A research paper on by our group on which I was the primary author titled “Conservative Fluid Management Prevents Age-Associated Ventilator Induced Mortality” was successfully submitted and published to the Journal of Experimental Gerontology. This chapter is contains the body of that work as published.

2.1.0 Introduction

Advanced age is known to be ventilator-associated with increased severity of ventilator-induced lung injury (VILI) ²⁹. Setzer et al recently demonstrated that HVT (24 ml/kg) MV caused more lung injury in old rat subjects than in their younger counterparts. Lung wet to dry ratios, lavage protein and cytokine concentrations, and systemic markers of inflammation were all elevated in the older HVT MV subjects ⁵⁹. Additionally, it has been shown that short-term mechanical ventilation with low tidal volume and hyperoxia increases pulmonary edema, lung inflammation, and decreases diaphragm function in old rats subjects compared to young adults ⁸⁴. However, the exact mechanism(s) through which this relationship between aging and VILI is mediated remain ill defined. Consequently, preventative strategies for the age-associated increase in ventilator mortality are currently unknown. The changing mechanical properties of the aging lung

lead to increases in lung compliance which can predispose the lung to over-distention and increased susceptibility to atelectasis during mechanical ventilation^{41,55,56,85}. Further, the aging lung exhibits increasingly dysregulated immune/inflammatory responses to injury leading to pathological increases in pro-inflammatory behavior^{57,59}.

Pulmonary edema is a hallmark of VILI⁵³. The incidence and in-hospital mortality rates of patients presenting with pulmonary edema is also known to increase with patient age^{86,87}. Both the presence of pulmonary edema in ventilated patients and their overall survival rates can be affected by fluid management strategies⁶¹. Recent studies show that conservative fluid management can decrease pulmonary edema, increase ventilator free days, and increase overall survival of patients with acute respiratory distress syndrome (ARDS)^{59,88}. However, patients undergoing mechanical ventilation with inadequate fluid support are also at risk of developing hypovolemia which overtime can lead to multiple organ system failure²⁸. Therefore administering optimal fluid balance is crucial for mechanical ventilator patient survival and recovery. Despite known benefits of conservative fluid protocols for patients with ARDS, its effects on VILI, interaction with patient age, and the role that they both may play in ventilator-associated mortality rates has yet to be established.

We hypothesized that high tidal volume (HVT) mechanical ventilation would induce lung injury, degrade pulmonary mechanics, and increase pulmonary edema in older murine subjects. Further, we hypothesized that a greater sensitivity to these pathologies would result in an age-associated increase in ventilator-associated mortality. Finally, we hypothesized that age-associated increases in injury and mortality could be attenuated with a conservative fluid support strategy. To establish the role

pulmonary edema plays in age-associated increases in VILI and ventilator-associated mortality and to evaluate fluid support protocols as a potential preventative treatment, we investigated the outcomes of both liberal and conservative fluid support strategies during high and low tidal volume mechanical ventilation in both young and old mice.

2.2.0 Materials and Methods

2.2.1 Animal Use: This study was approved by the VCU Institutional Animal Care and Use Committee (protocol number AD10000465). Male C57BL6 mice were used in these experiments. All animal experiments were carried out under IACUC University guidelines.

2.2.2 Age Groups: Age group I (Young): Young adult animals, 2-3 months of age, weighing 25 ± 3 g. Age group II (Old): Old animals, 20-22 months of age, weighing 35 ± 11 g. Ages of our young and old murine groups respectively were based on correlations between murine lifespan and known age-associated morphological changes in murine lung (17)(29).

2.2.3 Mechanical Ventilation: Young and old animal subjects were anesthetized with an intraperitoneal (IP) injection of 80mg/kg pentobarbital. In addition to anesthesia our MV regimen required that we arrest the subjects' spontaneous breathing with administration of a paralytic. This was accomplished with IP injection of 0.8 mg/kg pancuronium bromide at the 0hr and 2hr time points. Depth of subject anesthesia was monitored continuously via EKG transducer monitors included in FlexiVent small animal ventilator (Scireq) hardware. To maintain an appropriate level of anesthesia over the course of ventilation pentobarbital redoses of 40mg/kg were administered as needed

when subject heart rate exceeded 350 bpm. Each subject was randomized into the following treatment groups according to age: Young Low Tidal Volume (LVT), Young High Tidal Volume (HVT), Old LVT, and Old HVT. Following group assignment, subjects were mechanically ventilated with either LVT (8mL/kg, 125 BPM, 3cm H₂O positive end expiratory pressure, [PEEP]) or HVT (25mL/kg for Young, 18mL/kg for Old, 90 BPM, 0cm H₂O PEEP) ventilation protocol for either 1hr or 4hrs using a FlexiVent small animal ventilator (Scireq). LVT and HVT ventilation patterns and four-hour ventilation protocol were based on previously published *in vivo* models⁸⁹. Difference in tidal volumes of young and old HVT groups reflects a normalization of tidal volume across age based upon ideal body weight. Mice are considered to be adult at 2-3 months, but our measurements indicated that our 20-22 month old animal subjects were on average ~30% more massive than their younger counterparts. To better replicate clinical protocols the tidal volumes for our HVT ventilation were established using ideal/predicted body weights. The tidal volume for the old HVT group was therefore multiplied by 0.7, or the ratio of the average weight of the young subjects to that of the old. This gave an adjusted average tidal volume of 625ul±50ul and 630ul±62ul for the young and old HVT groups respectively.

2.2.4 Fluid Support Protocol: Animal subjects were administered either liberal (high) or conservative (low) fluid management protocols. Animals managed under high fluid received anesthesia with pentobarbital at a concentration of 10 mg/ml in saline and received IP infusions of saline at 100µL/hr. For a 25 gram subject requiring an hourly redose of pentobarbital the total 4hr saline infusion volume would be ~1ml. Animals managed under low fluid protocol were anesthetized with pentobarbital at 20 mg/ml and

received no IP saline infusions. For a 25 gram subject requiring an hourly redose of pentobarbital the total 4hr saline infusion volume would be ~0.35ml.

2.2.5 Lung Mechanics: At the 0, 1, 2, 3, and 4hr time points the following forced inspiratory maneuvers: 1) Deep Inflation v7.0, 2) Snapshot-150 v7.0, and 3) PVs-V v7.0 were performed using the included FlexiWare software package (Scireq). Deep inflation acts as a recruitment maneuver and measures total lung capacity (TLC). Snapshot measures lung tissue compliance. The pressure volume (PV) maneuver inflates the lung to a sequence of linearly increasing then decreasing volumes while measuring the corresponding airway pressures. With these data the PV maneuver generates respiratory pressure-volume loops from which the PV-loop area (hysteresis) is calculated. For subjects who died during ventilation the last set of mechanical data points taken prior to death were included in analysis where possible.

2.2.6 Euthanasia: At the end of the 1hr and 4hr ventilations respectively each animal subject was fully exsanguinated and removed from mechanical ventilation.

2.2.7 Bronchoalveolar Lavage Fluid Collection: Bronchoalveolar lavage was performed by instillation of saline using gravity feed driven flow at a height 30cm. This method was preferred over a forced installation to preserve lung architecture for histological analysis of alveolar airspace enlargement. Saline flowed freely into the lung until it stopped naturally. The installation tube and mouse were then inverted to allow the saline to flow freely back out and into a collection tube. This process was repeated three times. An average of 2.5 - 3.5mls of total bronchoalveolar lavage fluid (BALF) per subject was obtained using this technique.

2.2.8 Bronchoalveolar Lavage Fluid Cytology: BAL fluid was centrifuged at 300 x G, 4°C for 8 minutes. Supernatants were removed and cell pellets re-suspended in saline. Cells were then mounted onto glass slides using a cytopsin device (Shandon). Cells were stained (3 Diff-Quik solutions staining kit) and cover-slipped. Cell populations were then analyzed using microscopy (Olympus) and the ratios of lymphocytes, leukocytes, and macrophages were determined.

2.2.9 Bronchoalveolar Lavage Fluid Protein Concentration: BCA assay analysis (Pierce) of protein concentration was performed on all BAL fluid supernatants according to manufacturer's instructions.

2.2.10 Lung Histology: Left lungs were held at constant pressure, fixed with 10% formalin, sectioned, and stained with H&E. Airspace enlargement, which quantifies relative differences in alveolar airspace area within lung histology sections, was measured and analyzed using in-house custom code written in MATLAB. This code quantified enlargement using a previously defined mean weighted enlargement metric (18). The weight of each airspace in the metric was dependent on the variance and skewness of its size. Stained slides were dehydrated and mounted using Permount mounting medium (Fisher) and imaged using an Olympus IX71 Microscope (Olympus).

2.2.11 Lung Wet to Dry Weight Ratios: From each animal subject, right lungs were excised, weighed, fully desiccated then lyophilized for 48 hours. Specimens were then weighed and a wet weight to dry weight ratio calculated⁹⁰. To prevent introduction of erroneous fluid to this measurement wet to dry ratios were not performed on subjects for whom BALF had been collected.

2.2.12 Non-Ventilated Controls: Measurements of each experimental variable except for pulmonary biomechanics was performed on non-ventilated control animals.

2.2.13 Statistical Analysis: All quantitative experimental studies were performed with a minimum of n=3 however the values vary between individual groups experiments. A more in-depth explanation of the variation in N values is given in the supplement. Survival statistics were performed with Kaplan-Meyer estimation. For wet to dry data analysis two way ANOVA was used to establish pairwise differences across age and one way ANOVA with Tukey tests were used to establish within group differences. All other statistics were performed using two way ANOVA. P values of <0.05 were considered significant. We used GraphPad Prism 5 statistical analysis software.

2.3.0 Results

2.3.1 Four Hour High Fluid Survival Rate: 4hr survival curve for old subjects ventilated with HVT and high fluid support was statistically significantly lower than that observed in all other groups (figure 20). In all, only four of twelve old HVT subjects survived the 4Hr duration of their respective ventilations. By contrast, only one old HVT subject on the low fluid support protocol died during mechanical ventilation. Additionally, only one old LVT subject and one young LVT subject died during mechanical ventilation. No young HVT subjects died during mechanical ventilation (figure 20).

4Hr Ventilation Survival

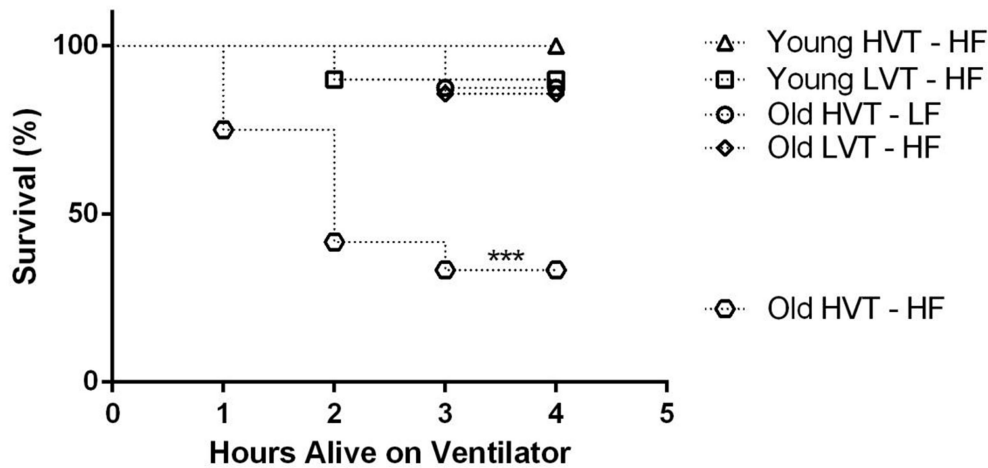


Figure 20: 4Hr Survival Rate. Survival rate in the Old HVT-HF group was significantly less than all other groups. Data is presented as survival percentage N = 10 for Young LVT-HF, 10 for Young HVT-HF, 3 for Young HVT-LF, 7 for Old LVT-HF, 12 for Old HVT-HF, 8 for Old HVT-LF ***p<0.001.

2.3.2 One Hour Lung Wet to Dry Ratios: Wet to dry ratios for each of the 1hr ventilation groups were measured (figure 21A). A statistically significant group-wise difference across age was observed with the older murine groups exhibiting significantly greater wet to dry ratios than the young. The wet to dry ratios for young HVT subjects receiving high fluid protocol was significantly greater than that observed in the young non-ventilated group (figure 21A). The wet to dry ratio of old HVT subjects receiving low fluid protocol was significantly lower than that observed in the old HVT subjects who received high fluid protocol and the old non-ventilated group (figure 21A).

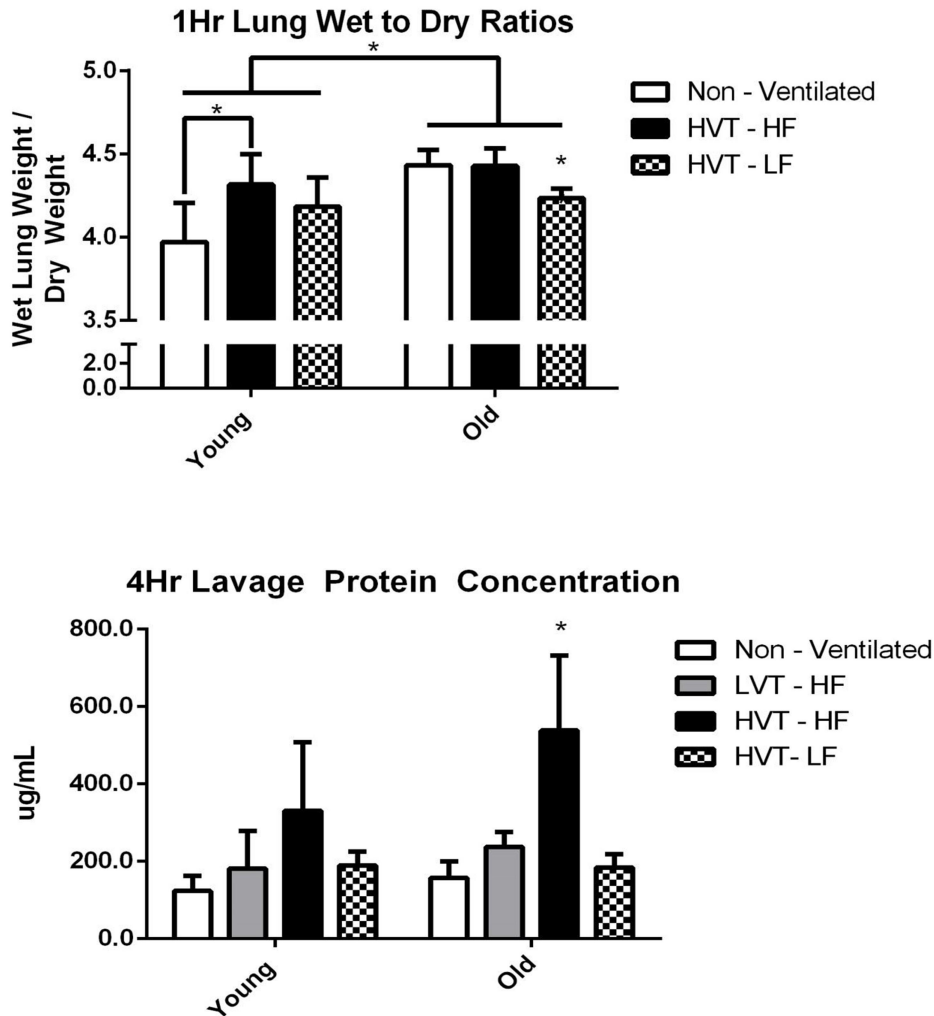


Figure 21: A. 1Hr Lung Wet to Dry Ratios. There was a group wise statistically significant difference across age with old groups having significantly greater lung wet to dry ratio than young. The Young HVT-HF group was significantly greater than in the Young Non-Ventilated group. The Old HVT-LF group was significantly less than in all other old groups respectively. Data are presented as mean +/- st.dev N = 4 for Young Non-Vent, 4 for Young HVT-HF, 4 for Young HVT-LF, 4 for Old Non-Vent, 4 for Old HVT-HF, 5 for Old HVT-LF. **B.** 4Hr Lavage Protein Concentration. The Old HVT-HF group concentration was significantly greater than that of all other old groups respectively. N = 4 for Young Non-Vent, 4 for Young LVT-HF, 7 for Young HVT-HF, 3 for Young HVT-LF, 4 for Old Non-Vent, 4 for Old LVT-HF, 4 for Old HVT-HF, 5 for Old HVT-LF *p<0.05.

2.3.3 Four Hour Bronchoalveolar Lavage Fluid Protein Concentration: BAL fluid

protein concentrations were measured for each animal subject surviving 4hr ventilation

(figure 21B). There was not a statistically significant group wise difference in lavage

protein concentration across age. Within the old group, the lavage protein concentration of subjects ventilated with HVT and high fluid support was significantly greater than that of all other old groups respectively. Similar trends were seen between the young groups but none reached statistical significance.

| | Young Non-Vent | Young LVT-HF | Young HVT-HF | Young HVT-LF | Old Non-Vent | Old LVT-HF | Old HVT-HF | Old HVT-LF |
|------------------------|----------------|--------------|--------------|--------------|--------------|------------|-------------|------------|
| Lymphocytes (%) | 1.58±0.8 | 5.89±4.1 | 4.69±3.4 | 2.5±5 | 2.66±0.7 | 3.79±1 | 9±4.2 | 6.9±3.2 |
| Neutrophils (%) | 0.33±0.2 | 0.67±0.4 | 3.14±3.1 | 0 | 0.33±0.1 | 4.42±3 | 8.42±7.2 | 6.4±6.2 |
| Monocytes (%) | 98.08±0.8 | 93.33±4.6 | 92.22±5.6 | 97.5±5 | 97±0.7 | 91.7±3.4 | 79.55±9.1 * | 86.4±6.1 |

Table 1: Cellularity in BALF. Data presented as absolute cell numbers in bronchoalveolar lavage and as cell differentials (percentage of counted cells). Monocyte differential < Young Non-Ventilated and Old Non-Ventilated. Data are presented as mean +/- st.dev N=4 for Young Non-Vent, 3 for Young LVT – HF, 6 for Young HVT – HF, 3 for Young HVT – LF, 6 for Old Non-Vent, 4 for Old LVT – HF, 4 for Old HVT – HF, 5 for Old HVT – LF *p<0.05.

2.3.4 Bronchoalveolar Lavage Fluid Cytology: Cytological differentials were measured on the BAL fluid of each subject surviving 4Hr ventilation (Table 1). The monocyte differentials of Old HVT high fluid group were significantly greater than those of both the Young Non-Ventilated and Old Non-Ventilated groups. No other statistically significant differences were observed.

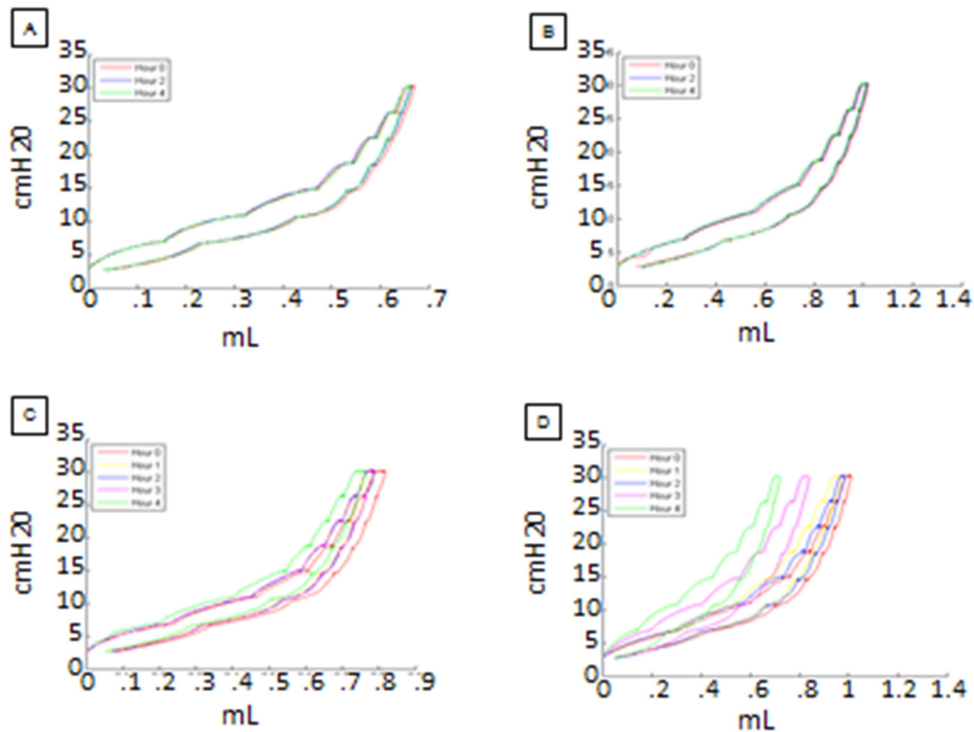


Figure 22: **A.** Representative 4Hr PV Loop for a Young LVT-HF subject. **B.** Representative 4Hr PV Loop for an Old LVT-HF subject. **C.** Representative 4Hr PV Loop for a Young HVT-HF subject. **D.** Representative 4Hr PV Loop for an Old HVT-HF subject.

2.3.5 PV Loop Hysteresis: PV loops were generated hourly using the Flexivent software (Scireq) for each surviving animal subject. Representative PV loops are shown in figure 22. The hysteresis values of each group were normalized with their respective 0hr values (figure 23). There was a group wise difference across age with old groups having significantly greater 1Hr PV loop hysteresis than young. 1Hr PV loop hysteresis of Old HVT high fluid group was significantly greater than that of the Old HVT low fluid group (figure 23A). The 4Hr PV loop hysteresis of the old HVT high fluid was significantly greater than that of both the old LVT high fluid and old HVT low fluid groups (figure 23B). Similar trends were seen between the young groups but none reached statistical significance.

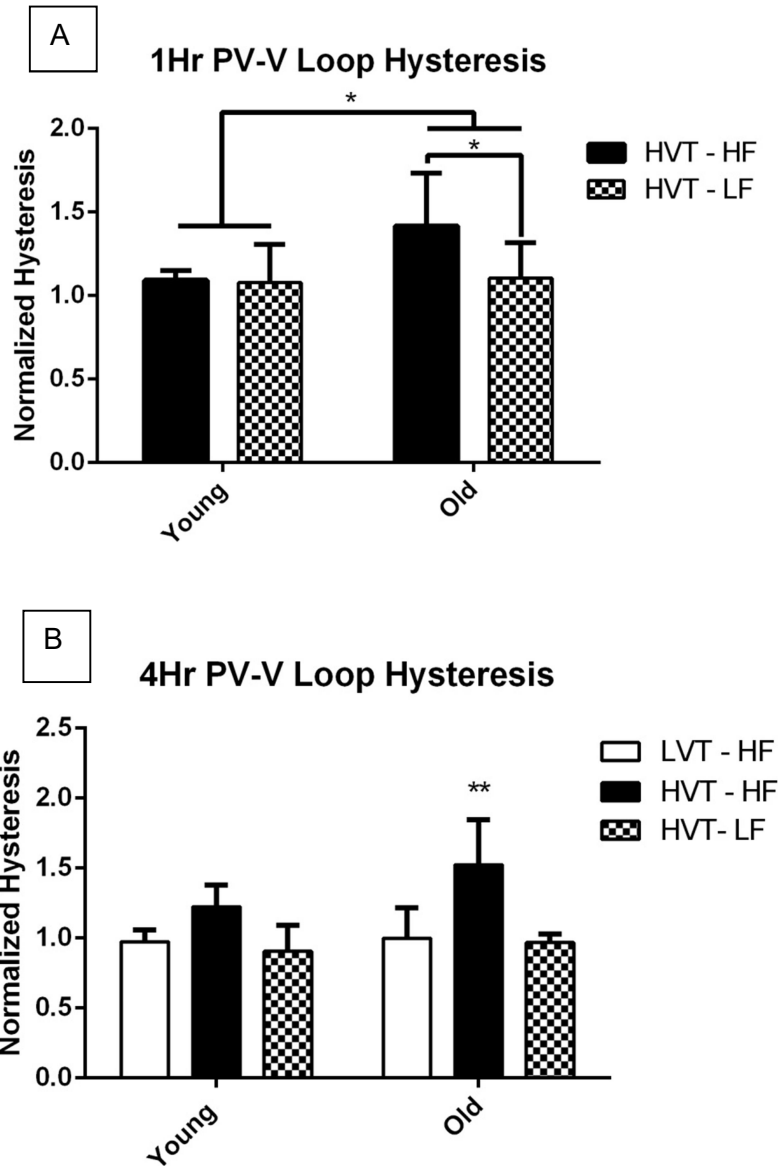


Figure 23: A. 1Hr PV Loop Hysteresis. Hysteresis in the Old HVT-HF group was significantly greater than Young HVT-HF and Old HVT-LF groups. Data are presented as mean +/- st.dev N=7 for Young HVT-HF, 7 for Young HVT-LF, 9 for Old HVT-HF, 12 for Old HVT-LF. **B.** 4Hr PV Loop Hysteresis. Hysteresis of the Old HVT-HF group was greater than that of the Old LVT-HF and Old HVT-LF groups. N=5 for Young LVT-HF, 6 for Young HVT-HF, 3 for Young HVT-LF, 5 for Old LVT-HF, 4 for Old HVT-HF, 5 for Old HVT-LF *p<0.05 **p<0.01.

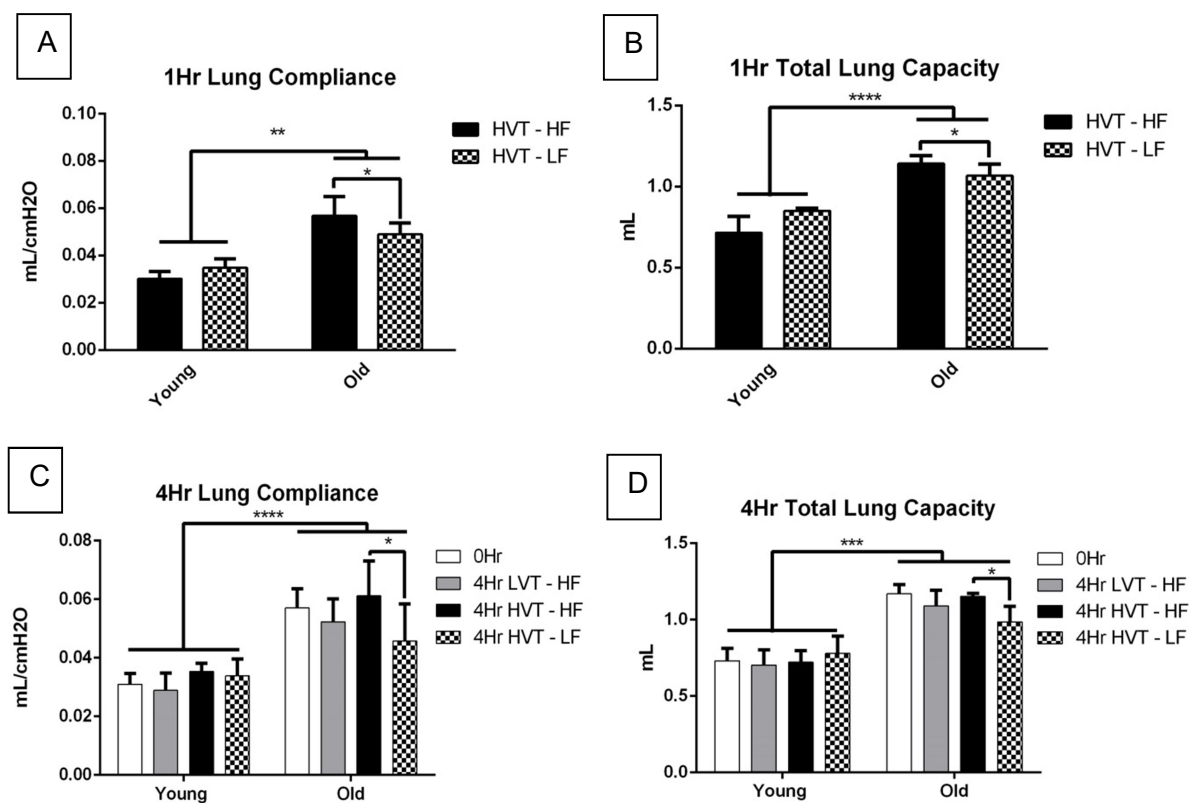


Figure 24: **A.** 1Hr Lung Compliance. There was a significant group wise across age with the old groups having a greater compliance than the young. 1Hr lung compliance in the Old HVT-HF group was significantly greater that of the Old HVT-LF group. Data are presented as mean +/-st.dev N=11 for Young HVT – HF, 4 for Young HVT – LF, 14 for Old HVT – HF, 7 for Old HVT – LF. **B.** 1Hr Total Lung Capacity. There was a significant group wise difference across age with the old groups having a greater TLC than young. 1Hr TLC in the Old HVT-HF group was significantly greater that of the Old HVT-LF group. N=4 for Young HVT – HF, 4 for Young HVT – LF, 14 for Old HVT – HF, 14 for Old HVT – LF. **C.** 4Hr Lung Compliance. There was a significant group wise difference across age with the old groups having greater lung compliance than the young. 4Hr lung compliance in the Old HVT-HF group was significantly greater that of the Old 0Hr and Old HVT-LF groups. N=11 for 0Hr Young, 7 for Young LVT – HF, 8 for Young HVT – HF, 3 for Young HVT – LF, 16 for 0Hr Old, 6 for Old LVT – HF, 4 for Old HVT – HF, 6 for Old HVT – LF. **D.** 4Hr Total Lung Capacity. There was a significant group wise difference across age with the old groups having a greater TLC than young. 4Hr TLC in the Old HVT-HF group was significantly greater that of the Old HVT-LF group. N=11 for 0Hr Young, 7 for Young LVT – HF, 9 for Young HVT – HF, 3 for Young HVT – LF, 16 for 0Hr Old, 6 for Old LVT – HF, 4 for Old HVT – HF, 6 for Old HVT – LF, *p<0.05 **p<0.01 ***p<0.001 ****p<0.0001.

2.3.6 Lung Compliance: Lung compliance was measured hourly using the Flexivent software (Scireq) for each surviving animal subject (figure 24). There was a significant group wise difference across age of both the 1Hr and 4Hr lung compliance with old groups having greater compliance than young. (figure 24 A, C). The 1Hr lung compliance of the old HVT high fluid group was significantly greater than that of the HVT low fluid group (figure 24A). The 4Hr lung compliance of the old HVT high fluid group was greater than that of the old HVT low fluid group (figure 24C). There was a strong non-significant trend with the old 4Hr HVT high fluid groups having a greater mean than the old 4Hr LVT low fluid group.

2.3.7 Total Lung Capacity: Total Lung Capacity (TLC) was measured hourly using the Flexivent software (Scireq) for each surviving animal subject (figure 24). There was a statistically significant group wise difference across age of both the 1Hr and 4Hr TLC with the old groups having greater TLC than young (figure 24 B, D). The 1Hr TLC of the old HVT high fluid group was significantly greater than that of the HVT low fluid group (figure 24B). The 4Hr TLC of the old HVT high fluid group was significantly greater than that of the old HVT low fluid group (figure 24D). There was a strong non-significant trend with the old 4Hr HVT high fluid group having a greater mean than the old 4Hr LVT high fluid group.

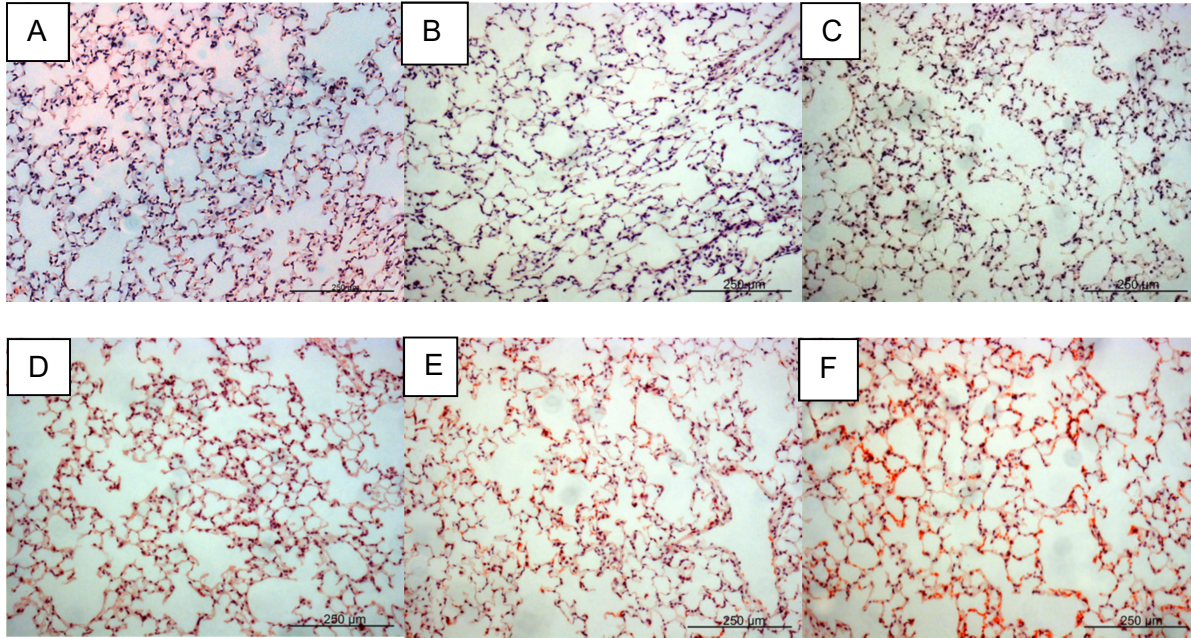


Figure 25: A, B, C, D, E, F. Representative 4Hr histological H&E images of **A.** Young LVT-HF, **B.** Young HVT-HF, **C.** Young HVT-LF, **D.** Old LVT-HF, **E.** Old HVT-HF, and **F.** Old HVT-LF lung sections respectively.

2.3.8 Airspace Enlargement: Representative histological images of lung stained with H&E of both young and old animal subjects ventilated with HV or LV are presented in figure 25A-D. Airspace enlargement and an increased infiltration of erythrocytes could clearly be seen in images corresponding to both increased age and HVT ventilation. Low fluid protocols visually attenuated these effects. Airspace enlargement was quantified and calculated for each subject reaching 4hrs of mechanical ventilation. There was a significant group wise difference in airspace enlargement across age with old groups having a greater value than young. Airspace enlargement of old subjects ventilated with HVT and high fluid was significantly greater than that of all other groups (figure 26).

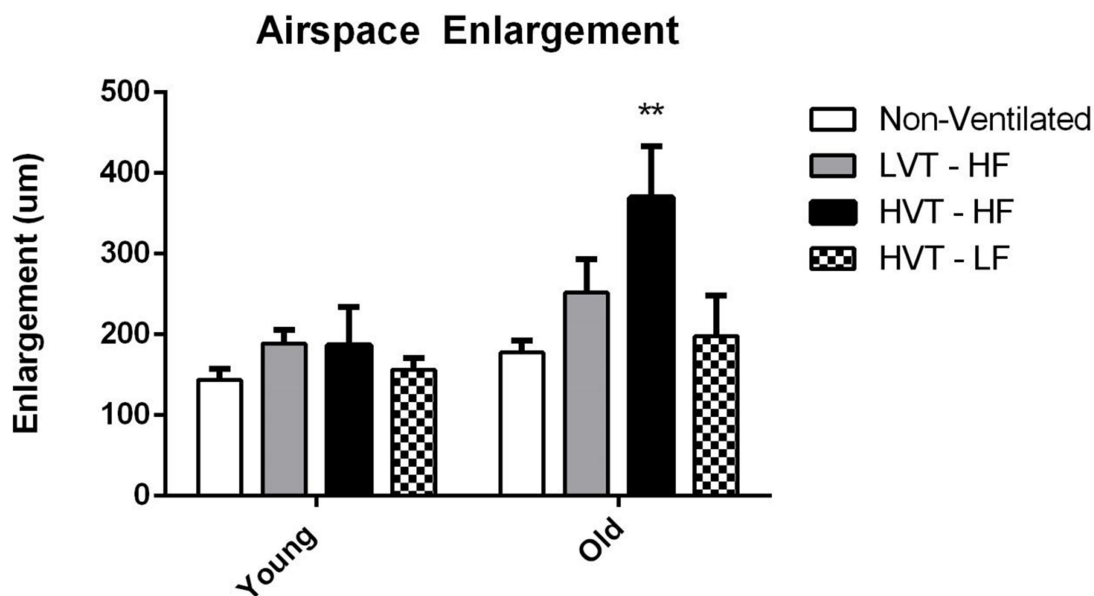


Figure 26: Airspace Enlargement. There was a statistically significant groupwise difference across age with old groups having significantly greater enlargement than young. Enlargement was greater in the Old HVT-HF group than in all others. Data are presented as mean +/- st.dev N = 3 for Young Non-Vent, 6 for Young LVT-HF, 6 for Young HVT-HF, 3 for Young HVT-LF, 3 for Old Non-Vent, 3 for Old LVT-HF, 4 for Old HVT-HF, 3 for Old HVT-LF **p<0.01.

2.4 Discussion

The first aim of this study was to establish that older mouse subjects when subjected to HVT MV exhibit an increased severity of ventilator-induced lung injury as was recently reported in an aging rat model⁵⁹. Wilson et al established that significant stretch induced lung injury in young healthy mice requires mechanical ventilation with tidal volumes approaching 40mg/ml⁹¹. Consequently most models of VILI use similarly high (>30mg/ml) VT and/or inspiratory pressures to induce injury. These settings however are generally considered significantly higher than those used in the clinical management of patients^{91,92}. Setzer et al demonstrated that the increased sensitivity of the aging rat lung to mechanical ventilation allowed their group to achieve significant VILI with tidal volumes of 16-24mg/kg⁵⁹. So while a tidal volume of 40mg/kg may be more conventionally referred to as “High Tidal Volume”, our HVT protocol is both sufficient to

cause ventilator induced injury and mortality in our older subjects and is closer to clinical relevance than other higher HVT standards.

Each of our experimental measures demonstrates a significant pattern of age-associated increase in inflammation and injury. Our second aim was to determine whether administration of a conservative fluid management strategy alone would attenuate these effects. While fluid management has long been an important issue in clinical medicine; the role of fluid management on the development and outcome of VILI had yet to be quantitatively studied *in-vivo*. The addition of conservative fluid support to our HVT ventilation protocol attenuated VILI and significantly decreased the mortality rate in older subjects.

Patient mortality is the gravest complication of mechanical ventilation. In our study neither advanced age nor HVT ventilation alone significantly increased subject mortality. Only with the combination of advanced age and HVT did our study yield a profound decrease in our subjects' survival (figure 18). Considering the epidemiology of VILI the experimental validation of the age-associated increase in ventilator mortality is already of paramount importance. Potentially even more meaningful however was that we were able to completely attenuate the age-associated increase in our subject's HVT mortality with the administration of a low fluid protocol. Pulmonary edema, pulmonary mechanics, lung histology, and BALF cytology data all give a strong testimony that the resolution of VILI induced edema itself is a primary mechanism through which this low fluid protocol is able to enact such a dramatically protective effect.

Pulmonary edema is a hallmark of VILI and the severity and susceptibility to pulmonary edema increases with age^{50,93-95}. Some of the driving forces behind

development and progression of pulmonary edema both in general and in VILI are increases in pulmonary intravascular pressure, decreased epithelial barrier integrity/increased permeability, and increased local and systemic inflammatory cytokine presence. Since conservative fluid strategies decrease intravascular pressure, it is not surprising that a body of data has emerged linking them to decreased pulmonary edema and increased survival rates both in animal and human studies of ARDS^{88,95,96}. However, liberal fluid management strategies are not wholly without merit. Liberal fluid resuscitation is known to have positive effects on blood pressure and other hemodynamic factors in human studies⁹⁵.

The role of aquaporin channels in pulmonary fluid clearance and how they may specifically interact with VILI, aging, and edema is complicated at the very least. Zhongguo et al showed that aquaporin channel 1 and 5 (AQP1& AQP5) expression decreases in rats with hyperoxia induced lung injury and correlates with increases in pulmonary edema. And although low tidal volume mechanical ventilation was not found to increase alveolar barrier permeability or pulmonary edema in rats, it was shown to increase AQP1 and AQP5 expression. Age is known to be a predictive factor in the incidence and severity of pulmonary edema^{29,97}. Zhang et al showed that aging lungs exhibit decreased aquaporin channel expression⁶⁰. Additionally, it is known that age-associated changes in lung physiology increase susceptibility to and severity of both VILI and pulmonary edema independently during mechanical ventilation. In the present study, we hypothesized that the negative synergy of the age-associated increases allows them to be powerful regulators of the age-associated increases in ventilator

mortality rates observed both in animal models and in older patients who are mechanically ventilated.

In our 1hr ventilations we found significant increases in lung wet to dry ratios ventilator-associated with both advanced age and liberal fluid support. These results support the general finding that age increases the incidence and severity of edema^{59,94}. They also demonstrate our experimental model's ability to induce ventilator-associated pulmonary edema with HVT mechanical ventilation and subsequently attenuate it through conservative fluid administration alone.

Increased lavage protein concentration is a general marker of lung injury and of enhanced pulmonary permeability and edema⁹⁸. In our 4hr subjects, lavage protein concentration was significantly increased by HVT ventilation. Importantly, old subjects on low fluid protocol exhibited near complete attenuation of the high protein containing BAL fluid produced by HVT ventilation. As with our 1hr ventilation results, these data establish our ability to use HVT mechanical ventilation and conservative fluid management both induce and ablate pulmonary edema respectively.

Pulmonary disease changes the physiology of the lungs, which manifests as changes in respiratory mechanics. Therefore, measurement of respiratory mechanics allows a clinician to monitor closely the course of pulmonary disease⁹⁹. The area of the pressure volume loop (i.e., the hysteresis) is the geometric representation of the energy lost during each breath cycle. Increased hysteresis is indicative of compromised lung mechanics function and is a hallmark of aging and various lung pathologies^{25,100}. The one hour PV-Loop data demonstrated that conservative fluid support in the old HVT subjects attenuated age-related increase in MV induced pulmonary mechanical

disruption. The success of these conservative fluid strategies in decreasing the severity of pulmonary edema and improving pulmonary mechanics in our 1Hr HVT subjects precipitated us to confidently apply our conservative fluid protocols to a group of old subjects being mechanically ventilated for 4hrs in hopes of increasing their survival rate. Predictably the four hour PV-Loop data showed an even more significant pattern of disruption and resolution of pulmonary mechanics with the administration of liberal and conservative fluid protocols respectively in our old murine subjects. In young subjects we saw a similar pattern but none of hysteresis differences reached statistical significance.

In addition to their hysteresis values, the PV loops also contain information in the shape of their ascending limb. In figure 22, we see that while the shapes of the PV loops of young LVT and HVT and old LVT subjects vary only minimally over time, the old HVT loops splay strongly to the left. This represents an increasing rise in pulmonary compliance over time. Increased lung compliance is a hallmark of the age-associated decline in lung mechanics and of many pathological conditions^{53,58,101}. TLC is not considered to significantly change with age¹⁰². It is generally known that this effect results from the almost perfect balance between the age-associated increase in lung compliance, the decrease in respiratory muscle tone, and the increase in chest wall stiffness²⁴. However, in our experiments, the Flexivent system calculates TLC based upon the volume of air required to inflate the lung to a specified pressure. Therefore, the age-associated loss of muscle tone does not affect the TLC measurements. Consequently, we expect the loss of lung compliance to dominate these measurements and expect to see TLC measurements taken with the Flexivent system to increase with

age. Furthermore, certain types of lung injury (e.g., emphysema) increase lung compliance, and thus, they further increase total lung capacity as measured by our Flexivent system¹⁰³.

Both age and injury related increases in these pulmonary mechanical measures were observed in our study. The significantly increased 0hr lung compliance and total lung capacity in old mice demonstrates the predicted age-associated changes in pulmonary physiology and mechanics. The strong trend toward increased mean values of both lung compliance and TLC observed in HVT vs LVT ventilator protocols seen in our older subjects therefore notable as well. Even more striking is that both lung compliance and TLC values are significantly decreased in older HVT subjects when treated with conservative fluid protocols. These findings demonstrate that HVT ventilation promotes greater injury compared to LVT ventilation in old animal subjects, and that this injury can be attenuated with a low fluid protocol alone.

Collectively these mechanics data paint a picture of an aging lung whose mechanical dysfunction is a downstream effect of the loss of elasticity and subsequent increase in compliance. This is in agreement with the known age-associated decrease in elastin fibers of the lung parenchyma¹⁰⁴. However, it must be noted that in general having increased pulmonary edema classically decreases lung compliance. This would seem to be in opposition to the pattern we observed of increasing lung compliance with injury. However, VILI induced changes in the lung parenchyma do operate in the direction of increasing lung compliances. In our histological analysis, we found a qualitative decrease in the presence and quality of elastin in older mice (Supplemental Figure).

We further investigated our model's effect on lung parenchyma destruction through measurement of ventilation-induced alveolar airspace enlargement. Increased airspace enlargement values are ventilator-associated with both increased age and pathophysiological conditions such as emphysema and VILI^{105,106}. In our case, the differences we observed in the airspace enlargement values for the experimental groups represent the extent of the alveolar barrier injury/destruction resulting from mechanical ventilation. Just as with our mechanics, edema, and cytology data, we expected to observe a group-wise difference in the airspace enlargement values across age, with older mice exhibiting greater airspace enlargement values than younger mice. Further, we expected to see significant increases in airspace enlargement values of HVT subjects over non-ventilated controls and LVT subjects. Our data not only showed both of these patterns, but additionally there was a significant interaction effect of increased airspace enlargement when advanced age combined with HVT ventilation. These pro-pulmonary compliance changes in the lung parenchyma work in opposition to the anti-compliant mechanics classically observed in an edematous lung. The fact we seen an increasing compliance in our most injured subjects despite their increasingly edematous lungs suggests that the mechanical effect of the injury/destruction of the parenchyma has a more profound impact on the overall lung mechanics than the edema.

Our cytological analysis of BAL fluid demonstrates a pattern of inflammatory cell recruitment that further validates our experimental model of VILI in aging mice. Recruitment of lymphocytes, neutrophils, basophils, and eosinophils to the site of an injury is part of the normal immuno-inflammatory and wound healing response^{40,107}.

Literature, experimental data, and our research lead us to conclude that age-related increases in the severity of VILI should amplify this damage-associated pattern both systemically and in the microenvironment of the lung^{57,59,90}. However, several studies have found little or no differences in BAL fluid cell count ratios between young and old healthy mice^{96,103,108}. For this reason, we expected that we would only see significant differences in differential cell counts between ventilation control and HVT subjects and that furthermore; this pattern would be more exaggerated in the old vs. the young subjects.

As expected, our cytological analysis failed to yield significant differences between young and old control groups. The only significant differences we observed were between old subjects ventilated with HVT and young and old control groups. These cytology data support our hypothesis by demonstrating the synergistic effect of advanced age and HVT ventilation on lung inflammation and injury. This age-associated increase in ventilator –induced pulmonary “biotrauma” is decidedly “mid-stream” in the VILI process. Alveolar epithelial cell barrier function is known to be disrupted by inflammatory cytokines. Increased pro-inflammatory cytokine levels in the lung promote disruption of the lung’s barrier function thus resulting in enhanced permeability and development of pulmonary edema.

Thus, the work reported here demonstrates that a low fluid support strategy alone can reverse the age-associated increases in the 4hr hour mortality rate of older subjects ventilated with HVT. The significantly important finding arising from this work is that development of pulmonary edema has both deleterious up and down stream

impacts on the development of VILI. Further, we have identified the crucial role conservative fluid administration has in diminishing lung edema and the severity of VILI.

In conclusion, our findings suggest that the age-associated increase in VILI-induced pulmonary edema is not simply a downstream marker of injury but also a mechanism for further injury and increased mortality. And while already known that conservative fluid support strategies give favorable outcomes to patients with ARDS, this is the first evidence that these strategies also attenuate VILI and its age-associated increase in severity. Considering the relative lack of preventative treatments for VILI and the age-associated increases in injury and death, the development of age-dependent fluid support strategies may be of critical importance in increasing the survival rate of elderly ventilator patients.

2.5 Limitations

The volume parameter of mechanical ventilations is generally determined by the application of a ratio between tidal volume and patient weight. For this purpose it is often the preferred clinical practice to use a calculation of the patient's ideal body weight instead of their actual weight as to not over or under ventilate under or overweight patients. This is of particular importance in our study as 20 month old mice are reliably ~30% more massive than their younger counterparts. If not accounted for, this would result in the lungs of the older subjects being systematically inflated to larger volumes based on their size than those of their younger counterparts. However, it has also been noted that while the lungs of the older mice may not be larger than those of the young adult mice, the increased mass of the older mice does correlate with an increased

circulatory volume. Therefore while the weight-adjusted tidal volume may provide a lung volume normalized tidal volume, the older mice are receiving a lower tidal volume relative to their circulatory volume. This is of course not different from how overweight human patients may be ventilated but is still a potentially important limitation to consider.

3.0

The Role of ER Stress and Aging in an *In Vitro* Models of Ventilator Induced Lung Injury

3.1.0 Introduction

Ventilator induced lung injury is initiated by mechanical insult to the lung. However, it is the systemic release of cytokines that if unabated develops into systemic inflammatory response syndrome (SIRS). SIRS in turn promotes multiple organ system dysfunction (MODS) which is the primary cause of death in VILI patients¹⁰⁹.

The majority of patients requiring mechanical ventilation are over the age of 65 and advanced age is known to increase the severity of VILI and in-hospital mortality rates²⁹. However, the mechanisms which predispose aging ventilator patients to increased severity of VILI and ventilator-associated mortality rates are not fully understood. Age-associated pathological changes in lung mechanics are well known and have been implicated in the severity of VILI but the relationship has not yet been fully elucidated. Additionally, the role of the aging alveolar epithelium in VILI is wholly unknown at this time.

There is however evidence to suggest that there may be a causal link between

epithelial cell aging and the age-associated increase in the severity of VILI. In general, advanced age is also known to promote an increasingly dysregulated innate immune/inflammatory response to injury with an overall shift towards a proinflammatory state^{57,58}. Additionally, mechanical stretch alone has been shown to cause injury and promote a proinflammatory cascade in multiple cell lines^{40,110,111}. Mechanical stretch of lung epithelial cells has been shown to increase cell injury and death, increase apoptosis, increase acidification and bacterial growth, and increase general inflammatory response including gene expression and release of IL-6 and IL-8¹¹². Additionally, mechanical stretch compromises epithelial barrier integrity by damaging the plasma membrane, increasing barrier permeability, and decreasing overall barrier function^{113–116}.

Mechanical stretch has also been shown to increase oxidative stress and promote epithelial to mesenchymal transition in alveolar epithelial^{113,114,117}. However, to date no research has been done to establish the effect of aging on mechanical stretch induced injury and inflammation in pulmonary epithelial cells. Age alone is also known to increase inflammation and injury to various types of insult through the senescence-associated secretory phenotype (SASP) pathway^{118,119}. Aging has also been shown to promote chronic inflammation in the murine lung¹¹⁵. Aging has also been shown to promote damage and inhibit repair in the lung epithelium following insult with influenza¹²⁰. We hypothesize that aged lung epithelia respond to mechanical stretch with a dysregulated inflammatory cytokine production which may be triggered by endoplasmic reticulum (ER) stress and the unfolded protein response (UPR).

The endoplasmic reticulum is a multifunctional organelle responsible for lipid biosynthesis, calcium storage, and protein folding and processing⁶⁴. Because of the innate inefficiency of protein folding as many as 30% of proteins never acquire their fully folded conformation¹²¹. The unfolded protein response (UPR) suppresses aggregation of these improperly folded proteins through three independent pathways which inhibit protein synthesis, chaperone nascent or unfolded proteins, and discern then transport them through a degradation pathway before they can aggregate¹²². However, if the UPR is unable to restore protein homeostasis inside the ER and resolve the aggregation of misfolded proteins, the apoptotic arms of the UPR are activated and apoptosis is accordingly promoted. Thus prolonged unresolved ER stress can cause accumulation of misfolded proteins, disruption of cellular functions, apoptosis, and has been shown to play a key role in many chronic inflammatory disease states. Specifically in alveolar epithelial cells, ER stress has been shown to regulate apoptosis, idiopathic pulmonary fibrosis, and epithelial to mesenchymal transition¹²³.

The UPR is also known to become increasingly dysregulated with age¹²⁴. There is a general age-associated increase in the occurrence of protein misfolding and accumulation. There is also a downregulation of the three non-apoptotic arms of the UPR while the pro-apoptotic arm is semi-independently upregulated^{125,126}. Unsurprisingly ER stress is implicated as a promoter of many pathological disease states associated with aging⁷². Additionally, ER stress has been implicated in the age-associated increase in pulmonary fibrosis¹²⁷.

However, despite the clear path the VILI must take through systemic inflammation to claim MODS as its main cause of death, there have been no studies to

date of the role of ER stress in VILI. Therefore unsurprisingly despite the well known the role of age-associated ER stress in many inflammatory disease states, VILI is not among them.

To investigate this relationship we isolated and cultured primary alveolar epithelial ATII cells (ATIIs) from young and old murine subjects. These cells were treated with 24h of cyclic mechanical stretch to promote mechanical stretch induced injury. We measured age-associated differences in ER stress response, cell injury/inflammation, and apoptosis. To help establish the position of ER stress relative to these measures of inflammation and injury in the VILI pathway we also inhibited ER stress using known ER stress inhibitor 4-phenylbutyrate (4-PBA)¹²⁸. 4-PBA is already in use as a successful treatment for systemic inflammatory diseases such as diabetes¹²⁹. So in addition to determining location of ER stress in cellular inflammatory VILI cascade we are also evaluating a critically needed treatment for VILI in aging patients.

3.2.0 Methods

3.2.1 ATII cell isolation and culture: For this project we harvested, isolated, and cultured ATII primary alveolar epithelial cells from young (8 week) and old (20 months) C57BL/6J wild type mice (WT) using previously cited methods [40]. Once cells were isolated we suspend them in Bronchial Epithelial Cell Growth Media (BEGM, Lonza) with all included supplemented added except hydrocortisone and supplemented with 10 ng/ml KGF (keratinocyte growth factor, PeproTech). Cells were then plated on collagen I coated 6-well silicone bottomed plates (Flexcell).

3.2.2 ATII Cellular Phenotyping: Cellular phenotyping was used to validate isolation

protocols. 48 hours after isolation both young and old cells were phenotyped using positive surfactant protein C (Abcam) primary antibody followed by AlexaFluor 488 secondary and counter stained with prolong gold anti-fade reagent with DAPI nuclear stain. A random sampling of images were qualitatively evaluated to pure ATII population in culture.

3.2.3 CHOP Immunofluorescence: Old and young mice were ventilated for 4 hours with ventilation protocol cited in chapter 2. After 4 hour ventilation subjects were sacrificed, lungs were extracted and fixed, and serological lung sections were obtained using histology methods cited in chapter 2. Slides were then stained with a primary antibody to CHOP (Cell Signaling, 1:1000) followed by AlexaFluor 594 secondary counter stained with DAPI nuclear stain, and imaged using an Olympus IX71 Microscope (Olympus).

3.2.4 Cell Stretch: After a 48 hour incubation we used the Flexcell Tension Plus System (Flexcell) to cyclically equibiaxially stretch the cells to a 15% change in surface area for durations of 4, 24, 48 and 96 hours. This stretch percentage corresponds to the stretch seen by ATII cells during injurious MV. Statically cultured ATII cells were used as controls. After cells were stretch treated, we collected the media and mRNA from each well.

3.2.5 ER Stress Inhibition: One hour prior to mechanical stretch each well received either 100ul vehicle (phosphate buffered saline; PBS) or 10 mmol/L sodium 4-phenylbutyrate (PBA) (Calbiochem, San Diego, CA) in 100ul PBS.

3.2.6 MTT Assay: MTT assays (Roche) were performed to measure net metabolic processing. These results can be used to infer relative rates of cellular or cytostatic

activity. Decreases in MTT values represent increases in cell injury and/or death.

Increases in MTT values indicate the shift of the ATII cells from a resting to proliferative state.

3.2.7 mRNA Analysis: We collected mRNA from each treatment group (RNeasy Mini Kit, Qiagen), purified the mRNA and used a standard RT kit (Biorad) to convert the RNA to CDNA. We used custom QPCR plates (Biorad) to perform QPCR analysis on 27 inflammatory genes of interest (Aimp1, B2m, Ccl12, Ccl2, Ccl20, Ccl3,Ccl4, Ccl6, Ccl7, Ccl9, Ccr1, Csf1, Cxcl12, Cxcl15, Cxcl5, Gusb, HSP90ab1, Il10rb, Il15, Il1a, Il1r1, Il2rg, Il6st, Nampt, Sgpp1, Tnfrsf11b, Vegfa).

3.2.8 Media Protein Concentration: We performed BCA assays (Pierce) on all collected cell media samples to measure cell media protein concentrations.

3.2.9 Inflammatory Mediator Analysis: We measured the concentrations of select inflammatory cytokines of interest in the collected cell media of each experimental group using 10 protein (IL-1a, IL-1b, IL-4, IL-6, IL-10, IL-12, MCP-1, MIP-1a, RANTES, TNF-a) custom Bio-Plex ELISAs (BioRad). Values were normalized to each samples protein concentration levels.

3.3.0 Results

3.3.1 Phenotyping: In both young and old ATII cells a random sampling of images confirmed positive staining for surfactant protein C (figure 27).

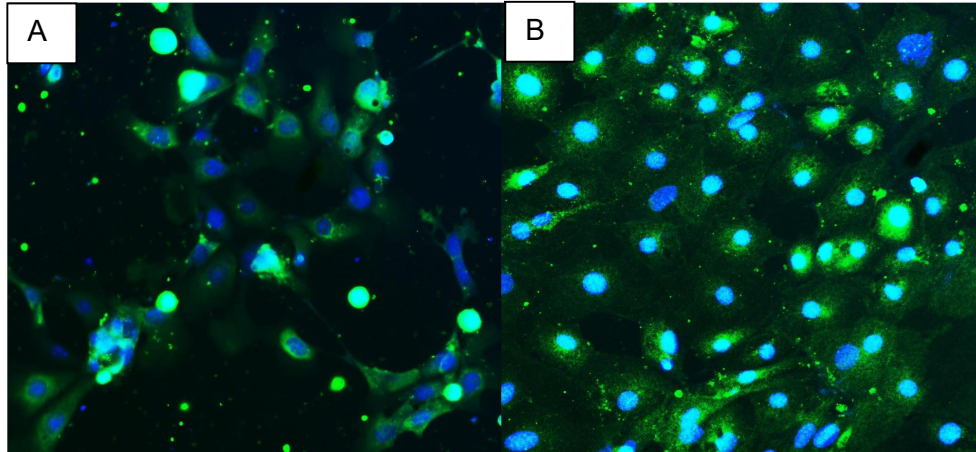


Figure 27: Representative 20X surfactant C images of **A.** Old 24Hr and **B.** Young 24Hr cells. Green are pro-SPC positive cells, blue are nuclei stained with DAPI

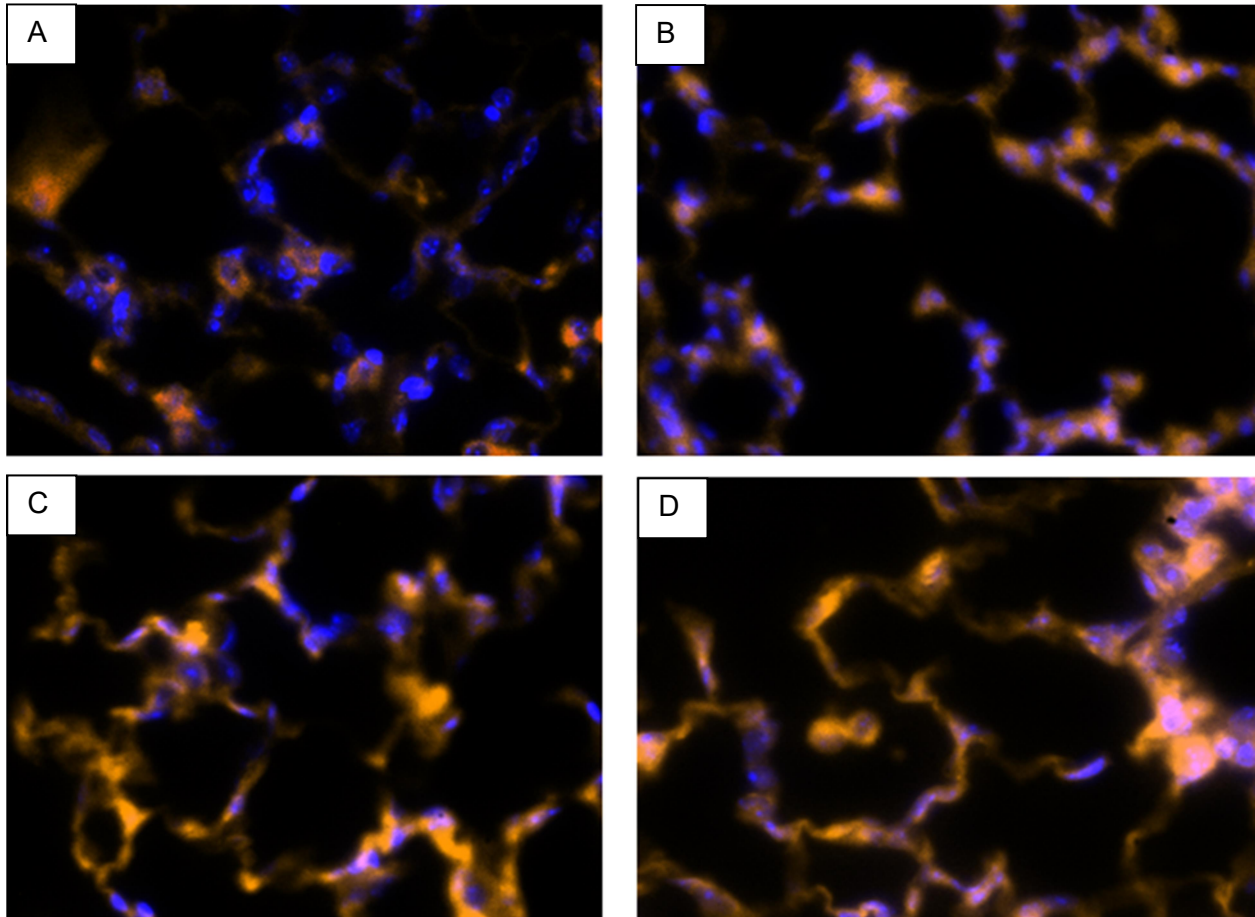


Figure 28: Representative 20X 4Hr histological CHOP images of **A.** Young LVT-HF, **B.** Old LVT-HF, **C.** Young HVT-HF, **D.** Old HVT-HF lung sections. Yellow are CHOP positive cells, blue are nuclei stained with DAPI

3.3.2 CHOP Staining: Representative CHOP staining of lungs tissue displayed both a general age-associated and ventilator protocol associated difference in CHOP expression (figure 28). Advanced age and HVT ventilation increased CHOP expression both independently and in combination.

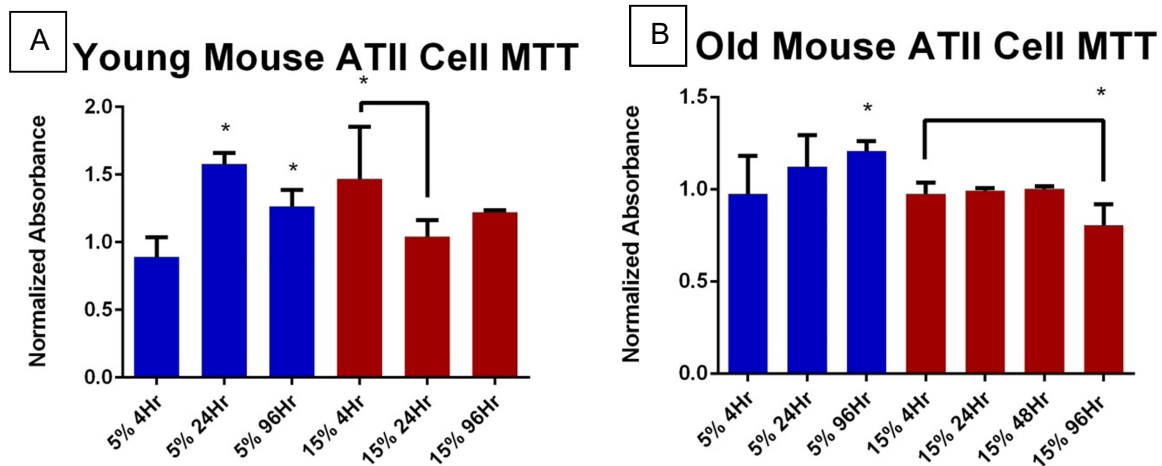


Figure 29: Normalized MTT absorbance values. **A.** MTT values for Young 5% 24hr and 96hr groups were significantly higher than static controls. MTT Value for Young 15% 4hr group was significantly higher than static control, **B.** MTT value for Old 5% 96hr group was significantly greater than static control. MTT value for old 15% 96hr was significantly lower than static control. Data presented as mean +/- st.dev n=3 *p<0.05

3.3.3 MTT Assay: In Young 5% stretch groups 24Hr and 96Hr each had significantly higher MTT values than static controls. In Young 15% stretch only 4Hr group had significantly higher MTT value than static control (figure 27A). In Old 5% stretch groups only 96Hr group had significantly higher MTT value than static control. In Old 15% stretch groups only 96Hr had significantly lower MTT value than static control (figure 29B).

3.3.4 Inflammatory Gene Expression: ER stress-associated Chop and ATF4 gene expression was significantly greater in Old 24Hr stretch ER control groups compared to every other group (figure 30). No other relationships were significant. However, Chop and ATF4 gene expression in Old 24Hr stretch ER Control group showed an increase in

mean compared to Old 24Hr static ER control. Additionally, Chop and ATF4 gene expression in Old static ER inhibited groups showed a decrease in compared to Old 24Hr static ER control but the trend was not significant.

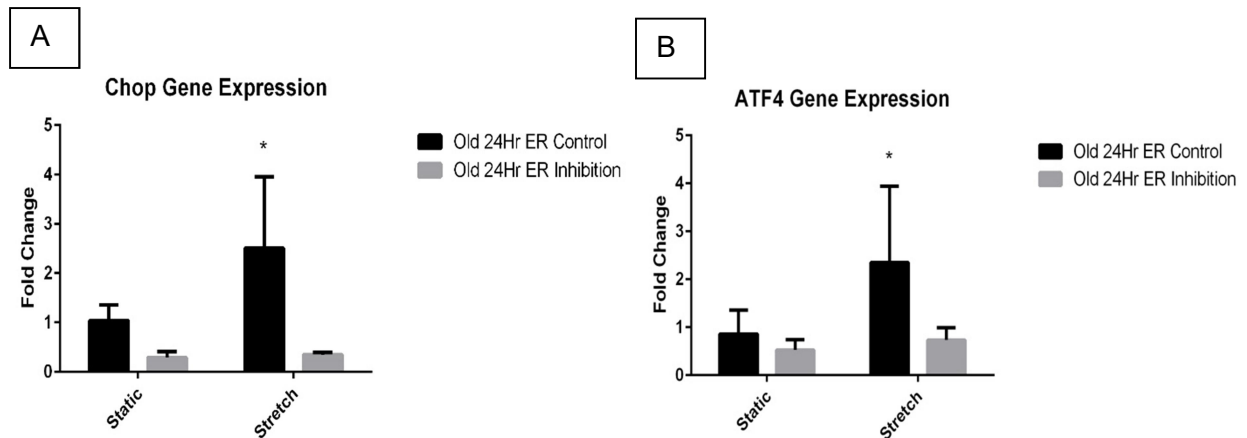


Figure 30: Age, stretch, and ER inhibitor induced inflammatory gene expression. **A,B.** Old 24Hr Static ER Control, Old 24Hr Stretch ER Control, Old 24Hr Static ER Inhibited, Old 24Hr Stretch ER Inhibited, normalized to Old 24Hr Static ER Control. Columns are fold change differences in gene expression. Data are presented as mean +/- st. deviation, n=3, *p<0.05.

Advanced age alone and advanced age combined with mechanical stretch were associated with general increases in inflammatory gene expression (figure 31A).

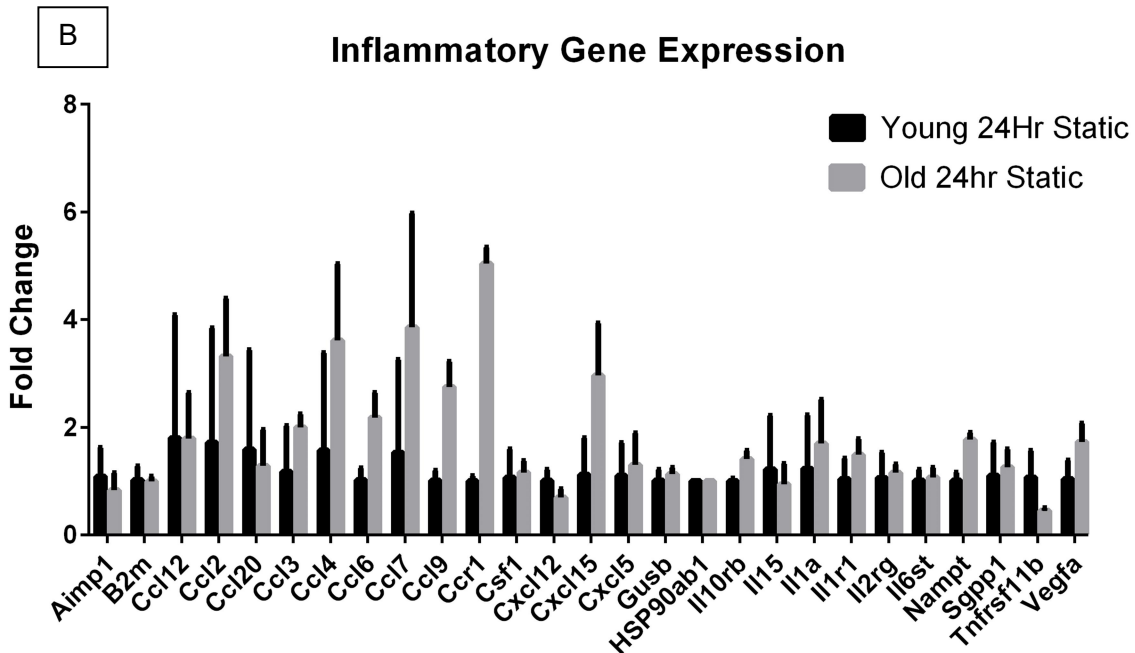


Figure 31: Age and stretch induced inflammatory gene expression. **A.** Young 24Hr Static, Old 24Hr Static, Young 24Hr Stretch, Old 24Hr Stretch normalized to Young 24Hr Static. **B.** Young 24Hr Static and Old 24Hr Static normalized to Young 24Hr Static. Columns are fold change differences in gene expression. Data are presented as mean +/- st. deviation, n=3.

Advanced age alone significantly increased the gene expression of Ccl6, Ccl9, Ccr1, Il10rb, and Nampt in statically cultured old VS young cells (figure 31B and 32A).

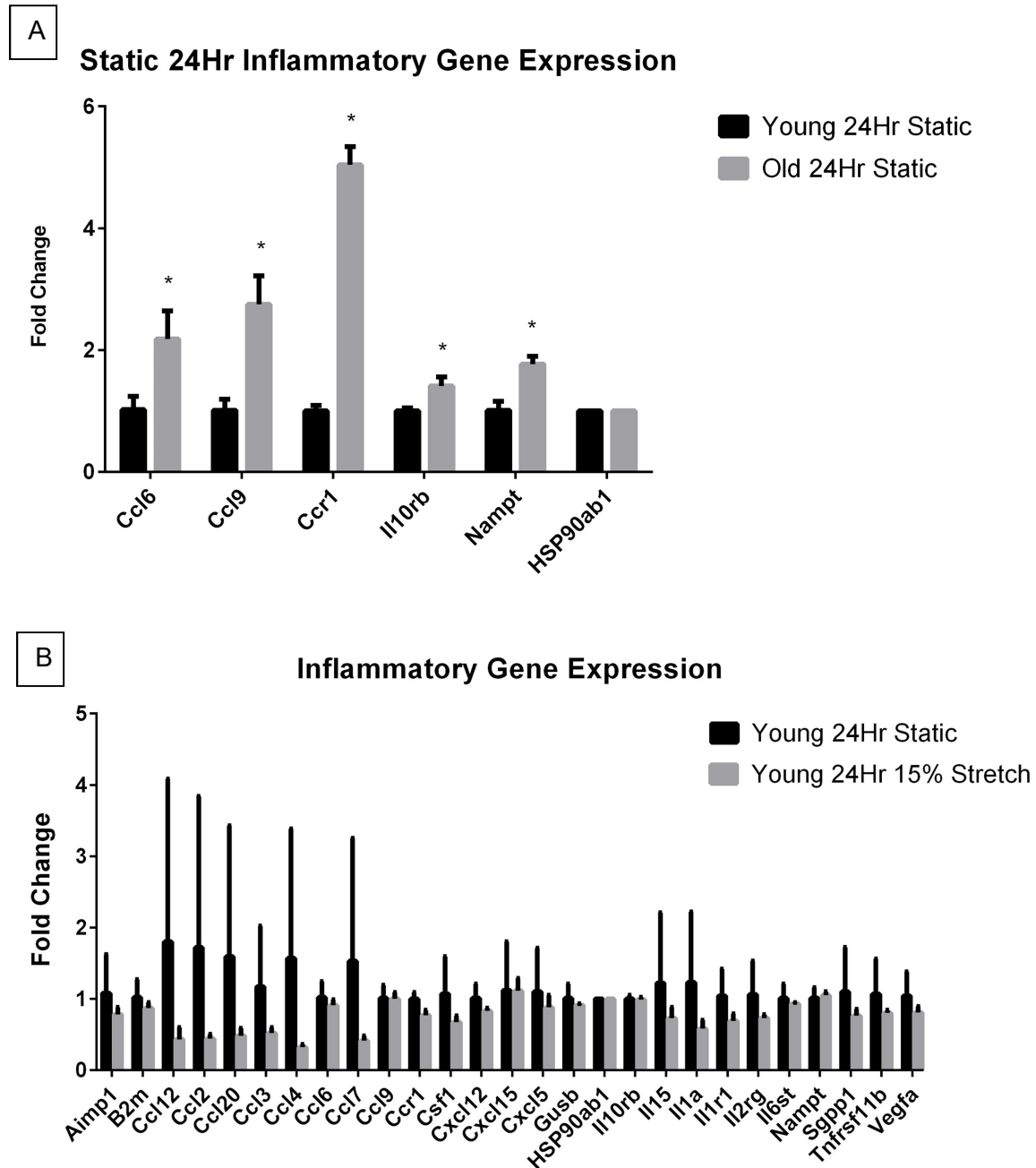


Figure 32: Age and stretch induced inflammatory gene expression. **A.** Young 24Hr Static and Old 24Hr Static normalized to Young 24Hr Static. **B.** Young 24Hr Static and Young 24Hr Stretch normalized to Young 24Hr Static. Columns are fold change differences in gene expression. Data are presented as mean +/- st. deviation, n=3, *p<0.05.

Mechanical stretch alone did not increase the expression of any inflammatory genes measured in young cell cells treated with 24Hr 15% stretch VS those statically cultured (figure gene 32B).

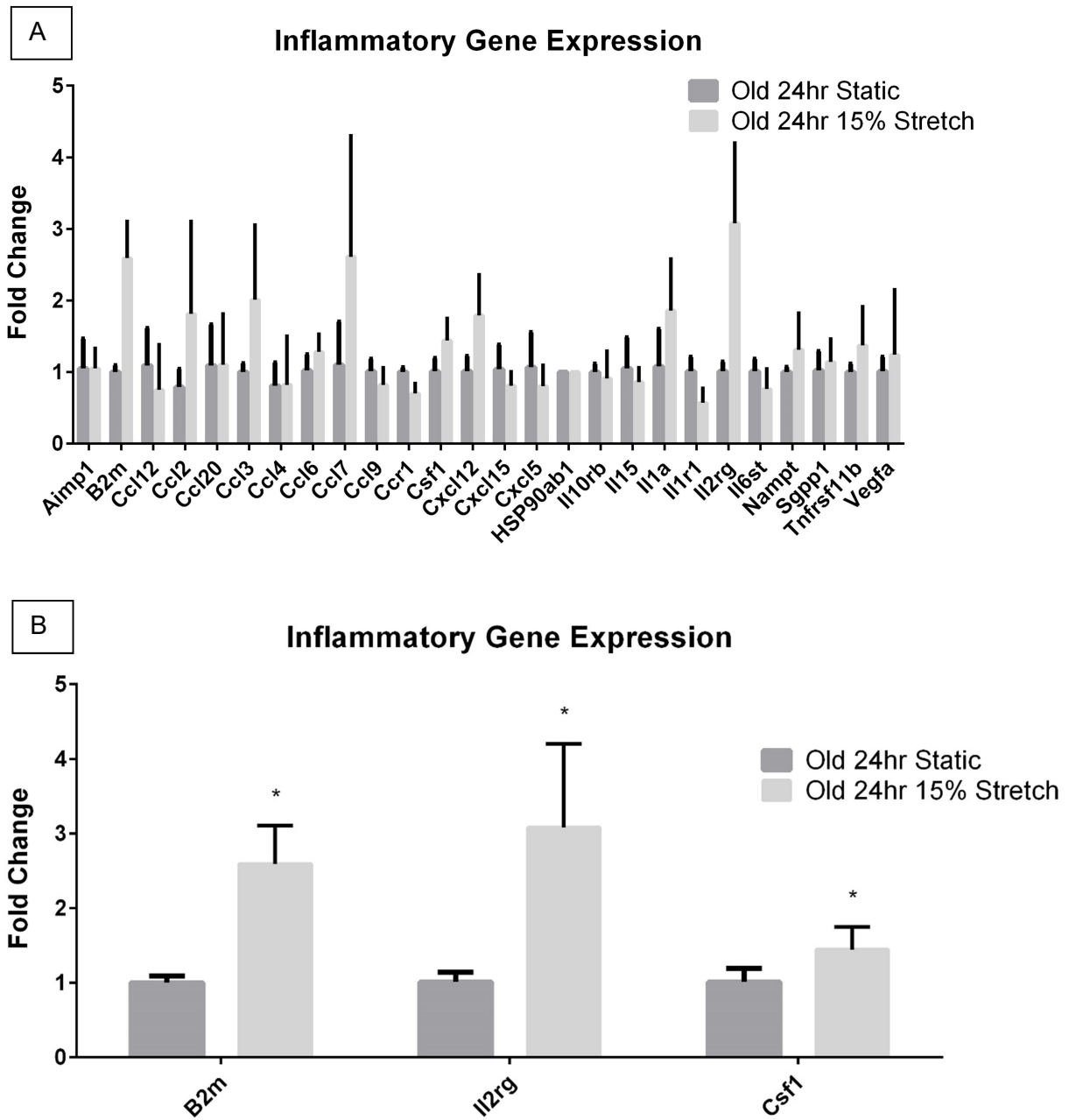


Figure 33: Age and stretch induced inflammatory gene expression. **A,B.** Old 24Hr Static and Old 24Hr Stretch normalized to Old 24Hr Static. Columns are fold change differences in gene expression. Data are presented as mean +/- st. deviation, n=3, *p<0.05.

Mechanical stretch alone increased gene expression of B2m, Ccl4, Csf1, and Il2rg in old cells treated with 24Hr 15% stretch VS old statically cultured cells (figure 33 A, B).

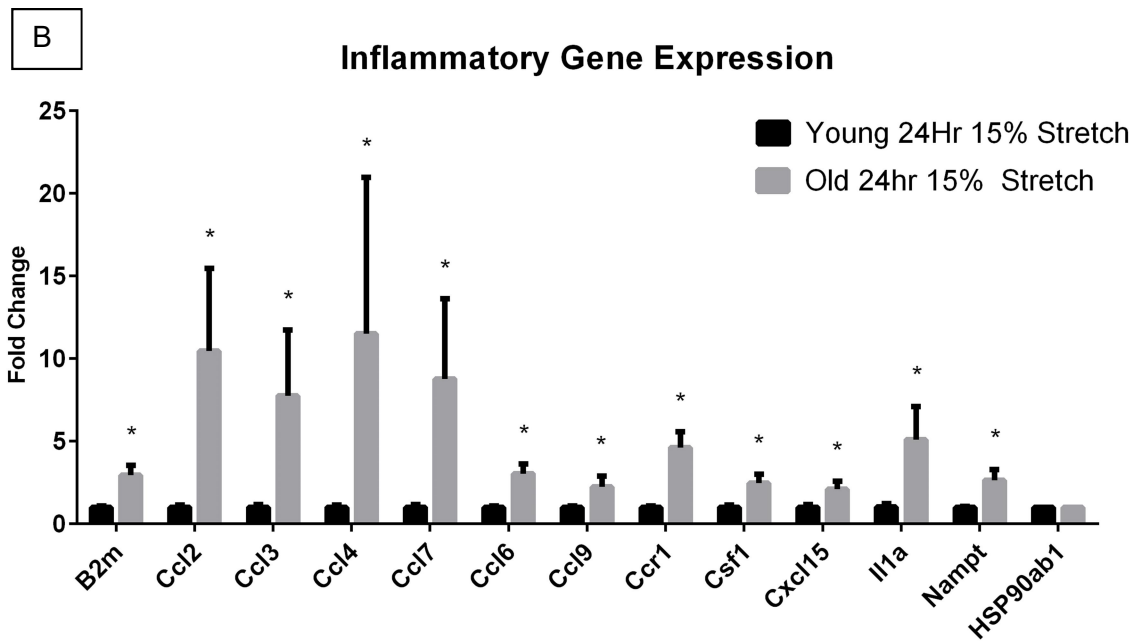
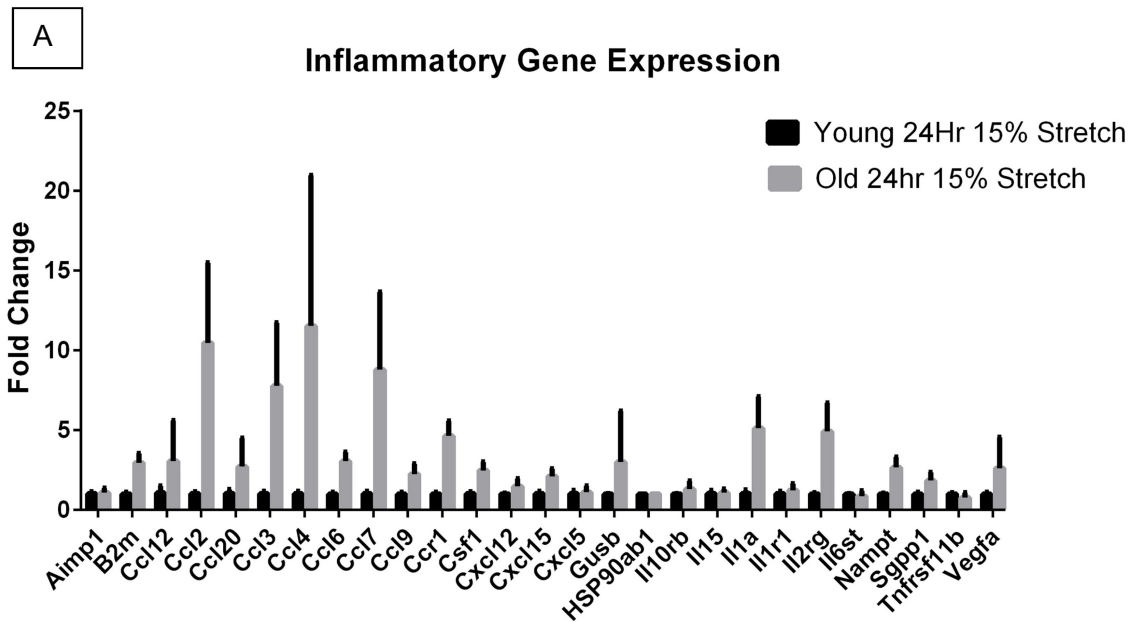


Figure 34: Age and stretch induced inflammatory gene expression. **A,B.** Young 24Hr Stretch and Old 24Hr Stretch normalized to Young 24Hr Stretch. Columns are fold change differences in gene expression. Data are presented as mean +/- st. deviation, n=3, *p<0.05.

Old cells treated with 24Hr 15% mechanical stretch had significantly increased expression of B2m, Ccl2, Ccl3, Ccl4 Ccl7, Ccl6, Ccl9, Ccsf1, Cxcl15, Il1a and Nampt compared to similarly treated young cells (figure 32A, B).

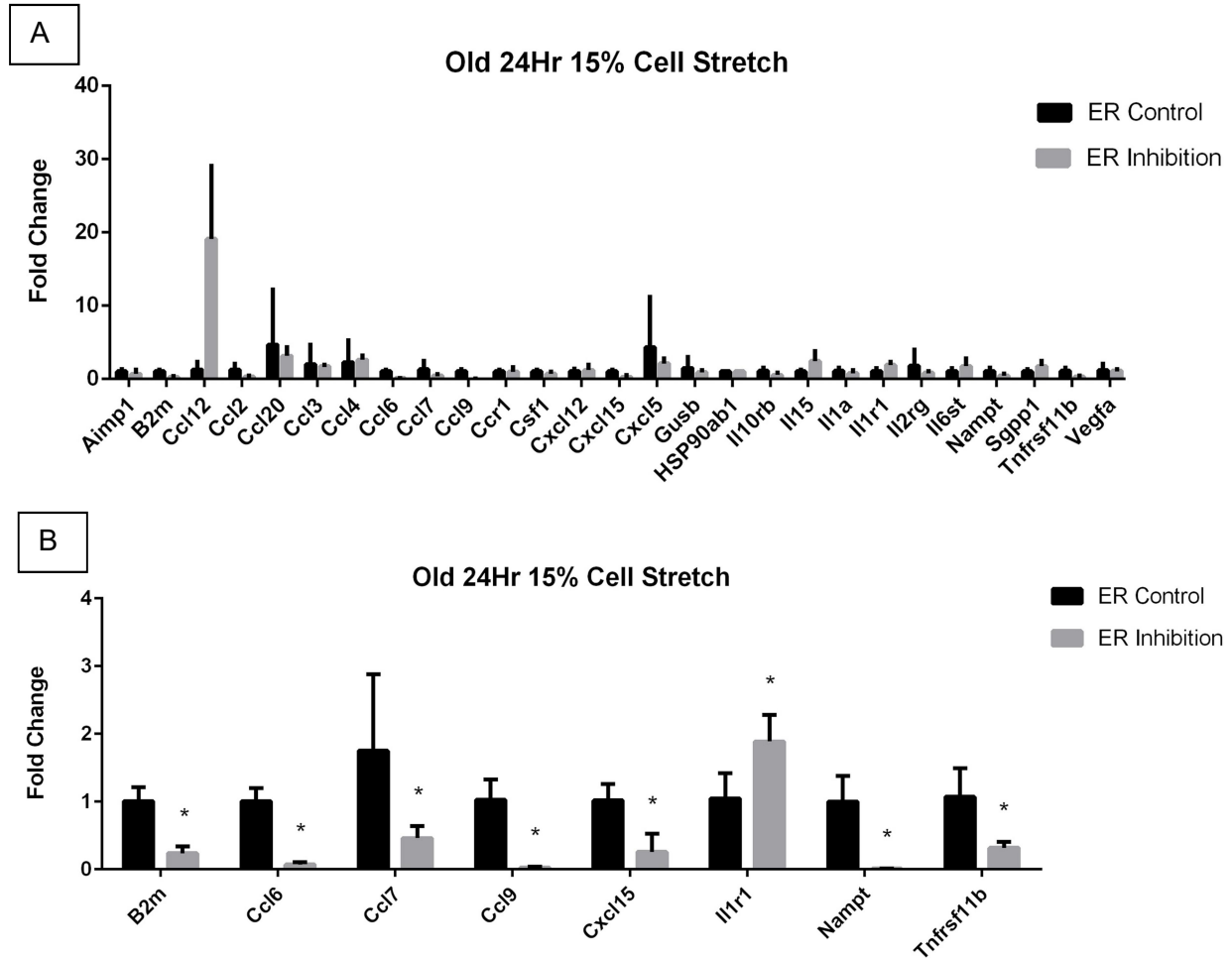


Figure 35: Age and stretch induced inflammatory gene expression. **A,B.** Old 24Hr Stretch ER Control and Old 24Hr Stretch ER Inhibited normalized to Old 24Hr Stretch ER Control. Columns are fold change differences in gene expression. Data are presented as mean +/- st. deviation, n=3, *p<0.05.

Old cells stretched and treated with 4-PBA exhibited significantly decreased expression of B2m, Ccl6, Ccl7, Ccl9, Cxcl15, Nampt, Tnfrs11b and an increased expression of Il1a relative to old cells stretched and treated with sham ER inhibition (figure 35 A, B).

Treatment with 4-PBA significantly increased the expression of IL-1a and decreased expression of IL-6 in both old cells treated with 24Hr 15% stretch and those statically cultured (figure 36).

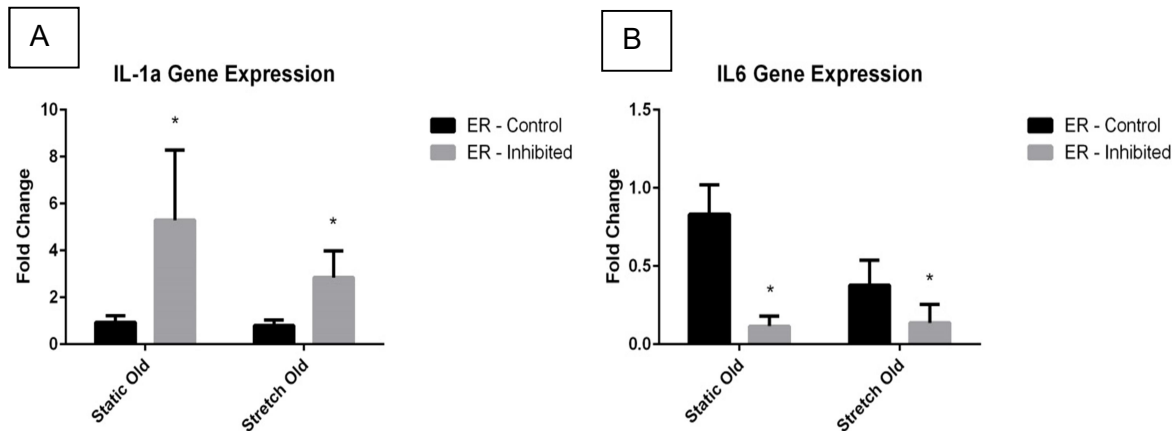


Figure 36: Age and stretch induced inflammatory gene expression. **A,B.** Old 24Hr Stretch ER Control and Old 24Hr Stretch ER Inhibited normalized to Old 24Hr Stretch ER Control. Columns are fold change differences in gene expression. Data are presented as mean +/- st. deviation, n=3, *p<0.05.

3.3.5 Media protein concentration: Treatment with 4-PBA decreased the media concentrations of inflammatory cytokines IL-6, MIP-1b, MCP-1, and Rantes in both old cells treated with stretch and old statically cultured cells (figure 35 A,B,C,D). Treatment with 4-PBA increased the media concentrations of inflammatory cytokines proteins IL1a, IL-1b, IL-10 and MIP-1a in both old cells treated with stretch and old statically cultured cells (figure 37z E,F,G,H).

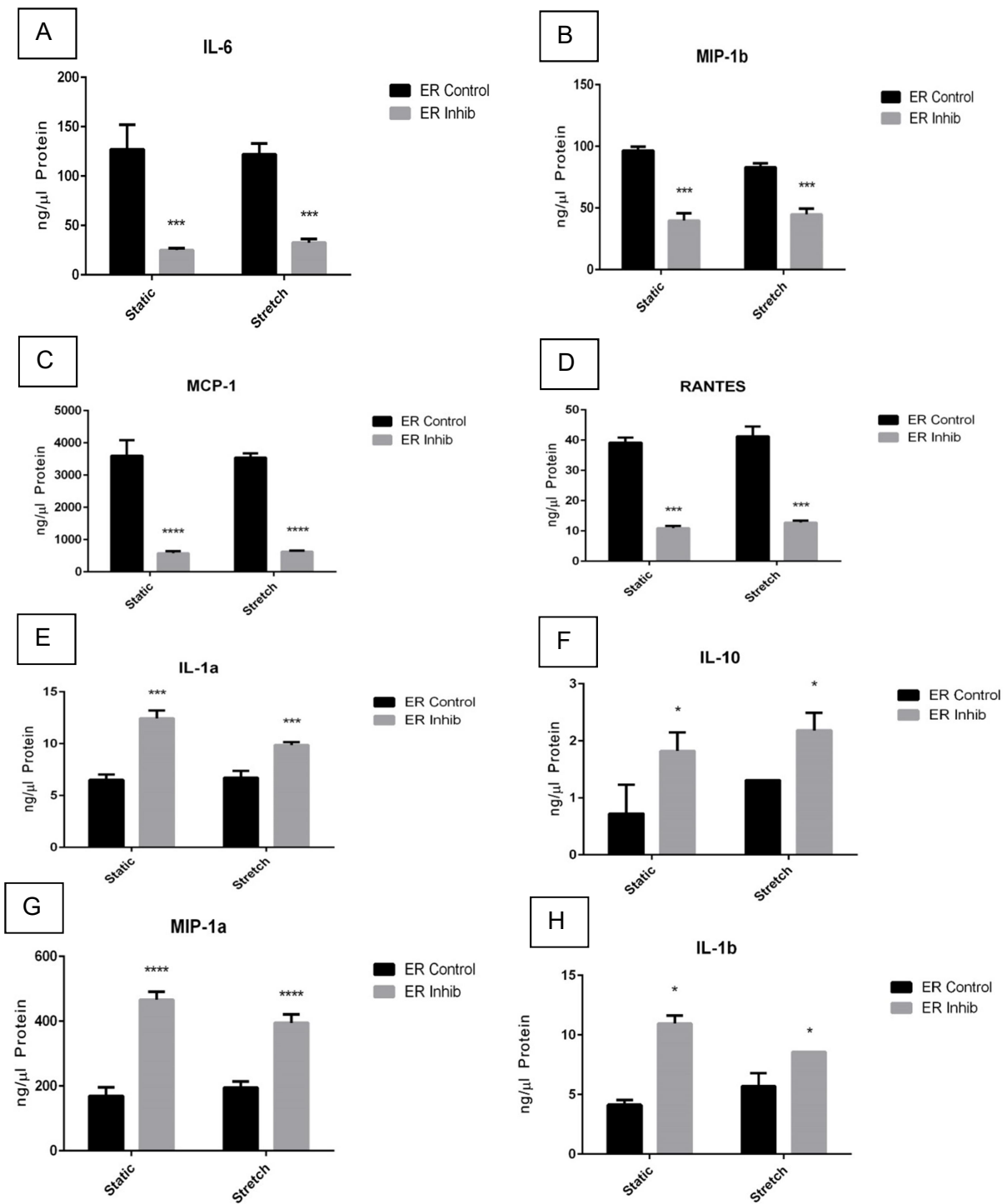


Figure 37: Cell media protein concentration. A,B,C,D,E,F,G,H. Old 24Hr Static ER Control, Old 24Hr Stretch ER Control, Old 24Hr Static ER Inhibited, Old 24Hr Stretch ER Inhibited. Data are presented as mean +/- st. deviation, n=3, *p<0.05.

3.4.0 Discussion

Although the lung is undoubtedly one of the most physiologically complex organ systems, it is unique in that its operation can be almost completely automated through external stimulation long after the lung itself is too injured to function normally. However, like any other system in a profound state of injury the lung produces a predictable tirade of inflammatory cytokines^{27,41}. And the lungs vascularity and prominent position in the circulatory system guarantee that this inflammatory response is efficiently exported to all of the major organs systems of the body.

Therefore while mechanical ventilation has the ability to force the physiologically compromised lung to continue to oxygenate a patient's body, in doing so the lung is transformed into a powerful inflammation exporting engine. And because each other organ system has a maximum amount of inflammation it can tolerate before physiological failure, MODS rather than hypoxia is the leading cause of death associated with VILI¹³⁰.

We know that systemic inflammation itself can lead to ARDS which is characterized by lung inflammation/injury, pulmonary edema, and compromised pulmonary mechanics. Thus it is theoretically possible that mechanical ventilation itself is not innately injurious to the lung but rather the circulation of cytokines caused by pre-existing lung pathologies could lead to systemic inflammation which in turn leads to a ventilator induced form of ARDS. However, there are multiple experimental examples that demonstrate that systemic levels of cytokines in the circulatory system are increased by the ventilation of a previously uninjured lung even with "protective" ventilation protocols¹³¹⁻¹³³. This clearly establishes that mechanical forces alone and

the resultant deformations imparted to the lung during mechanical ventilation are sufficient to cause an inflammatory response independent of other factors. This combined with the relatively straightforward nature of measuring, describing, and manipulating the mechanical forces associated with both spontaneous and mechanical ventilation has made modification of ventilation protocols the obvious initial target for the attenuation of VILI. The two most common modifications to ventilation protocols associated with improved patient outcomes are decreased tidal volumes and the inclusion of PEEP in the ventilation cycle¹³⁴.

However, despite the success of these kinds of protocols in attenuating VILI, mortality rates for ventilator patients is still extremely high. The physiological pathway that leads these mechanical forces exerted on the lung to have MODS as their chief cause of death necessarily travels through cellular and inflammatory processes. This means that it is critical to pursue cellular therapeutic targets for VILI as well. Thus just as the known mechanical changes associated with the aging lung immediately suggest themselves as mechanism for increased susceptibility to VILI, an exploration of the MV to MODS inflammatory pathway does the same. There is both a known increase in the inflammatory known age-associated increase in the upregulation of ER stress may further explain the age-associated increase in the severity of VILI and ventilator-associated mortality rates.

Although there is a known increase in the severity of ER stress-associated with age, the underlying mechanisms are not known at this time. To establish a link between this age-associated ER stress and ventilator induced lung injury in a murine model we began by staining lung sections from you young and old mechanically

ventilated murine subjects for CHOP. A qualitative analysis of the alveolar CHOP expression confirmed an elevated level of ER stress-associated with both advanced age and HVT mechanical ventilation.

In order to confirm the role of this ER stress in the inflammatory VILI process we next isolated the effects of age and mechanical both independently and in combination on inflammation and injury. We accomplished this by isolating, culturing, and mechanically stretching young and old ATII cells.

In statically cultured ATII cells we demonstrated that there was a significant increase in the expression of Ccl6, Ccl9, Ccr1, Il10rb, and Nampt with age. With the exception of Il10rb, each of these cytokines are associated with an increased level of inflammation in the lung which is not surprising owing to the known increase in systemic inflammation-associated with advanced age. Ccr1 in particular is the receptor to Ccl3 (MIP-1a) which is known to be upregulated in ventilator induced lung injury. Additionally, the blocking of Ccr1 has been shown to decrease lung damage and neutrophilic infiltration caused by high-pressure ventilation *in vivo*¹³⁵.

There was however no significant increase in expression of these or any other inflammatory genes we measured in our young mechanically stretched ATII groups compared to young static groups. This is somewhat surprising. But when considering the increase in proliferation associated with this group it is entirely possible that the proliferative signaling of 15% cell stretch is not significant to substantially activate pro inflammatory gene pathways in our ATII cells in a 24hr time frame. Multiple studies have suggested that 15% stretch is insufficient to injure young alveolar epithelial cells^{113,116}.

The old AT2 cells were much more sensitive to mechanical stretch. When compared to the gene expression of young cells stretched cells the old cells showed a significant increase in the expression of numerous inflammatory genes. Not surprisingly they showed an increase in the expression of all of the inflammatory genes we saw previously upregulated with age alone.

However, there were a host of pro-inflammatory genes upregulated with only with the combination of age and stretch. These genes are B2m, Ccl2, Ccl3, Ccl4, Ccl7, Cxcl15, IL1a, and IL6. B2m has long been recognized as a potential marker for inflammation, but its role in that process has yet to be elucidated. Furthermore to date no specific role for B2m within the lungs has been established^{136,137}. This is important to note, because B2m is utilized in many models as a housekeeping gene.

Ccl2 is critical to leukocyte recruitment in the lung as well as being a regulator of numerous inflammatory disease states including ARDS, fibrosis, and cancer.^{138–140} As described previously, we demonstrated an age-associated increase in Ccr1 indicating that the aging lung epithelium may already be primed to be more sensitive to Ccl3 which is itself upregulated by mechanical stretch in old ATII cells. Ccl7 has been shown to be a strong regulator of neutrophilic lung inflammation. Antibody neutralization of CCL2 and CCL7 significantly reduced LPS-induced total leukocyte and neutrophil accumulation in the lung alveolar lavage fluid of mice.

Ccl4 (MIP 1-b) is a macrophage inflammatory protein and is well established as a regulator in pulmonary inflammation in host of pathophysiological disease states of the lung^{141,142}. Cxcl15 is a neutrophil recruiting chemokine that is located in many mucosal organs including the gastrointestinal tracts, endocrine organs and adrenal glands.

Cxcl15 is expressed so abundantly in the lung however that it is known as lungkine.

IL-1a is an inflammatory cytokine that operates as an early necrosis alarmin and a juxtacrine signaling molecule¹⁴³. IL-1a release from damaged epithelial cells is both necessary and sufficient to trigger an inflammatory response in human lung fibroblasts.¹⁴⁴ Additionally, IL-1a is an upstream regulator of the senescence associated secretory pathway and the release of IL-6 and IL-8¹⁴³. And lastly IL-6 is a pro-inflammatory cytokine which is involved in a wide variety of inflammatory disease states including VILI¹⁴⁵ and was significantly upregulated in our old stretched cells.

To establish the mechanistic role of ER stress in these age-associated increases in mechanical stretch induced inflammatory gene expression we administered the ER stress inhibitor 4-PBA. As stated previously the mechanism that increases the severity of ER stress with age are currently unknown. However, we hypothesized that the molecular chaperone 4-PBA would still attenuate ER stress in our aged cell model.

Our gene expression results generally validate this hypothesis. There were many inflammatory genes down regulated by the administration of 4-PBA. Of particular interest are the genes B2m, Ccl7, Cxcl15, IL-6. Each of these 4 inflammatory genes is known to contribute to pathological inflammatory processes in the lung, each was upregulated in the previous experiment with a combination of advanced age and stretch, and each was successfully downregulated with the administration of ER stress inhibitor 4-PBA alone.

Ccl6 and Ccl9 gene expression were both upregulated in old stretched cells VS static old cells as well. And the gene expression of both were reduced with 4-PBA treatment. However, since these were also both elevated in static old cells VS static

young cells their role in mechanical stretch induced inflammation is less clear.

Tnfrsf11b was also downregulated by 4-PBA but the meaning is also less than straightforward. Tnfrsf11b is a decoy receptor for Nf-kb and is thought to mainly function as an inflammatory inhibitor. It is also known to play an important role in inhibiting osteoclastogenesis but its role in the lung epithelium is unknown to date¹⁴⁶. It is possible that if this gene is activated to attenuate inflammation then a 4-PBA induced reduction in inflammation may have reduced upstream activation of Tnfrsf11b gene expression.

Lastly and most puzzlingly, there was a 4-PBA induced increase in IL-1a expression. IL-1a is known only as an inflammatory cytokine and has no known anti-inflammatory roles that would suggest a reason why it and it alone would be upregulated in old stretched cells treated with 4-PBA.

To further establish the translatability of these results into a novel *in vivo* target for treatment of VILI we investigated the 4-PBA induced changes in concentrations of inflammatory cytokines secreted into the cell media. These results revealed the inhibition of the secretion of several different inflammatory cytokines. Furthermore the patterns of changes are generally in good agreement with the with the corresponding changes 4-PBA induced changes in gene expression.

IL-6, Ccl2 (MCP-1), Cc-I4 (MIP-1b), and RANTES media concentrations were all significantly decreased with ER inhibition in both stretched and statically cultured ATII cells. Of these RANTES is the only one not already discussed thus far. RANTES is pro-inflammatory neutrophil recruiter implicated in multiple pathological pulmonary inflammatory conditions including pulmonary fibrosis, lung cancer, and viral lung

infections¹⁴⁷⁻¹⁴⁹. 4-PBA upregulated IL-10 media concentration in both stretched and static old cells. IL-10 has a somewhat complex role in the pulmonary has an inflammatory process but is primarily anti-inflammatory supporting results of the 4-PBA as attenuating ER stress

Additionally, 4-PBA treatment upregulated media concentrations of both IL-1a and IL-1b in stretched and statically cultured old cells. This result is internally consistent with our findings regarding the upregulation of IL-1a and IL-1r1 gene expression. It confirms that these gene expression results are not just anomalous gene results but rather translate into a meaningful difference in the cytokine excretion into the cell media. The meaning of this effect and how to integrate it with known inflammatory physiology is however unclear.

And lastly, the media concentration of Ccl3 (MIP1a) is strongly upregulated in media samples of both stretch and static old cells treated with 4-PBA. This result is difficult to contextualize for two reasons. Firstly, this is the only protein secretion result that seems to be at odds with our gene expression data. While 4-PBA decreased the Ccl3 gene expression, it seems to have increased the secretion of Ccl3 cells into the surrounding media. Additionally, there is not an easily forthcoming explanation based on our current understanding of MIP-1a and MIP-1b for why there would be any single chemical chaperone what would have the effect of simultaneously and promoting and attenuating the excretions of these two cytokines respectively.

In summation with the exception of Ccl3 of effects of 4-PBA treatments on cell media cytokine concentrations are in good agreement with the gene expression data. And with the exception of an upregulation of IL-1a the gene expression data is in good

agreement with our hypothesis that 4-PBA successfully attenuates the age-associated stretch induced increase in inflammatory gene expression.

4.0.0

VitC treatment attenuates VILI induced pulmonary edema and partially normalized pulmonary mechanics.

4.1.0 Introduction

The pulmonary system is unique in its design in that each incremental step towards its most distal region sees a meaningful increase in the complexity of the mechanical, molecular, and physiological environment^{7,24}. This organizational facet of the pulmonary systems owes in part to the exponential manner in which succeeding generations decrease in size terminating with the alveolar sacs having a structure in the micrometer range. Furthermore the contribution to the lungs primary function of gas exchange exhibit a parallel asymmetry with the alveolar sacs hosting of 90% of all gas exchange. Thus the alveolar barrier is at once one of the most complex, biologically essential, difficult to observe, and consequently least well understood regions of the body. Not surprisingly many pathophysiological conditions of the alveolar barrier are poor elucidated as well.

Furthermore the molecular pathophysiological effects of aging have only begun to be recognized and thoroughly studied relatively recently. Thus the effects of aging on alveolar barrier function are at a time both of such critical importance and so understudied that the American journal of physiology has put out a call for studies on this topic. Since then there have been some studies conducted to establish the

pathophysiology of senescent alveolar cell types and the aging extra cellular network but few studies address the effect of aging on alveolar barrier integrity directly. In addition to our investigation of the aging lung and its interaction with VILI, in this project we are involved in an ongoing investigation of VitC as a possible treatment for VILI and other lung pathologies.

VitC is an essential nutrient for humans and many other animal species which means that prolonged VitC deficiency results in a myriad of serious health complications and eventually results in death¹⁵⁰. VitC has a number of vitamers including its reduced form ascorbic acid (AscA) and its anion ascorbate¹⁵¹. Most animals that require VitC are able to fully meet their requirements by synthesizing VitC from glucose. Humans and other primates however cannot synthesize VitC as a result of a loss of function in the gene for the enzyme *L-gulono-gamma-lactone oxidase (Gulo)* which is required in the terminal step of ascorbate synthesis. By contrast, mice and rats produce endogenous VitC and maintain high levels of ascorbate in their tissues. This complicates the translatability of VitC studies from mice and rats to humans. To overcome this limitation C57BL/6J wild type mice (WT) with a homozygous knockout of the crucial *Gulo* producing gene (*gulo*^{-/-} mice) are often employed for VitC research¹⁵². Additionally, (WT) mice with a knockout of senescence marker protein-30 (SMP30) are unable to synthesize VitC and are useful for VitC research as well¹⁵³.

VitC has many known biological functions all of which originate from its chemical activities as a 1- or 2-electron reducing agent for several antioxidants¹⁵¹. Specialized cells throughout body can take up AscA through Na⁺-dependent ascorbate cotransporters (SVCT1 and SVCT2). Most other cells take up VitC in its oxidized form

(DHA) via facilitative glucose transporters¹⁵⁴. VitC is also a known cofactor in at least 8 enzymatic reactions 7 of which are collagen synthesis reactions. As a result VitC's corresponding avitaminosis, scurvy, is characterized by a generally increase in sensitivity to oxidative stress. Additionally, over time VitC deficiency promotes malformation of collagen in many of the bodies tissues including the skin, gums, cartilage, blood vessel walls, and lung parenchyma¹⁵⁰. These malformations can lead to bruising, bleeding, and inhibited wound healing in all of these tissues.

In addition to the generalized effects, VitC deficiency is known to have multiple pathogenic effects on the lung. VitC deficient *gulo*^{-/-} mice have been experimentally shown to have an increased lung pathology following infection with influenza¹⁵⁵. One study also showed that by their third month of life VitC deficient SMP 30 knockout mice showed an 82.2% decrease in collagen I mRNA and the development of emphysema (21.6% increase of mean linear intercepts (MLI) and 42.7% increase of destructive index measured as described by Koike et al¹⁵⁶).

VitC levels have been shown to decrease with age in both humans and in animals who make their own VitC. An analysis of the ascorbic acid levels in the hepatic cells of 24-26 month old rats showed a 68% decrease from the levels seen in 3-5 month old rats¹⁵⁷. Similarly in humans it has been known for several decades that serum levels of VitC decrease with age. A meta-analysis of 30 publications showed a significantly lower serum plasma VitC level older adults (aged 60-96) than in younger adults (aged 15-65) with similar VitC intake¹⁵⁶. The exact reason for this disparity is not yet known however one study demonstrated that in older rats there was a 45% decrease in the mRNA levels of one of the isoforms of the sodium dependent VitC

transporter (SVCT1)¹⁵⁷. Furthermore there are multiple studies which suggest that the decrease in VitC associated with aging promote the development of chronic obstructive pulmonary disease^{158,159}. All of this research suggests that elderly people have both higher VitC requirements than the young and a greater susceptibility to lung and injury are related illnesses because of decreased VitC levels.

There are also experiments that demonstrate that levels of VitC that far exceed those found in human and murine plasma and tissues can have a therapeutic effect. In one experiment fibroblasts derived from human skin biopsies were cultured separated in groups that were passaged 5, 10, 15, 20, 25 or 30 times respectively¹⁶⁰. Cells that were passage 20 or more times showed a significant loss of all enzyme activities. The addition of ascorbate to the cell media equivalent to that of normal human plasma concentrations ($100 \mu\text{mol l}^{-1}$) had no effect on the enzyme activities of the fibroblasts. The addition of $300 \mu\text{mol l}^{-1}$ ascorbate however totally restored Complex II-IV and citrate synthase activities and partially restored the activity of Complexes I-III.

VitC has also been shown recently to be a powerful regulator of sepsis across several experimental models and of sepsis induced ALI. Sepsis is a leading cause of death in the United States and is the most common cause of death among critically ill patients outside of coronary intensive care units¹⁶¹. The respiratory tract is the most common site of septicemic infection and is associated with the highest mortality. Patients who develop severe sepsis have a 25% in hospital mortality rate which jumps to 50% in the case of septic shock. The incidence of severe sepsis in the United States is estimated to be 300 cases per 100,000 population and septicemia related hospital costs are estimated at \$14 annually. MODS is the leading cause of

death in sepsis patients and consequently the number of organs failing and the degree of organ dysfunction is the leading predictor of patient mortality¹⁰⁹. Additionally, septicemia incidence and septicemia-related deaths have increased over the past 2 decades in United States.

It is also known that a significant percentage of patients with severe sepsis develop acute lung injury (ALI)¹⁶². Thus inducing sepsis is frequently used in *in vivo* animal models to experimentally induce ALI. Sepsis is known to compromise alveolar barrier integrity in a number of ways stemming from its associated systemic pro inflammatory responses and the degradation of endothelial tight cell junctions¹⁶³. The immune inflammatory response to the initial onset of sepsis is activation and tissue infiltration of polymorphonuclear neutrophils PMNs. In the microenvironment of the alveolus PMNs upregulate inflammation, increase the permeability of microvascular barriers, and promote in extravascular accumulation of protein-rich edema fluid. Alveolar infiltration of PMN is a hallmark of ALI and is known to be a primary mechanism for sepsis-induced pulmonary dysfunction and injury^{154,164,165}.

This PMN infiltration and the general inflammatory pathway that lead sepsis to promote ALI is strongly regulated by NFkB. NFkB is proinflammatory transcription factor that plays a key role in host defense, inflammation, and apoptosis^{164,165}. NFkB is activated by proinflammatory cytokine induced phosphorylation and degradation of inhibitor kB proteins. And TNFa induced NFkB activation has been shown to be inhabitable with VitC in multiple studies and over multiple cell population.

Sepsis is also associated with a profound systemic oxidative stress which not surprisingly has been demonstrated to severely lower antioxidant level in patient plasma

including AscA. Therefore not surprisingly low levels of AscA correlate with multiple organ system failure and inversely with patient survival¹⁵⁴. It has also already been shown experimentally that in VitC deficient animal models of sepsis that parenteral ascorbate attenuates the effects of sepsis^{154,166}. Experiments have also shown that in WT mice administered parenteral VitC treatments have a strong therapeutic effect on sepsis induced ALI.

Sepsis is modeled in a variety of ways *in vivo*. Endotoxin, a component of the outer membrane of Gram-negative bacteria, is involved in the pathogenesis of sepsis, and an LPS infusion/injection model has been widely used for sepsis research. LPS administration induces systemic inflammation that mimics many of the initial clinical features of sepsis, including increases in proinflammatory cytokines such as TNF- α and IL-1, but without bacteremia¹⁶⁷.

Sepsis also has a powerful interaction with patient age. Sepsis is the tenth leading cause of death in patients over the age of 65 in the US since. Advanced aged patients also account for 58–65% of all sepsis patients. Additionally, both the incidence and mortality rates of sepsis patients increase significantly with advanced age¹⁶⁸

Owing to the fact that inhibition of LPS induced NFkB activation had not yet been investigated, our collaborators conducted an *in vivo* study of VitC treatment on LPS induced sepsis and ALI. ALI was induced in WT mice with an injection of a lethal lipopolysaccharide (LPS) dose (10 ug/g of body weight). 30 minutes after the LPS injection mice either received an intraperitoneal (i.p.) injection of 200 mg/kg AscA, the oxidized form of AscA (DHA) at 200 mg/kg, or saline. There was a 100% mortality after 28 hours for mice receiving saline. In contrast there was a 60% survival for mice

receiving AscA and a 75% survival rate for mice receiving DHA even after 72 hours. In addition compared to saline controls, WT mice treated with AscA/DHA had suppressed inflammatory chemokine expression, decreased microvascular thrombosis in the lungs, suppressed proinflammatory gene expression, and attenuated neutrophilic capillaritis and vascular leak in the lungs.

Another common method for modeling sepsis is through injection of fecal solution known as fecal-induced peritonitis (FIP). Conventional animal models of sepsis are typically microbial-based responses which may be mono- or poly-microbial in design. Using a single organism results in a septic state that is dependent on the type and amount used as well as the animal and route of administration, whereas a polymicrobial model typically mimics intra-abdominal sepsis, which affects 20% of patients admitted with sepsis. Polymicrobial models of sepsis typically involve either FIP or cecal ligation and puncture (CLP). In the FIP model, a freshly prepared fecal solution is derived from murine colonic stool and injected intraperitoneally into mice at a defined concentration to result in acute peritonitis^{163,169}.

Additionally, the same research group performed experiments directly tested the effects of VitC deficiency on sepsis induced ALI in mice with and without VitC treatment. Sepsis was induced with an i.p. injection of fecal stem solution which induced peritonitis (FIP). They showed that the pathogenic effects of sepsis induced ALI were strongly attenuated in VitC sufficient *gulo*^{-/-} mice (*gulo*^{-/-} supplemented with dietary VitC) and in VitC deficient *gulo*^{-/-} mice treated 30 minutes after FIP exposure with 200 mg/kg AscA compared to their VitC deficient *gulo*^{-/-} counterparts that received only saline treatment. *Gulo*^{-/-} mice who had either VitC supplementation or VitC treatment had less

proinflammatory response in the lung, greater capillary barrier function in the lung, less lung water accumulation, and better preservation of their lung architecture than mice without any VitC treatment and the mice with both VitC supplementation and VitC treatment had the greatest attenuation of sepsis induced ALI¹⁵⁴.

In addition to its usefulness in experimentally inducing ALI, sepsis bears a close resemblance to the disease process of VILI. Experiments employing gene array methodology to measure lung gene expression have identified differential patterns of gene expression in animal models of VILI which are similar to those gene pathways activated during experimental and clinical sepsis^{170,171}. All of this has lead our group to hypothesize that VitC treatments would confer a protective effect against ventilator induced lung injury to our older mouse subjects.

Just as with LPS induced ALI, we hypothesize that VitC treatment's down regulation of NFkB, decrease of alveolar barrier permeability, and restoration of alveolar barrier integrity will attenuate VILI induced edema in our aged mice. And based on the wide spread protective effect that our novel low fluid protocol conferred we hypothesis that VitC attenuation of edema will decrease injury and inflammation, improve pulmonary mechanics, and increase subject survival. To test this hypothesis we ventilated old mice old mice each either receiving VitC treatment or sham. During ventilation we measured pulmonary mechanics. After ventilation treatments each mouse was sacrificed and lung we to dry ratios were measured.

4.2.0 Methods

4.2.1 Animal Use: This study was approved by the VCU Institutional Animal Care and Use Committee (protocol number AD10000465). Male C57BL6 mice were used in these experiments. All animal experiments were carried out under IACUC University guidelines.

4.2.2 Age Groups: Old animals, 20-22 months of age, weighing 35 ± 11 g. Ages of our murine subjects were based on correlations between murine lifespan and known age-associated morphological changes in murine lung (17)(29).

4.2.3 Mechanical Ventilation: 20 month old Murine subjects were anesthetized and mechanically ventilated for 1 hour using the same protocols outlined in chapter 2 methods section.

4.2.4 VitC Treatment: Each VitC treatment mouse received an IP injection of 200 mg/kg AscA in 100ul saline immediately prior to ventilation. Control mice received a VitC sham IP injection of 100ul saline just prior to ventilation.

4.2.5 Pulmonary Mechanics: Pulmonary mechanics measurements were taken for each subject at the 0hr and 1hr time points using the same protocol described in chapter 2 methods.

4.2.6 Lung Wet to Dry Ratios: After 1hr each subject was sacrificed, its lungs were removed, and wet to dry ratios were collected using methods described in chapter 2 methods.

4.2.7 Data Analysis: Data analysis was performed on the pulmonary mechanics and wet to dry ratio data using the same methods outlined in the chapter two methods section.

4.3.0 Results

4.3.1 One Hour Lung Wet to Dry Ratios: Wet to dry ratios for each of the old 1hr groups (figure 38). The wet to dry ratios for HVT high fluid subjects receiving VitC protocol was significantly lower than that observed in all other old groups (figure 38). The wet to dry ratio of old HVT subjects receiving low fluid protocol was significantly lower than that observed in the old HVT subjects who received high fluid protocol and the old non-ventilated group (figure 38).

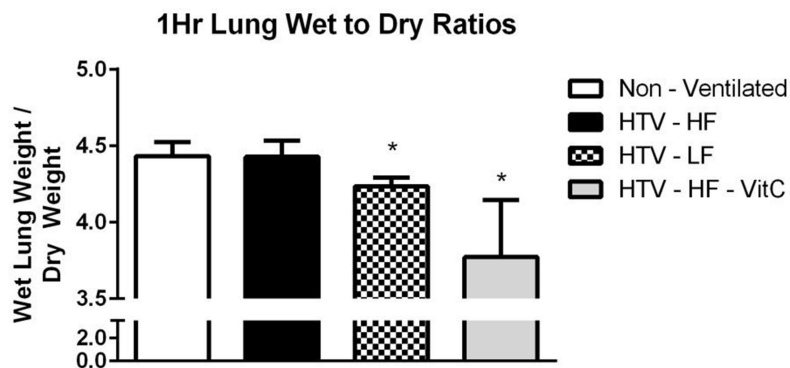


Figure 38: 1Hr Lung Wet to Dry Ratios. The Old HVT-HF-LF and Old HVT-HF-VitC groups were significantly lower than that of Old non-ventilated and Old HVT-HF groups. Data are presented as mean +/- st.dev N = 3, *p<0.05

4.3.2 PV Loop Hysteresis: PV loops were generated hourly using the Flexivent software (Scireq) for each surviving subject. Representative PV loops shown in figure 39. The hysteresis values of each group were normalized with respective 0hr values (figure 39). 1Hr PV loop hysteresis of Old HVT high fluid group was significantly greater than that of the Old HVT low fluid and Old HTV high fluid VitC group (figure 39).

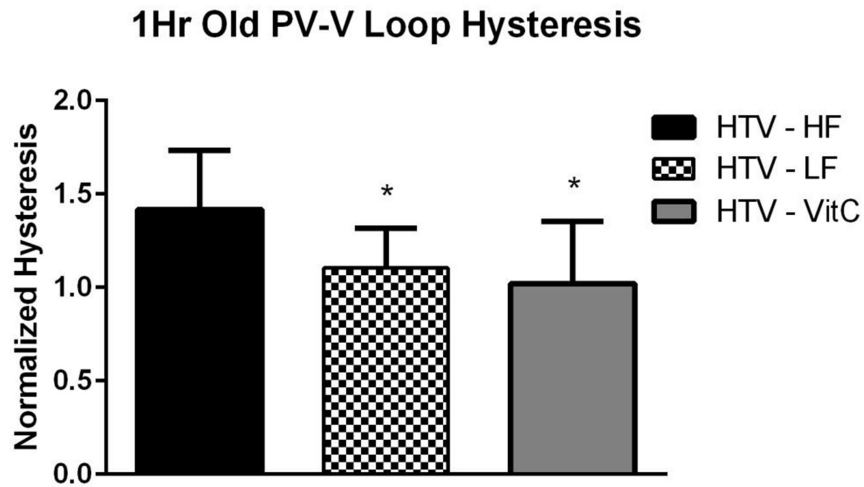


Figure 39: 1Hr PV Loop Hysteresis. Hysteresis in the Old HVT-LF and Old HVT-HF-VitC group were significantly greater than Old HVT HF. Data are presented as mean +/- st.dev N=3, *p<0.05

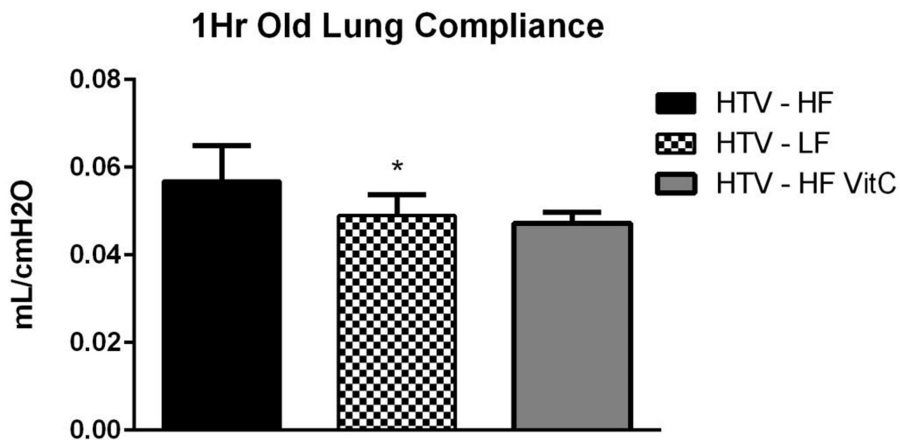


Figure 40: 1Hr Lung Compliance. Lung Compliance in the Old HVT-LF group was significantly lower than Old HVT-HF. Data are presented as mean +/- st.dev N=3, *p<0.05

4.3.3 Lung Compliance: Lung compliance was measured hourly using the Flexivent software (Scireq) for each surviving animal subject (figure 40). The 1Hr lung compliance of the old HVT high fluid group was significantly greater than that of the HVT low fluid group. There was a strong non-significant trend with the old 14Hr HVT high fluid VitC group having a lower mean than the old 4Hr high fluid group that fell just

short of significance. This HTC VitC has no significant differences with the HTV-LF values with a one way anova P-value of .08. However, due to the need to exclude one data outlier the groups has an N value of only N= 2. We suspect this relationship will become significant with additional subjects.

4.4.0 Discussion

The only ventilation mechanics statistic that was collected but yielded no significance was the measurement of inspiratory capacity. The low fluid treatment was able to create a treatment based difference in the inspiratory capacity but it is possible that one hour is simply insufficient for the VitC treatments to remodel this aspect of the pulmonary mechanics.

The success of these early results is highly promising and offers a potentially powerful therapeutic option for patients requiring mechanical ventilation. Considering the natural decrease in VitC levels associated with age and the corresponding increase in the severity of VILI seen with increasing patient age this development of age based VitC treatments protocols for patients requiring mechanical ventilation may be critically important for ensuring the health and wellbeing of elderly patients.

5.0.0

Implications of completed work

Close to a million patients in the US require mechanical ventilation annually. Knowing that proper mechanical ventilation can literally mean the difference between life and death for many of these patients means that the importance of mechanical ventilation

cannot be overstated. Additionally, for a patient population this large, a 30% in hospital mortality rate is devastating. However, the historical perspective on this mortality rate is very elucidating as well. As recently as the 1970's the in hospital mortality rate of patients with severe ARDS was 90%¹⁷². And there are still particularly vulnerable patient populations today. For example patients requiring MV as a result of ischemic stroke have a short term mortality rate of 50-90%¹⁷³. In fact many of the most common comorbidities with mechanical ventilation (ARDS, Phenomena, COPD, etc.) are known to increase ventilator-associated mortality rates.

This reinforces the urgency with which we must not only drive down the overall ventilator-associated patient mortality rates, but also identify populations particularly sensitive to VILI and tailor specific treatments for them. Demographically the largest sub population of ventilator patients with a significantly increased risk of mortality is the elderly. In fact, patients over the age of 65 represent over half of all mechanically ventilated patients. Furthermore the aging population in the US is poised to precipitously grow over the next few decades¹⁷⁴ which will only see an increase in the urgency with which we must address this issue. While some of the mechanical changes of the lung associated with aging have been studied and understood for the better part of the last century, aging on the cellular level has only recently been studied.

Our initial four hour injurious mechanical ventilation protocol, while readily survivable by young mice, proved to be too challenging for our older subjects with very few surviving. In searching for protocol modifications that would aid elderly subject survival we discovered a recent research consensus and resultant recommendation from ARDSNet concerning the protective effects of fluid restriction. Critically ill ARDS

patients with conservative fluid management had consistently better outcomes than those treated with liberal fluid protocols. We hypothesized that a conservative fluid protocol might confer protection to our aging VILI subjects as well.

Despite our hypothesis, our level of success at increasing the survival of our older subjects by simply changing their fluid treatment protocol was more dramatic than we had originally anticipated. A careful examination of the presence of pulmonary edema as well as other markers of inflammation and injury clearly indicated that our conservative fluid protocol alone was capable modulating VILI-associated edema. Furthermore it established that resolution of this edema has a strong protective effect on other downstream ventilator induced injuries.

Pulmonary edema is well established as a hallmark of VILI and is considered to be a downstream inevitability of the type lung damage and inflammation there in. What is so unique about this research is its establishment that pulmonary edema is actually upstream of much of the injury and inflammation associated and VILI and that the resolution of edema alone can dramatically increase the survival of elderly murine subjects.

The implication of the research for elderly ventilator patients is both dramatic and immediate. However, just as with all biomedical challenges it is important to pursue multiple vectors of attack. Identifying pulmonary edema as a target in the age-associated increase in ventilator-associated mortality opens the door for us to both seek a more mechanistic explanation of these underlying processes and to pursue additional treatment targets.

Moving forward, we had to attempt to answer the question as to why the lungs of

our young subjects were so readily able clear or even avoid the accumulation addition¹⁷ al of alveolar fluid load but this challenge proved fatal for our older subjects. The answer to this question begins with the fulfilment of our second specific aim. Our understanding of the aging lung epithelium as a physiological unit is radically underdeveloped. Currently there are no major physiological mechanisms of the aging alveolar epithelium itself that have been identified as major contributors to VILI.

Inflammation itself however, especially the presence of inflammatory cytokines, is known to severely compromise epithelial barrier integrity and in the micro environment of the lung strongly promoted edema. Furthermore there has been a recent explosion in the understanding of the role of biotrauma as a mechanism of VILI. Furthermore, ER stress is known to play a key role in many organ systems and pathological disease states to promote age associate increases in inflammation. We hypothesized that ER stress was likely a key player in the age-associated increase in VILI as well.

Knowing that stretch induced inflammation and injury can be achieved in cultured primary alveolar epithelial cells, we hypothesized that cells harvested from old mice would be significantly more injured/inflamed than young. Furthermore if our hypotheses were correct, we would be able to attenuate this age-associated increase in inflammation with the administration of an ER stress inhibitor. Our success at achieving this result validates our hypothesis and establishes the importance of ER stress in the age-associated increase in alveolar epithelial inflammatory response to mechanical stretch. To establish the effect of this relationship on the development VILI-associated edema in vivo experiments are clearly needed and represent an obvious avenue for future research.

The success of both of our first aims direct us to further expand our search for treatments that might further fortify the alveolar epithelial barrier against insult and injury. Our first aim identifies pulmonary edema as an important mechanism for the age-associated increase VILI mortality rates in our subjects. Inflammation is known to be a powerful promoter of alveolar edema and the completion of our second aim offers a possible age-associated inflammatory mechanism driving our VILI-associated edema. So an ideal preventative treatment for VILI would be one that was profoundly anti-inflammatory, was known to decrease alveolar permeability, and had already been proven to dramatically decrease pulmonary edema. VitC is well known to be anti-inflammatory, to decrease alveolar membrane permeability, and VitC treatments have been shown to aid in the resolution of pulmonary edema. Additionally, VitC has already been shown to have a dramatic effect on both ARDS and Sepsis. This is also particular value in a potential VILI treatment owing to the fact that these diseases more than any others either mimic or are direct pro/antecedent to VILI.

We naturally hypothesized that VitC would confer a protective effect to our older murine subjects and attenuate their VILI-associated edema and the downstream injurious effects. Our pilot study confirmed just this by showing a dramatic decrease in the wet to dry ratios of old subjects treated with VitC prior to HVT mechanical ventilation. Furthermore, impaired pulmonary mechanics which were identified in our first project to be a downstream effect of VILI-associated edema were attenuated as well. These preliminary results provide a strong proof of concept that VitC treatments can attenuate the age-associated increase in VILI-associated edema. The next experimental step is clearly outlined and will consist of a repeating our previous survival

study with the addition of VitC treated subjects.

Each of these aims contributes indispensably to the picture of how the aging lung interacts with VILI. The repositioning of pulmonary edema as a “mid-stream” mechanism in VILI for the first time opens up anti-edema measures as a powerful protective therapeutic target. Additionally, the identification of ER stress as a regulatable source of age-associated stretch induced alveolar epithelial inflammation makes the ER an invaluable target for attenuating age-associated pulmonary edema. And finally the success that VitC has already enjoyed as a treatment for ARDS and sepsis in mice combined with our pilot data demonstrating its ability to attenuate VILI-associated edema starkly confirm the need for its pursuance as a preventative treatment for VILI.

Our sincerest hope is that all three of these experimental avenues both independently and in consort will push forward the development of much needed lifesaving age dependent ventilator protocols in clinic.

References

1. McNulty, W. & Usmani, O. S. Techniques of assessing small airways dysfunction. *Eur. Clin. Respir. J.* **1**, (2014).
2. Kerr, J. B. *Functional Histology*. (Elsevier Mosby Australia, 2010).
3. File:Alveolus diagram.svg. *Wikipedia, the free encyclopedia*
4. Sherwood, L. & Sherwood, L. *Human physiology : from cells to systems*. (Australia ; United States : Brooks/Cole, Cengage Learning, 2010).
5. Weibel, E. R. Morphological basis of alveolar-capillary gas exchange. *Physiol. Rev.* **53**, 419–495 (1973).
6. Toshima, M. Three-dimensional architecture of elastin and collagen fiber networks in the human and rat lung. *Arch. Histol. Cytol.* **67**, 31 (2004).
7. Hicks, G. H. & Hicks, G. H. *Cardiopulmonary anatomy and physiology*. (Philadelphia : W.B. Saunders, 2000).
8. Meyer, K. C., Ershler, W., Rosenthal, N. S., Lu, X. G. & Peterson, K. Immune dysregulation in the aging human lung. *Am. J. Respir. Crit. Care Med.* **153**, 1072–1079 (1996).
9. Lumb, A. B. *Nunn's applied respiratory physiology*. (Edinburgh : Churchill Livingstone; Askews and Holts, 2010).
10. Cotes, J. E., Chinn, D. J. & Miller, M. R. *Lung Function: Physiology, Measurement and Application in Medicine*. (Wiley, 2009).
11. Rogers, D. F. Physiology of airway mucus secretion and pathophysiology of hypersecretion. *Respir. Care* **52**, 1134–1146; discussion 1146–1149 (2007).
12. ROGERS, D. F. & ROGERS, D. F. *AIRWAY GOBLET CELLS - RESPONSIVE AND ADAPTABLE FRONT-LINE DEFENDERS.* **7**,

13. Ochs, M. *et al.* The number of alveoli in the human lung. *Am. J. Respir. Crit. Care Med.* **169**, 120
14. Antranik. The Respiratory System. *Antranik.org* Available at: <http://antranik.org/the-respiratory-system/>. (Accessed: 11th August 2016)
15. Crandall, E. D., M., Crandall, E. D. & Matthay, M. A. Alveolar epithelial transport. Basic science to clinical medicine. *Am. J. Respir. Crit. Care Med.* **163**, 1021
16. Flodby, P. *et al.* Knockout Mice Reveal a Major Role for Alveolar Epithelial Type I Cells in Alveolar Fluid Clearance. *Am. J. Respir. Cell Mol. Biol.* (2016). doi:10.1165/rcmb.2016-0005OC
17. Wong, M. H. & Johnson, M. D. Differential Response of Primary Alveolar Type I and Type II Cells to LPS Stimulation. *PLOS ONE* **8**, e55545 (2013).
18. Berthiaume, Y., Voisin, G. & Dagenais, A. The alveolar type I cells: the new knight of the alveolus? *J. Physiol.* **572**, 609–610 (2006).
19. Meyer, K. & Meyer, K. Lung Surfactants: Basic Science and Clinical Applications. *Crit. Care Med.* **30**, 266
20. Roan, E. & Waters, C. M. What do we know about mechanical strain in lung alveoli? *Am. J. Physiol. Lung Cell. Mol. Physiol.* **301**, L625–635 (2011).
21. Vaccaro, C. A., B., Vaccaro, C. A. & Brody, J. S. Structural features of alveolar wall basement membrane in the adult rat lung. *J. Cell Biol.* **91**, 427
22. Rubins, J. B. Alveolar macrophages: wielding the double-edged sword of inflammation. *Am. J. Respir. Crit. Care Med.* **167**, 103–104 (2003).
23. Alveolar macrophage seeking E. coli. Available at: <http://www.denniskunkel.com/detail/180.html>. (Accessed: 11th August 2016)
24. Cotes, J. E. & Cotes, J. E. *Lung function : physiology, measurement and application in medicine.* (Malden, Mass. ; Oxford : Blackwell Pub, 2006).

25. Harris, R. S. Pressure-volume curves of the respiratory system. *Respir. Care* **50**, 78–98; discussion 98–99 (2005).
26. Gattinoni, L. *et al.* Physical and biological triggers of ventilator-induced lung injury and its prevention. *Eur. Respir. J.* **22**, 15s–25s (2003).
27. Gattinoni, L., Protti, A., Caironi, P. & Carlesso, E. Ventilator-induced lung injury: the anatomical and physiological framework. *Crit. Care Med.* **38**, S539–548 (2010).
28. Plötz, F. B., Slutsky, A. S., van Vught, A. J. & Heijnen, C. J. Ventilator-induced lung injury and multiple system organ failure: a critical review of facts and hypotheses. *Intensive Care Med.* **30**, 1865–1872 (2004).
29. Wunsch, H. *et al.* The epidemiology of mechanical ventilation use in the United States. *Crit. Care Med.* **38**, 1947–1953 (2010).
30. Slutsky, A. S. & Ranieri, V. M. Ventilator-induced lung injury. *N. Engl. J. Med.* **369**, 2126 (2013).
31. Carrasco Loza, R., Villamizar Rodríguez, G. & Medel Fernández, N. Ventilator-Induced Lung Injury (VILI) in Acute Respiratory Distress Syndrome (ARDS): Volutrauma and Molecular Effects. *Open Respir. Med. J.* **9**, 112–119 (2015).
32. Pesau, B. *et al.* Influence of age on outcome of mechanically ventilated patients in an intensive care unit. *Crit. Care Med.* **20**, 489–492 (1992).
33. Burr, M. L., Phillips, K. M. & Hurst, D. N. Lung function in the elderly. *Thorax* **40**, 54–59 (1985).
34. Janssens, J.-P. Aging of the Respiratory System: Impact on Pulmonary Function Tests and Adaptation to Exertion. *Clin. Chest Med.* **26**, 469–484 (2005).
35. Dreyfuss, D., Soler, P., Basset, G. & Saumon, G. High Inflation Pressure Pulmonary Edema: Respective Effects of High Airway Pressure, High Tidal Volume, and Positive End-expiratory Pressure. *Am. Rev. Respir. Dis.* **137**, 1159–1164 (1988).

36. Plötz, F. B. *et al.* Mechanical ventilation alters the immune response in children without lung pathology. *Intensive Care Med.* **28**, 486–492 (2002).
37. Kotecha, S. *et al.* The role of neutrophil apoptosis in the resolution of acute lung injury in newborn infants. *Thorax* **58**, 961 (2003).
38. Pugin, J. *et al.* Activation of human macrophages by mechanical ventilation in vitro. *Am. J. Physiol. - Lung Cell. Mol. Physiol.* **275**, L1040–L1050 (1998).
39. Lukkarinen, H. P., Laine, J. & Käätä, P. O. Lung epithelial cells undergo apoptosis in neonatal respiratory distress syndrome. *Pediatr. Res.* **53**, 254–259 (2003).
40. Hammerschmidt, S. *et al.* Mechanical stretch alters alveolar type II cell mediator release toward a proinflammatory pattern. *Am. J. Respir. Cell Mol. Biol.* **33**, 203–210 (2005).
41. Halbertsma, F. J. J., Vaneker, M., Scheffer, G. J. & van der Hoeven, J. G. Cytokines and biotrauma in ventilator-induced lung injury: a critical review of the literature. *Neth. J. Med.* **63**, 382–392 (2005).
42. Douzinas, E. E. *et al.* The regional production of cytokines and lactate in sepsis-related multiple organ failure. *Am. J. Respir. Crit. Care Med.* **155**, 53–59 (1997).
43. Whitehead, T. C., Zhang, H., Mullen, B. & Slutsky, A. S. Effect of mechanical ventilation on cytokine response to intratracheal lipopolysaccharide. *Anesthesiology* **101**, 52–58 (2004).
44. Imai, Y. *et al.* Injurious mechanical ventilation and end-organ epithelial cell apoptosis and organ dysfunction in an experimental model of acute respiratory distress syndrome. *JAMA J. Am. Med. Assoc.* **289**, 2104 (2003).
45. The Acute Respiratory Distress Syndrome. Ventilation with lower tidal volumes as compared with traditional tidal volumes for acute lung injury and the acute respiratory distress syndrome. The Acute Respiratory Distress Syndrome Network. *N. Engl. J. Med.* **342**, 1301–1308 (2000).

46. Ventilation with Lower Tidal Volumes as Compared with Traditional Tidal Volumes for Acute Lung Injury and the Acute Respiratory Distress Syndrome. *Surv. Anesthesiol.* **45**, 19–20 (2001).
47. Corti, M., Brody, A. R. & Harrison, J. H. Isolation and primary culture of murine alveolar type II cells. *Am. J. Respir. Cell Mol. Biol.* **14**, 309–315 (1996).
48. Matthay, M. A., Folkesson, H. G. & Clerici, C. Lung epithelial fluid transport and the resolution of pulmonary edema. *Physiol. Rev.* **82**, 569 (2002).
49. Lemyze, M. & Mallat, J. Understanding negative pressure pulmonary edema. *Intensive Care Med.* **40**, 1140–1143 (2014).
50. Matthay, M. A. Resolution of pulmonary edema. Thirty years of progress. *Am. J. Respir. Crit. Care Med.* **189**, 1301–1308 (2014).
51. Zhang, Z. & Chen, L. The association between fluid balance and mortality in patients with ARDS was modified by serum potassium levels: a retrospective study. *PeerJ* **3**, e752 (2015).
52. Edoute, Y., Roguin, A., Behar, D. & Reisner, S. A. Prospective evaluation of pulmonary edema. *Crit. Care Med.* **28**, 330 (2000).
53. de Prost, N., Ricard, J.-D., Saumon, G. & Dreyfuss, D. Ventilator-induced lung injury: historical perspectives and clinical implications. *Ann. Intensive Care* **1**, 1–15 (2011).
54. Capaldo, C. T. & Nusrat, A. Cytokine regulation of tight junctions. *BBA - Biomembr.* **1788**, 864–871 (2009).
55. Baudouin, S. Ventilator induced lung injury and infection in the critically ill. *Thorax* **56**, ii50–ii57 (2001).
56. Putensen, C., Theuerkauf, N., Zinserling, J., Wrigge, H. & Pelosi, P. Meta-analysis: ventilation strategies and outcomes of the acute respiratory distress syndrome and acute lung injury. *Ann. Intern. Med.* **151**, 566–576 (2009).

57. Paxson, J. A. *et al.* Age-dependent decline in mouse lung regeneration with loss of lung fibroblast clonogenicity and increased myofibroblastic differentiation. *PLoS One* **6**, e23232 (2011).
58. Janssens, J. P., Pache, J. C. & Nicod, L. P. Physiological changes in respiratory function associated with ageing. *Eur. Respir. J.* **13**, 197 (1991).
59. Setzer, F. *et al.* Susceptibility to ventilator induced lung injury is increased in senescent rats. *Crit. Care* **17**, R99 (2013).
60. Zhang, Y.-W. *et al.* Reduced lung water transport rate associated with downregulation of aquaporin-1 and aquaporin-5 in aged mice. *Clin. Exp. Pharmacol. Physiol.* **36**, 734–738 (2009).
61. Zuurbier, C. J., Emons, V. M. & Ince, C. Hemodynamics of anesthetized ventilated mouse models: aspects of anesthetics, fluid support, and strain. *Am. J. Physiol. Heart Circ. Physiol.* **282**, H2099–2105 (2002).
62. Anfinsen, C. B. The formation and stabilization of protein structure. *Biochem. J.* **128**, 737–749 (1972).
63. Alberts, B. *et al.* The Shape and Structure of Proteins. (2002).
64. Alberts, B. *et al.* The Endoplasmic Reticulum. (2002).
65. Braakman, I. & Hebert, D. N. Protein Folding in the Endoplasmic Reticulum. *Cold Spring Harb. Perspect. Biol.* **5**, a013201 (2013).
66. Dobson, C. M. Protein folding and misfolding. *Nature* **426**, 884–890 (2003).
67. Reynaud, E. Protein Misfolding and Degenerative Diseases. *Nat. Educ.* **28**
68. Zhou, H.-X. Influence of crowded cellular environments on protein folding, binding, and oligomerization: Biological consequences and potentials of atomistic modeling. *FEBS Lett.* **587**, 1053–1061 (2013).
69. Scheuner, D. *et al.* Control of mRNA translation preserves endoplasmic reticulum function in beta cells and maintains glucose homeostasis. *Nat. Med.* **11**, 757–764 (2005).

70. Ma, Y. & Hendershot, L. M. ER chaperone functions during normal and stress conditions. *J. Chem. Neuroanat.* **28**, 51–65 (2004).
71. Araki, K. & Nagata, K. Protein Folding and Quality Control in the ER. *Cold Spring Harb. Perspect. Biol.* **3**, (2011).
72. Brown, M. K. & Naidoo, N. The endoplasmic reticulum stress response in aging and age-related diseases. *Front. Physiol.* **3**, (2012).
73. Bravo, R. *et al.* Endoplasmic Reticulum and the Unfolded Protein Response: Dynamics and Metabolic Integration. *Int. Rev. Cell Mol. Biol.* **301**, 215–290 (2013).
74. Osowski, C. M. & Urano, F. Measuring ER stress and the unfolded protein response using mammalian tissue culture system. *Methods Enzymol.* **490**, 71–92 (2011).
75. Harding, H. P., Zhang, Y., Bertolotti, A., Zeng, H. & Ron, D. Perk is essential for translational regulation and cell survival during the unfolded protein response. *Mol. Cell* **5**, 897–904 (2000).
76. Avivar-Valderas, A. *et al.* PERK integrates autophagy and oxidative stress responses to promote survival during extracellular matrix detachment. *Mol. Cell. Biol.* **31**, 3616–3629 (2011).
77. Yan, H., Wang, H., Zhang, X., Li, X. & Yu, J. Ascorbic acid ameliorates oxidative stress and inflammation in dextran sulfate sodium-induced ulcerative colitis in mice. *Int. J. Clin. Exp. Med.* **8**, 20245–20253 (2015).
78. Chiang, W.-C., Hiramatsu, N., Messah, C., Kroeger, H. & Lin, J. H. Selective Activation of ATF6 and PERK Endoplasmic Reticulum Stress Signaling Pathways Prevent Mutant Rhodopsin Accumulation. *Invest. Ophthalmol. Vis. Sci.* **53**, 7159–7166 (2012).
79. Hetz, C. The unfolded protein response: controlling cell fate decisions under ER stress and beyond. *Nat. Rev. Mol. Cell Biol.* **13**, 89–102 (2012).
80. Lindholm, D., Wootz, H. & Korhonen, L. ER stress and neurodegenerative diseases. *Cell Death Differ.* **13**, 385–392 (2006).

81. Paz Gavilán, M. *et al.* Cellular environment facilitates protein accumulation in aged rat hippocampus. *Neurobiol. Aging* **27**, 973–982 (2006).
82. Nuss, J. E., Choksi, K. B., DeFord, J. H. & Papaconstantinou, J. Decreased enzyme activities of chaperones PDI and BiP in aged mouse livers. *Biochem. Biophys. Res. Commun.* **365**, 355–361 (2008).
83. Takeda, N. *et al.* Altered unfolded protein response is implicated in the age-related exacerbation of proteinuria-induced proximal tubular cell damage. *Am. J. Pathol.* **183**, 774–785 (2013).
84. Andrade, P. V. *et al.* Influence of Hyperoxia and Mechanical Ventilation in Lung Inflammation and Diaphragm Function in Aged Versus Adult Rats. *Inflammation* **37**, 486–494 (2013).
85. Caironi, P., Langer, T., Carlesso, E., Protti, A. & Gattinoni, L. Time to generate ventilator-induced lung injury among mammals with healthy lungs: a unifying hypothesis. *Intensive Care Med.* **37**, 1913–1920 (2011).
86. Crane, S. D. Epidemiology, treatment and outcome of acidotic, acute, cardiogenic pulmonary oedema presenting to an emergency department. *Eur. J. Emerg. Med. Off. J. Eur. Soc. Emerg. Med.* **9**, 320–324 (2002).
87. Chioncel, O. *et al.* Epidemiology, pathophysiology, and in-hospital management of pulmonary edema: data from the Romanian Acute Heart Failure Syndromes registry. *J. Cardiovasc. Med. Hagerstown Md* (2014). doi:10.2459/JCM.0000000000000192
88. Matthew W. Semler, Art P. Wheeler, Gordon R. Bernard, B. T. Thompson & Todd W. Rice. in *C95. WHAT'S NEW IN ACUTE RESPIRATORY DISTRESS SYNDROME A5094–A5094* (American Thoracic Society, 2014).
89. Pedreira, P. R. *et al.* Effects of melatonin in an experimental model of ventilator-induced lung injury. *Am. J. Physiol. Lung Cell. Mol. Physiol.* **295**, L820–827 (2008).

90. Eckle, T., Grenz, A., Laucher, S. & Eltzschig, H. K. A2B adenosine receptor signaling attenuates acute lung injury by enhancing alveolar fluid clearance in mice. *J. Clin. Invest.* **118**, 3301–3315 (2008).
91. Wilson, M. R., Patel, B. V. & Takata, M. Ventilation with ‘clinically-relevant’ high tidal volumes does not promote stretch-induced injury in the lungs of healthy mice. *Crit. Care Med.* **40**, 2850–2857 (2012).
92. Wolthuis, E. K. *et al.* Mechanical ventilation using non-injurious ventilation settings causes lung injury in the absence of pre-existing lung injury in healthy mice. *Crit. Care Lond. Engl.* **13**, R1 (2009).
93. Wu, Y., Kharge, A. B. & Perlman, C. E. Lung ventilation injures areas with discrete alveolar flooding, in a surface tension-dependent fashion. *J. Appl. Physiol. Bethesda Md 1985* **117**, 788–796 (2014).
94. Chamorro-Marín, V., García-Delgado, M., Touma-Fernández, A., Aguilar-Alonso, E. & Fernández-Mondejar, E. Intratracheal dopamine attenuates pulmonary edema and improves survival after ventilator-induced lung injury in rats. *Crit. Care Lond. Engl.* **12**, R39 (2008).
95. National Heart, Lung, and Blood Institute Acute Respiratory Distress Syndrome (ARDS) Clinical Trials Network *et al.* Comparison of two fluid-management strategies in acute lung injury. *N. Engl. J. Med.* **354**, 2564–2575 (2006).
96. Valentine, S. L. *et al.* Fluid balance in critically ill children with acute lung injury. *Crit. Care Med.* **40**, 2883–2889 (2012).
97. Murray, J. F. Pulmonary edema: pathophysiology and diagnosis. *Int. J. Tuberc. Lung Dis. Off. J. Int. Union Tuberc. Lung Dis.* **15**, 155–160, i (2011).
98. Tsukimoto, K. *et al.* Protein, cell, and LTB4 concentrations of lung edema fluid produced by high capillary pressures in rabbit. *J. Appl. Physiol. Bethesda Md 1985* **76**, 321–327 (1994).

99. Grinnan, D. C. & Truwit, J. D. Clinical review: Respiratory mechanics in spontaneous and assisted ventilation. *Crit. Care* **9**, 472–484 (2005).
100. Fahlman, A. *et al.* Inflation and deflation pressure-volume loops in anesthetized pinnipeds confirms compliant chest and lungs. *Front. Physiol.* **5**, (2014).
101. Biehl, M., Kashiouris, M. G. & Gajic, O. Ventilator-induced lung injury: minimizing its impact in patients with or at risk for ARDS. *Respir. Care* **58**, 927–937 (2013).
102. Sharma, G. & Goodwin, J. Effect of aging on respiratory system physiology and immunology. *Clin. Interv. Aging* **1**, 253–260 (2006).
103. Papandrinopoulou, D., Tzouda, V. & Tsoukalas, G. Lung Compliance and Chronic Obstructive Pulmonary Disease. *Pulm. Med.* **2012**, e542769 (2012).
104. Huang, K., Rabold, R., Schofield, B., Mitzner, W. & Tankersley, C. G. Age-dependent changes of airway and lung parenchyma in C57BL/6J mice. *J. Appl. Physiol.* **102**, 200–206 (2007).
105. Muñoz-Barrutia, A., Ceresa, M., Artaechevarria, X., Montuenga, L. M. & Ortiz-de-Solorzano, C. Quantification of lung damage in an elastase-induced mouse model of emphysema. *Int. J. Biomed. Imaging* **2012**, 734734 (2012).
106. Loring, S. H. *et al.* Maintaining end-expiratory transpulmonary pressure prevents worsening of ventilator-induced lung injury caused by chest wall constriction in surfactant-depleted rats. *Crit. Care Med.* **38**, 2358–2364 (2010).
107. *Interstitial lung disease.* (Shelton, Conn. : People’s Medical Pub. House, 2011).
108. Elder, A. C., Finkelstein, J., Johnston, C., Gelein, R. & Oberdörster, G. Induction of adaptation to inhaled lipopolysaccharide in young and old rats and mice. *Inhal. Toxicol.* **12**, 225–243 (2000).
109. Systemic Inflammatory Response Syndrome: Background, Pathophysiology, Etiology. (2016).

110. Jia, L.-X. *et al.* Mechanical stretch-induced endoplasmic reticulum stress, apoptosis and inflammation contribute to thoracic aortic aneurysm and dissection. *J. Pathol.* **236**, 373–383 (2015).
111. Boudreault, F. & Tschumperlin, D. J. Stretch-induced mitogen-activated protein kinase activation in lung fibroblasts is independent of receptor tyrosine kinases. *Am. J. Respir. Cell Mol. Biol.* **43**, 64–73 (2010).
112. Chatzigeorgiou, A. *et al.* The pattern of inflammatory/anti-inflammatory cytokines and chemokines in type 1 diabetic patients over time. *Ann. Med.* **42**, 426–438 (2010).
113. Davidovich, N. *et al.* Cyclic stretch-induced oxidative stress increases pulmonary alveolar epithelial permeability. *Am. J. Respir. Cell Mol. Biol.* **49**, 156–164 (2013).
114. Song, M. J., Davis, C. I., Lawrence, G. G. & Margulies, S. S. Local influence of cell viability on stretch-induced permeability of alveolar epithelial cell monolayers. *Cell. Mol. Bioeng.* **9**, 65–72 (2016).
115. Gao, J. *et al.* Preconditioning effects of physiological cyclic stretch on pathologically mechanical stretch-induced alveolar epithelial cell apoptosis and barrier dysfunction. *Biochem. Biophys. Res. Commun.* **448**, 342–348 (2014).
116. Cohen, T. S., Cavanaugh, K. J. & Margulies, S. S. Frequency and peak stretch magnitude affect alveolar epithelial permeability. *Eur. Respir. J.* **32**, 854–861 (2008).
117. Heise, R. L., Stober, V., Cheluvvaraju, C., Hollingsworth, J. W. & Garantziotis, S. Mechanical Stretch Induces Epithelial-Mesenchymal Transition in Alveolar Epithelia via Hyaluronan Activation of Innate Immunity. *J. Biol. Chem.* **286**, 17435–17444 (2011).
118. Maciel-Barón, L. A. *et al.* Senescence associated secretory phenotype profile from primary lung mice fibroblasts depends on the senescence induction stimuli. *AGE* **38**, 1–14 (2016).
119. Kumar, M., Seeger, W. & Voswinckel, R. Senescence-Associated Secretory Phenotype and Its Possible Role in Chronic Obstructive Pulmonary Disease. *Am. J. Respir. Cell Mol. Biol.* **51**, 323–333 (2014).

120. Yin, L. *et al.* Aging exacerbates damage and delays repair of alveolar epithelia following influenza viral pneumonia. *Respir. Res.* **15**, 116 (2014).
121. Römisch, K. A cure for traffic jams: small molecule chaperones in the endoplasmic reticulum. *Traffic Cph. Den.* **5**, 815–820 (2004).
122. Schröder, M. & Kaufman, R. J. ER stress and the unfolded protein response. *Mutat. Res.* **569**, 29–63 (2005).
123. Zhong, Q. *et al.* Role of Endoplasmic Reticulum Stress in Epithelial–Mesenchymal Transition of Alveolar Epithelial Cells. *Am. J. Respir. Cell Mol. Biol.* **45**, 498–509 (2011).
124. Naidoo, N. ER and aging—Protein folding and the ER stress response. *Ageing Res. Rev.* **8**, 150–159 (2009).
125. Naidoo, N., Ferber, M., Master, M., Zhu, Y. & Pack, A. I. Aging impairs the unfolded protein response to sleep deprivation and leads to proapoptotic signaling. *J. Neurosci. Off. J. Soc. Neurosci.* **28**, 6539–6548 (2008).
126. Hussain, S. G. & Ramaiah, K. V. A. Reduced eIF2 α phosphorylation and increased proapoptotic proteins in aging. *Biochem. Biophys. Res. Commun.* **355**, 365–370 (2007).
127. Torres-González, E. *et al.* Role of Endoplasmic Reticulum Stress in Age-Related Susceptibility to Lung Fibrosis. *Am. J. Respir. Cell Mol. Biol.* **46**, 748–756 (2012).
128. Kim, H. J. *et al.* Inhibition of endoplasmic reticulum stress alleviates lipopolysaccharide-induced lung inflammation through modulation of NF- κ B/HIF-1 α signaling pathway. *Sci. Rep.* **3**, 1142 (2013).
129. Zhu, M., Guo, M., Fei, L., Pan, X.-Q. & Liu, Q.-Q. 4-phenylbutyric acid attenuates endoplasmic reticulum stress-mediated pancreatic β -cell apoptosis in rats with streptozotocin-induced diabetes. *Endocrine* **47**, 129–137 (2014).
130. Slutsky, A. S. & Brochard, L. *Mechanical Ventilation*. (Springer Science & Business Media, 2006).

131. Brégeon, F. *et al.* Conventional mechanical ventilation of healthy lungs induced pro-inflammatory cytokine gene transcription. *Respir. Physiol. Neurobiol.* **132**, 191–203 (2002).
132. Ignatenko, O., Protsenko, D., Yaroshetskiy, A. & Gelfand, B. Conventional mechanical ventilation can injury intact lungs in severe trauma patients. *Crit. Care* **14**, P200 (2010).
133. Meier, T. *et al.* Pulmonary cytokine responses during mechanical ventilation of noninjured lungs with and without end-expiratory pressure. *Anesth. Analg.* **107**, 1265–1275 (2008).
134. Sutherasan, Y., Vargas, M. & Pelosi, P. Protective mechanical ventilation in the non-injured lung: review and meta-analysis. *Crit. Care* **18**, 211 (2014).
135. Blázquez-Prieto, J. *et al.* Exposure to mechanical ventilation promotes tolerance to ventilator-induced lung injury by Ccl3 downregulation. *Am. J. Physiol. Lung Cell. Mol. Physiol.* **309**, L847–856 (2015).
136. Ertugrul, A. S., Sahin, H., Dikilitas, A., Alpaslan, N. & Bozoglan, A. Evaluation of beta-2 microglobulin and alpha-2 macroglobulin levels in patients with different periodontal diseases. *Aust. Dent. J.* **58**, 170–175 (2013).
137. Liabeuf, S. *et al.* Plasma beta-2 microglobulin is associated with cardiovascular disease in uremic patients. *Kidney Int.* **82**, 1297–1303 (2012).
138. Lehmann, M. H. *et al.* CCL2 expression is mediated by type I IFN receptor and recruits NK and T cells to the lung during MVA infection. *J. Leukoc. Biol.* **99**, 1057–1064 (2016).
139. Kitamura, T. *et al.* CCL2-induced chemokine cascade promotes breast cancer metastasis by enhancing retention of metastasis-associated macrophages. *J. Exp. Med.* **212**, 1043–1059 (2015).
140. Rose, C. E., Sung, S.-S. J. & Fu, S. M. Significant involvement of CCL2 (MCP-1) in inflammatory disorders of the lung. *Microcirc. N. Y. N 1994* **10**, 273–288 (2003).
141. Driscoll, K. E. Macrophage inflammatory proteins: biology and role in pulmonary inflammation. *Exp. Lung Res.* **20**, 473–490 (1994).

142. Chong, I.-W. *et al.* Expression and regulation of the macrophage inflammatory protein-1 alpha gene by nicotine in rat alveolar macrophages. *Eur. Cytokine Netw.* **13**, 242–249 (2002).
143. Orjalo, A. V. *et al.* Cell Surface-Bound IL-1 β Is an Upstream Regulator of the Senescence-Associated IL-6/ IL-8 Cytokine Network. *Proc. Natl. Acad. Sci. U. S. A.* **106**, 17031–17036 (2009).
144. Suwara, M. I. *et al.* IL-1 α released from damaged epithelial cells is sufficient and essential to trigger inflammatory responses in human lung fibroblasts. *Mucosal Immunol.* **7**, 684–693 (2014).
145. Ko, Y.-A., Yang, M.-C., Huang, H.-T., Hsu, C.-M. & Chen, L.-W. NF- κ B activation in myeloid cells mediates ventilator-induced lung injury. *Respir. Res.* **14**, 69 (2013).
146. Krakauer, T. Nuclear factor-kappaB: fine-tuning a central integrator of diverse biologic stimuli. *Int. Rev. Immunol.* **27**, 286–292 (2008).
147. Culley, F. J. *et al.* Role of CCL5 (RANTES) in Viral Lung Disease. *J. Virol.* **80**, 8151–8157 (2006).
148. Moran, C. J. *et al.* RANTES expression is a predictor of survival in stage I lung adenocarcinoma. *Clin. Cancer Res. Off. J. Am. Assoc. Cancer Res.* **8**, 3803–3812 (2002).
149. Pan, Z. Z., Parkyn, L., Ray, A. & Ray, P. Inducible lung-specific expression of RANTES: preferential recruitment of neutrophils. *Am. J. Physiol. Lung Cell. Mol. Physiol.* **279**, L658–666 (2000).
150. Kuo, S.-M. The Multifaceted Biological Roles of VitC. *J. Nutr. Food Sci.* **03**, (2013).
151. Figueroa-Méndez, R. & Rivas-Arancibia, S. VitC in Health and Disease: Its Role in the Metabolism of Cells and Redox State in the Brain. *Front. Physiol.* **6**, (2015).
152. Li, Y. *et al.* Restoration of VitC synthesis in transgenic Gulo $^{-/-}$ mice by helper-dependent adenovirus-based expression of gulonolactone oxidase. *Hum. Gene Ther.* **19**, 1349–1358 (2008).

153. Senmaru, T. *et al.* Pancreatic insulin release in VitC-deficient senescence marker protein-30/gluconolactonase knockout mice. *J. Clin. Biochem. Nutr.* **50**, 114–118 (2012).
154. Fisher, B. J. *et al.* Mechanisms of attenuation of abdominal sepsis induced acute lung injury by ascorbic acid. *Am. J. Physiol. Lung Cell. Mol. Physiol.* **303**, L20–32 (2012).
155. Li, W., Maeda, N. & Beck, M. A. VitC deficiency increases the lung pathology of influenza virus-infected *gulo*^{-/-} mice. *J. Nutr.* **136**, 2611–2616 (2006).
156. Brubacher, D., Moser, U. & Jordan, P. VitC concentrations in plasma as a function of intake: a meta-analysis. *Int. J. Vitam. Nutr. Res. Int. Z. Für Vitam.- Ernährungsforschung J. Int. Vitaminol. Nutr.* **70**, 226–237 (2000).
157. Michels, A. J., Joisher, N. & Hagen, T. M. Age-related decline of sodium-dependent ascorbic acid transport in isolated rat hepatocytes. *Arch. Biochem. Biophys.* **410**, 112–120 (2003).
158. Sargeant, L. A., Jaeckel, A. & Wareham, N. J. Interaction of VitC with the relation between smoking and obstructive airways disease in EPIC Norfolk. European Prospective Investigation into Cancer and Nutrition. *Eur. Respir. J.* **16**, 397–403 (2000).
159. Siedlinski, M. *et al.* Lung function loss, smoking, VitC intake, and polymorphisms of the glutamate-cysteine ligase genes. *Am. J. Respir. Crit. Care Med.* **178**, 13–19 (2008).
160. Ghneim, H. K. & Al-Sheikh, Y. A. The effect of aging and increasing ascorbate concentrations on respiratory chain activity in cultured human fibroblasts. *Cell Biochem. Funct.* **28**, 283–292 (2010).
161. Mayr, F. B., Yende, S. & Angus, D. C. Epidemiology of severe sepsis. *Virulence* **5**, 4–11 (2014).
162. Sheu, C.-C. *et al.* Clinical Characteristics and Outcomes of Sepsis-Related vs Non-Sepsis-Related ARDS. *Chest* **138**, 559–567 (2010).
163. Nemzek, J. A., Hugunin, K. M. & Opp, M. R. Modeling Sepsis in the Laboratory: Merging Sound Science with Animal Well-Being. *Comp. Med.* **58**, 120–128 (2008).

164. Hoesel, L. M. *et al.* Harmful and protective roles of neutrophils in sepsis. *Shock Augusta Ga* **24**, 40–47 (2005).
165. Perl, M. *et al.* Role of activated neutrophils in chest trauma-induced septic acute lung injury. *Shock Augusta Ga* **38**, 98–106 (2012).
166. Fisher, B. J. *et al.* Attenuation of sepsis-induced organ injury in mice by VitC. *JPEN J. Parenter. Enteral Nutr.* **38**, 825–839 (2014).
167. Doi, K., Leelahavanichkul, A., Yuen, P. S. T. & Star, R. A. Animal models of sepsis and sepsis-induced kidney injury. *J. Clin. Invest.* **119**, 2868–2878 (2009).
168. Starr, M. E. & Saito, H. Sepsis in Old Age: Review of Human and Animal Studies. *Aging Dis.* **5**, 126–136 (2014).
169. Shrum, B. *et al.* A robust scoring system to evaluate sepsis severity in an animal model. *BMC Res. Notes* **7**, 233 (2014).
170. Dixon, D.-L. & Bersten, A. D. Sepsis and ventilator-induced lung injury: an imperfect storm. *Crit. Care Med.* **41**, 354–355 (2013).
171. Chacon-Cabrera, A. *et al.* Influence of mechanical ventilation and sepsis on redox balance in diaphragm, myocardium, limb muscles, and lungs. *Transl. Res. J. Lab. Clin. Med.* (2014). doi:10.1016/j.trsl.2014.07.003
172. de Prost, N., Ricard, J.-D., Saumon, G. & Dreyfuss, D. Ventilator-induced lung injury: historical perspectives and clinical implications. *Ann. Intensive Care* **1**, 28 (2011).
173. Golestanian, E., Liou, J.-I. & Smith, M. A. Long-Term Survival in Older Critically Ill Patients with Acute Ischemic Stroke. *Crit. Care Med.* **37**, 3107–3113 (2009).
174. Mather, M., Jacobsen, L. A. & Pollard, K. M. Aging in the United States. *Popul. Bull.* **70**, 2–18 (2015).

Vita

Joseph Ames Herbert was born on March 11th, 1983, in Auburn, Alabama, and is an American citizen. He graduated from Franklin High School, Franklin, Virginia 2001. He received a Bachelor's of Science in Physics from the University of Mary Washington, Fredericksburg, Virginia in 2005. He worked in the Radiation Oncology Laboratory of Dr. Mark Dewhirst in Durham Virginia for 5 years.